The Dissertation Committee for Alexey V. Seregin Certifies that this is the approved version of the following dissertation:

Genetic Determinants of Junin Virus Attenuation

Committee:

Slobodan Paessler

Adolfo Garcia-Sastre

Robert B. Tesh

Tetsuro Ikegami

Stanley J. Watowich

Dean, Graduate School

Genetic Determinants of Junin Virus Attenuation

by

Alexey V. Seregin, M.S.

Dissertation

Presented to the Faculty of the Graduate School of

The University of Texas Medical Branch

in Partial Fulfillment

of the Requirements

for the Degree of

Doctor of Philosophy

The University of Texas Medical Branch

March, 2014

Dedication

To my family, who inspire me and for whom I live.

Acknowledgements

First of all, I would like to thank my mentor Dr. Slobodan Paessler for his great support, guidance and encouragement throughout my dissertation project. I was privileged to have him as my mentor and I have learnt so much from him about all aspects of being a scientist. I want to thank my committee: Drs. Robert Tesh, Tetsuro Ikegami, Stanley Watowich, and Adolfo Garcia-Sastre for their time, guidance, and invaluable input in my dissertation. I would also like to acknowledge Dr. Nadezhda Yun who taught me everything I know in the BSL-4 laboratory and everyone who was involved in this project. Finally, I would like to thank my parents for cultivating a thirst for knowledge in me throughout my childhood and, most importantly, my wife Nadya and our daughter Katya for their endless support and for always being there for me when I needed them. I could not absolutely have done this without them.

Genetic Determinants of Junin Virus Attenuation

Publication No._____

Alexey V. Seregin, Ph.D.

The University of Texas Medical Branch, 2014

Supervisor: Slobodan Paessler

The New World arenavirus Junin (JUNV) is the causative agent of the Argentine hemorrhagic fever (AHF), a deadly disease endemic to central regions of Argentina. The live-attenuated Candid #1 strain of JUNV is currently used to vaccinate human population at risk. However, the mechanism of attenuation of this strain is still largely unknown. Therefore, the identification and functional characterization of viral genetic factors implicated in JUNV pathogenesis or attenuation would significantly improve the understanding of the molecular mechanisms underlying AHF and facilitate the development of novel, effective and safe vaccines. To this end, an RNA polymerase I/II-based reverse genetics system was utilized to rescue the wild type pathogenic Romero and attenuated Candid #1 strains of JUNV. Both recombinant viruses exhibited similar *in vitro* growth kinetics and *in vivo* biological properties to their parental counterparts. This system was further used to generate chimeric JUNV variants encoding different gene combinations of Romero and Candid #1. Analysis of virulence of the chimeric viruses in a guinea pigs model of lethal infection that closely reproduces the features of AHF, identified the envelope glycoproteins (GPs) as the major determinants of pathogenesis and attenuation of JUNV. Therefore, the chimeric viruses expressing the GPs of Romero

and Candid #1 exhibited virulent and attenuated phenotypes in guinea pigs, respectively. Comparison of the transcriptional and protein expression profiles of the chimeric JUNV variants demonstrated marked differences in the levels of viral RNA synthesis and protein expression between the attenuated and virulent JUNV variants. Further analysis showed that the GPC of Candid #1 undergoes abnormal post-translational modification and induces endoplasmic reticulum (ER) stress, which may facilitate immune recognition of JUNV infection. In addition, the small RING finger protein Z that is a negative regulator of the viral polymerase complex was retained in infected cells when it was coexpressed with the GPs of Romero, but not the GPs of Candid #1, therefore suggesting a molecular mechanism for the higher levels of viral RNA synthesis in cells infected with attenuated JUNV variants expressing the GPC of Candid #1. Thus, these findings provided further insights into the mechanism of JUNV attenuation.

TABLE OF CONTENTS

List of Tables

List of Figures

CHAPTER 1: INTRODUCTION TO JUNV AND AHF[1]

PHYLOGENY AND GEOGRAPHICAL DISTRIBUTION

Junin virus, the causative agent of Argentine hemorrhagic fever (AHF) in humans, belongs to the family *Arenaviridae*. This family consists of a single genus, Arenavirus (Fig. 1.1) (Buchmeier, 2013). Arenaviruses are enveloped segmented negative-sense RNA (nsRNA) viruses that have a close phylogenetic relationship with virus members of families *Bunyaviridae* and *Orthomyxoviridae*. All of these viruses share basic principles of the intacellular life cycle but utilize different cellular compartments for replication. Phylogenetic analysis (Bowen et al., 1997), serological cross-reactivity tests (Wulff et al., 1978), and geographical distribution allowed to sub-divide all arenaviruses into the Old World and New World virus complexes. The Old World complex includes arenaviruses that circulate in Africa, Europe, and Asia (lymphocytic choreomeningitis (LCMV), Lassa (LASV), Mopeia (MOPV), Mobala (MOBV), Ippy (IPPYV), Morogoro (MORV), Kodoko (KODV), Dandenong (DANV), Merino Walk (MWV), Lujo (LUJV), Luna (LUNV), and Lunk (LNKV) virus) and comprise the LCMV-LASV serocomplex. LCMV is the only arenavirus that is distributed worldwide due to the association with its rodent host (species *Mus domesticus* and *Mus musculus*). The New World arenavirus complex (Tacaribe serocomplex) consists of four phylogenetic lineages designated as clades A, B, C, and A/Rec. Clade A includes Pirital (PIRV), Pichinde (PICV), Flexal (FLEV), Parana (PARV), and Allpahuayo (ALLV) virus. Clade B includes Sabia (SABV), Junin (JUNV), Machupo (MACV), Guanarito (GTOV), Amapari (AMAV), Tacaribe (TACV), Cupixi (CPXV), and Chapare (CHPV) virus. Clade C includes Oliveros (OLVV) and Latino (LATV) (Salvato et al., 2012).

[1] Adapted with permission form Grant A, Seregin A, Huang C, Kolokoltsova O, Brasier A, Peters C, Paessler S. Junín Virus Pathogenesis and Virus Replication. Review. Viruses 2012, 4, 2317-2339; doi:10.3390/v4102317

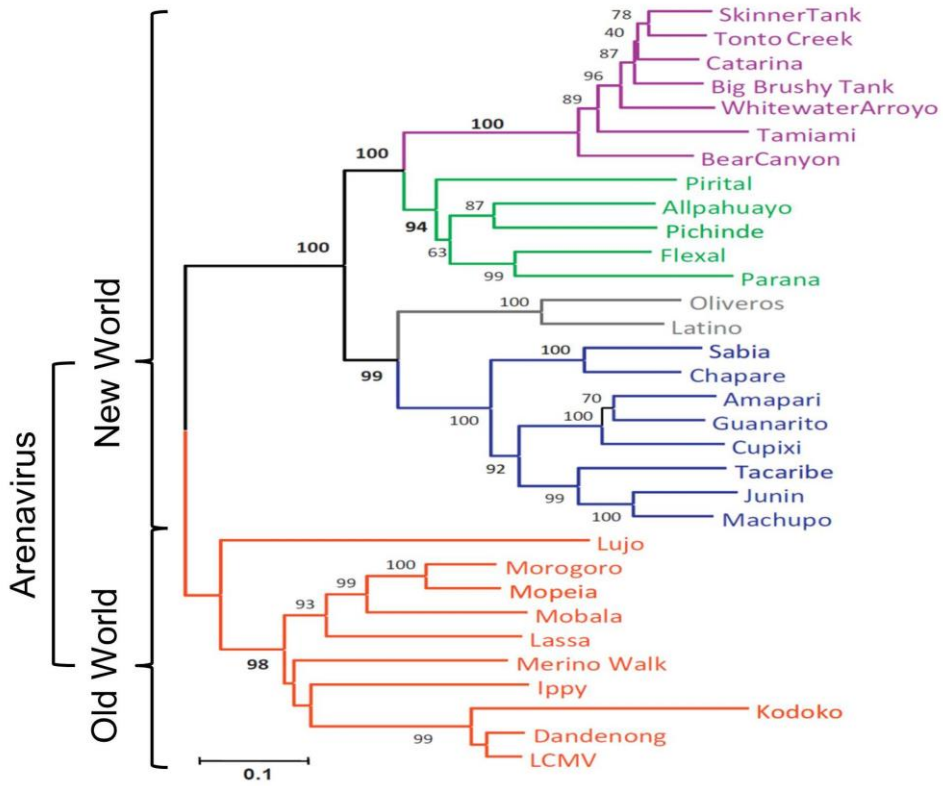

Figure 1.1. Phylogeny of the genus Arenavirus. Evolutionary lineages are designated with different colors. Red, Old World arenaviruses; green, clade A New World arenaviruses; blue, clade B New World arenaviruses, grey, clade C New World arenaviruses; purple, clade A/Rec New World arenaviruses. Adapted with permission from (Charrel, Coutard et al. 2011).

Clade A, B, and C arenaviruses circulate in South America. Clade A/Rec comprises several North American arenaviruses that are believed to result from recombination between ancestor viruses belonging to clades A and B (Archer and Rico-Hesse, 2002; Charrel et al., 2002; Fulhorst et al., 2001), namely Whitewater Arroyo (WWAV), Tamiami (TAMV), Bear Canyon (BCNV), Skinner Tank, Tonto Creek, Big Brushy Tank, and Catarina virus (Cajimat et al., 2008; Cajimat et al., 2007; Charrel et al., 2011; Milazzo M.L., 2008). However, a recent report has provided evidence that this phylogenetic phenomenon was observed due to the differences in the analytical methods that were used rather than recombination of genetic material between arenaviruses (Cajimat et al., 2011).

Arenaviruses are transmitted by rodents, with which they have established a long-term evolutionary relationship. TCRV is the only exception that was isolated from *Artibeus* bats in Trinidad (Downs et al., 1963) and no evidence of infection of other mammals, particularly rodents, has been found to date. Transmission of each arenavirus is usually associated with a single rodent species, less often two closely related species. Thus, the geographical distribution and migration patterns of the host species determine the geographical distribution of arenaviruses (Gonzalez et al., 2007).

EPIDEMIOLOGY

The primary rodent reservoir for JUNV is the drylands vesper mouse *Calomys musculinus* (Sabattini and Maiztegui, 1970). These rodents inhabit cornfields and surrounding weedy areas where their population reaches the highest density during the harvest season between March and June (Peters, 2006). AHF, the disease that is caused

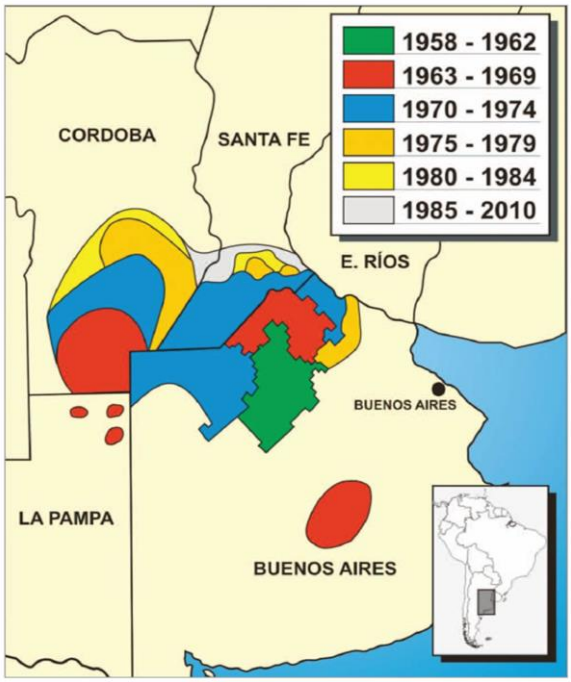

Figure 1.2. Progressive expansion of AHF-endemic area. Reproduced with permission from (Ambrosio et al., 2011).

by JUNV infection, emerged in 1958 in the Buenos Aires province of Argentina, a rich farming region. The appearance of AHF coincided with massive deforestation and rapid development of farming in the area, which significantly increased the frequency of interaction between humans and the rodent reservoir of JUNV. Most infected patients are agricultural workers involved in harvesting corn in endemic regions. Human infections are believed to occur through either direct contact with infected rodents from bites or inhalation of aerosolized virus particles produced from rodent excreta or from rodents that are caught and shredded in the harvesting machinery (Maiztegui, 1975). The initial endemic region was estimated to include a 16,000 km^2 area of humid pampas in the north of Buenos Aires province putting 270,000 people at risk. However, AHF has progressively spread to a larger area of 150,000 km^2 involving three more provinces, Santa Fe, Cordoba and La Pampa, inhabited by more than three million people (Fig. 1.2) (Enria, 1998). Currently, the human population at risk is estimated to be about five million people. Since 1958, and until the introduction of a specific vaccine, the number of cases reported annually ranged from several hundreds to more than three thousand (Enria et al., 2008). A live-attenuated vaccine, Candid #1, has been developed by the United States Army Medical Research Institute of Infectious Diseases (USAMRIID) and is currently used to vaccinate human population residing in the endemic regions of Argentina that allowed to significantly reduce the incidence of AHF to current 30 to 50 cases per year (Ambrosio et al., 2011).

Person-to-person transmission is rare; however, may occur via either exposure to body fluids or direct contact with infected patients. Nosocomial infections have also been reported (Grant et al., 2012).

CLINICAL DESCRIPTION AND PATHOGENESIS OF AHF

The incubation period for JUNV infection in human patients usually lasts for 6 to 14 days, with most infections (~80%) resulting in a clinical disease. There are free phases recognized in the illness: prodromal, neurological-hemorrhagic, and convalescence (Enria et al., 2004).

The prodromal phase lasts for the first week after the onset of symptoms. AHF patients most commonly experience headache, chills, anorexia, malaise, myalgia, and a fever of 38°C to 39°C. Very often, nausea or vomiting, retro-orbital pain, epigastric pain, photophobia, dizziness, and constipation or mild diarrhea are also observed. Upon physical examination the patients present with flushing of the face, neck and upper chest; conjunctival congestion and periorbital edema. Congestion of the gums that may bleed either spontaneously or under slight pressure, enanthem over the soft palate, and cutaneous petechiae in the axillary regions, upper chest and arms are among most common clinical manifestations. By the end of the prodromal phase, the patients may become lethargic, irritable, and experience fine tremor of tongue and upper limbs. Moderate ataxia, cutaneous hyperesthesia, and decrease in deep tendon reflexes and muscular tonicity are commonly observed. Oral candidiasis is frequent in patients at the end of the first week of illness (Enria et al., 2008).

Around 8 to 12 days after the onset of symptoms, 20% to 30% of patients progress to the neurological-hemorrhagic phase, which is associated with significant worsening of the patient's condition. During this phase patients develop severe hemorrhagic manifestations, including hematemesis, melena, hemoptysis, epistaxis, hematomas, metrorrhagia and hematuria. Neurological complications begin with increased irritability, tremors, ataxia, and mental confusion that are followed by delirium, generalized convulsions and coma. Frequently observed superimposed bacterial infections that lead to pneumonia and septicemia may significantly complicate the

disease. The terminal cases presumably succumb to shock, although the death of these patients cannot be attributed to blood loss alone. If untreated, the mortality rate of AHF can be up to 30% (Enria et al., 2008).

Patients that survive AHF experience prolonged, protracted convalescence that lasts up to 3 months. A number of symptoms are observed during this phase, such as asthenia, irritability, memory changes and hair loss (Enria et al., 2008).

Clinical findings during the first week of illness include progressive leukopenia and thrombocytopenia with cell counts falling to 1,000-2,000 white blood cells and 50,000-100,000 platelets per μL. Mild elevation of aspartate transaminase (AST), creatine phosphokinase (CPK), and lactate dehydrogenase (LDH) levels are characteristic findings in AHF patients. The rate of sedimentation either remains normal or slightly decreased. Proteinuria and urinary sediment consisting of hyaline-granular casts and red blood cells are also observed. The levels of creatinine and urea in serum are increased in severe cases of AHF proportionally to the degree of dehydration and shock (Enria et al., 2011).

Most cases of JUNV infection are believed to occur through inhalation of aerosolized viral particles from infected rodents. Initial viral replication takes place in lungs and is followed by subsequent spread to parenchymal tissues, which is presumably mediated by migration of infected alveolar macrophages to draining lymph nodes and further virus dissemination through the vascular system (González et al., 1980). As a result, the majority of organs are affected, including vascular endothelium, myocardium, kidneys, adrenal, lungs, central nervous system, and lymphoid organs (Buchmeier, 2013).

Macrophages have been demonstrated to be a primary target of arenavirus infection. Thus, macrophages isolated from patients with fatal AHF developed a cytopathic effect, JUNV virions budding from plasma membrane were shown by electron microscopy, and specific viral antigens were detected by immunofluorescent staining. In addition, the structure of white pulp of the spleen and lymph nodes was severely affected,

which strongly suggests the tropism of JUNV for lymphatic tissue (González et al., 1980). Virulent strains of both New World and Old World arenaviruses do not activate macrophages upon infection, which was evident from the failure of infected cells to express costimulation and antigen presentation cell surface markers and produce inflammatory cytokines, as has been demonstrated for PICV (New World) and LASV (Old World); however, they establish productive infection (Baize et al., 2004; Fennewald et al., 2002; Lukashevich et al., 1999). In line with these findings, survival of LASV-infected patients has been demonstrated to correlate with elevated levels of proinflammatory cytokines in the plasma of LF patients (Mahanty et al., 2001).

Hemorrhaging during AHF is believed to result from thrombocytopenia, abnormal platelet function, and altered blood coagulation (Marta et al., 2000). The JUNV infection-associated changes in blood parameters include an increase in activated partial thromboplastin time (APTT), low levels of factors VIII, and IX, elevated values of factor V, fibrinogen, and von Willebrand factor, which also demonstrates the involvement of endothelial cells, and decreased levels of antithrombin III and plasminogen (Enria et al., 2008; Heller et al., 1995). AHF patients develop viremia that persists through the acute febrile phase of the disease and is accompanied with very high levels of endogenous IFN-α that have been found to positively correlate with the disease severity. Thus, higher titers of IFN-α indicate a poor clinical prognosis (Levis et al., 1984; Levis et al., 1985).

IMMUNE RESPONSE TO JUNV INFECTION

Role of Adaptive Immune Response

In general, JUNV infection is associated with decreased numbers of T and B lymphocytes and reduced ratio of CD4 to CD8 T cells that is observed during the acute phase of disease. These alterations disappear with the onset of convalescence in AHF

patients (Vallejos et al., 1989). The analysis of the ability of peripheral blood mononuclear cells (PBMC) and polymorphonuclear cells (PMNC) to mediate antibody-dependent cell cytotoxicity (ADCC) revealed that both effector subsets can perform ADCC with comparable efficiency during the acute phase of AHF and in early convalescence to that of effector cells from normal, uninfected donors. These findings suggest that ADCC may be important for the clearance of JUNV-infected cells during the resolution of AHF (Ambrosio et al., 1992). Accordingly, necrosis of lymphoid tissue in the spleen and impaired immunological parameters were observed in JUNV-infected guinea pigs (Kenyon et al., 1985; Weissenbacher et al., 1975).

Humoral immunity plays one of the most important roles in the control of JUNV infection. Thus, guinea pigs infected with attenuated strains of JUNV or immunized with envelope glycoproteins develop high levels of neutralizing antibodies and acquire protection against lethal challenge with virulent strains of JUNV (Avila et al., 1979; Seregin et al., 2010; Weissenbacher et al., 1975). In contrast, immunosuppressed animals infected with attenuated strains and immunocompetent animals infected with virulent strains of JUNV succumb to infection due to the failure to produce neutralizing antibodies and mount antibody-dependent cytotoxic spleen cell activity (Kenyon et al., 1985). The central role of neutralizing antibodies in protective immune response was also demonstrated in marmosets, in which treatment with homologous immune serum reduced mortality from 100% to 25% (Avila et al., 1987). In humans, the use of immune plasma from patients in convalescence allowed to lower the mortality rate from historical 15%-30% to less than 1% (Enria et al., 2008). However, around 10% of patients develop a late neurological syndrome (LNS) that is specifically associated with immune therapy (Enria et al., 1985; Maiztegui et al., 1979). LNS is characterized by febrile symptoms, cerebellar signs and cranial nerve palsies (Enria et al., 2008).

Role of Innate Immune Response

High levels of endogenous IFN-α detected in sera of AHF patients during the acute phase of the disease correlate with the presence of fever, chills, backache and indicate poor prognosis for the disease outcome (Levis et al., 1984; Levis et al., 1985). The high titers of IFN-α are associated with low platelet counts and abnormal platelet function (Lerer et al., 1991). In an *in vitro* model of platelet formation, infection with JUNV did not affect survival of human CD34+ hematopoietic progenitor cells, neither formation of megakaryocytes. However, the infection triggered production of antiviral cytokines, which was mediated by type I IFN that acted via paracrine route and caused abnormal platelet formation. Thus, these findings suggested a central role for IFN-α in the development of thrombocytopenia (Pozner et al., 2010). Similarly, JUNV infection-mediated induction of IFN-α production has also been demonstrated in animal models of AHF (Dejean et al., 198; Kenyon et al., 1992).

Elevated levels of IL-6, IL-8, IL-10 and TNF-α are detected in patients with severe, moderate, and mild AHF indicating activation of both pro- and anti-inflammatory cytokine pathways (Marta et al., 1999). However, it is very unlikely that macrophages or monocytes are sources of these cytokines, since *in vitro* infection of peripheral blood mononuclear cells (PBMCs) from human donors with the pathogenic Romero strain of JUNV did not result in increased production of IFN-α, IFN-β, IL-6, IL-10, IL-12, or TNF-α. However, expression of IL-6, IL-10, and TNF-α was upregulated in response to infection with naturally attenuated TACV that is closely related to JUNV (Groseth et al., 2011).

At least two viral proteins, nucleoprotein (NP) and matrix protein Z, have been demonstrated to be involved in the inhibition of signaling by the antiviral sensing mechanisms of the host cell. Thus, overexpression of JUNV NP resulted in blockage of nuclear translocation of the interferon regulatory factor (IRF)-3 and following inhibition

of expression from IRF-3-dependent promoters and production of IFN-β (Martinez-Sobrido et al., 2007). The Z proteins of four New World arenaviruses, GTOV, MACV, SABV, and JUNV, were shown to bind to the retinoic acid-inducible gene I product (RIG-I) and inhibit expression of IFN-β in response to synthetic RNA bearing 5' phosphates (5'pppRNA). Interaction between the Z proteins and RIG-I was demonstrated by co-immunoprecipitation and co-localization experiments. In addition, expression of JUNV Z prevented interaction between RIG-I and the mitochondrial antiviral-signaling protein (MAVS) and blocks activation of IRF-3/NF-κβ pathway (Fan et al., 2010). Recently, a highly conserved interaction between NP and the IκB kinase (IKK)-related kinase (IKKε) was identified. In LCMV-infected cells, NP was found to bind the kinase domain of IKKε and block its autophosphorylation, which prevented phosphorylation of IRF-3 (Pythoud et al., 2012). Further studies revealed that NPs of both Old World and New World arenaviruses inhibit nuclear translocation and transcriptional regulatory activity of the nuclear factor kappa B (NF-κB) (Rodrigo et al., 2012). Thus, these findings demonstrate that NP of arenaviruses plays a critical role in the inhibition of the host's innate immune and inflammatory responses.

Parenchymal cells infected with JUNV may at least partially be the source of high levels of IFN-α detected in patients during the acute stage of AHF. Thus, infection of human lung epithelial carcinoma cells (A549) with either virulent Romero or attenuated Candid #1 strain of JUNV resulted in production of type I IFN, expression of IFN-stimulated genes (ISG), and phosphorylation of the signal transducer and activator of transcription (STAT) 1. In addition, RIG-I was shown to serve as a primary sensor of JUNV infection, which triggered type I IFN signaling in infected cells (Huang et al., 2012). Collectively, the results from *in vitro* experiments with live JUNV and expression constructs for NP and Z demonstrated that, although, these viral proteins are involved in the suppression of innate immune response, in the early stages of infection there might not be sufficient amounts of NP and Z to block the sensing of viral replication by the host

cell that would trigger type I IFN production. This may be one of the mechanisms that determine the faith of a patient in fatal versus non-fatal AHF cases.

TREATMENT AND PREVENTION

Live-Attenuated Vaccines

TACV is a heterologous New World arenavirus that is not known to cause disease in humans (Buchmeier, 2013). The ability of this virus to induce a cross-protective immune response against lethal JUNV infection has been evaluated in guinea pigs and NHPs. Immunization of guinea pigs with a single dose of TACV resulted in complete protection against lethal challenge (Weissenbacher et al., 1975-1976). Further experiments demonstrated that guinea pigs fully cleared TACV by 30 days after injection and raised high titers of JUNV-cross-reactive neutralizing antibodies that persisted for up to two years and mediated complete protection of the experimental animals against JUNV challenge 18 months after immunization (Weissenbacher et al., 1975-1976). Marmosets inoculated with TACV did not develop any disease symptoms and the analysis of blood parameters demonstrated normal values for erythrocyte, leukocyte, reticulocyte, and platelet counts, as well as unchanged levels of hematocrit and hemoglobin. No viremia was detected in any of the animals and anti-TACV neutralizing antibodies were readily present at 3 weeks post-inoculation. Immunization with TACV resulted in the induction of a strong cross-protective immune response against the pathogenic XJ strain of JUNV, which was confirmed to be protective in subsequent challenge experiments carried out two months after initial TACV infection. The immunized animals did not show any signs of disease or viremia development in contrast to control animals that developed classical AHF symptoms, high levels of viremia, and high viral titers in organs. In addition, the survivors developed high anti-JUNV neutralizing antibody titers (Weissenbacher et al.,

1982). These studies suggested the utility of TACV as a platform for vaccine development against JUNV.

The pathogenic XJ strain of JUNV was isolated by Parodi *et al* in 1958 from a clinical human case (Parodi et al., 1958). This virus has been used to develop several live-attenuated strains of JUNV by passaging in tissue culture, suckling mouse brains, or guinea pigs. XJCl3 strain, derived from parental XJ strain by plaquing the virus on immortalized rabbit kidney MA-111 cells, was demonstrated to be significantly attenuated in mice, and guinea pigs. Accordingly, experimental animals cleared the infection and developed high titers of neutralizing antibodies (Avila et al., 1979; Candurra et al., 1989). Based on the promising results obtained in pre-clinical studies, it was decided to evaluate XJCl3 in a clinical trial in human patients. Thus, XJCl3 strain was administered over a two-year period to 636 volunteers, whose health and immunological status were followed for up to nine years. Most vaccinees developed a subclinical disease with mild symptoms. Out of 165 volunteers tested nine years after immunization, 153 (90.3%) had detectable levels of neutralizing antibodies. All clinical and laboratory parameters were within normal limits for all examined vaccine recipients. However, due to the passage history of XJCl3 strain in suckling mouse brains and a heteroploid cell line, the clinical trials were interrupted (Ambrosio et al., 2011; Ruggiero et al., 1981). Another derivative of a JUNV variant that was the predecessor of XJCl3 strain, XJ0 strain, was attenuated and highly immunogenic in guinea pigs. Immunization induced a protective immune response as early as 3 days after vaccine administration and at 30 days all experimental animals were completely protected. Further development of XJ0 as a live-attenuated vaccine was discontinued after detection of persistent infection of lymphohematopoietic organs of inoculated guinea pigs (Ambrosio et al., 2011; de Guerrero et al., 1985).

Live-attenuated Candid #1 strain of JUNV was developed by the US Army Medical Research Institute of Infectious Diseases (USAMRIID) in collaboration with the

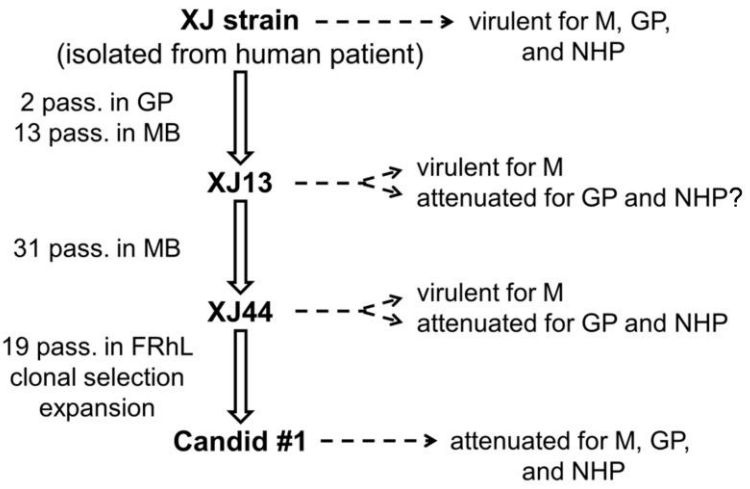

Figure 1.3. Development of Candid #1 vaccine strain of JUNV. M, mouse. MB, mouse brain. GP, guinea pig. NHP, non-human primate. FRhL, fetal rhesus monkey lung cells. Reproduced with permission from (Grant et al., 2012).

Argentine Ministry of Health and Social Action. Candid #1 was derived from XJ strain of JUNV, which gradually lost virulence for mice, guinea pigs, and non-human primates (NHP) during the process of attenuation (Fig. 1.3). The parental XJ virus was initially passages two times in guinea pigs followed by 44 passages in newborn mouse brains. The brain homogenate from the last brain passage (XJ44) was then used to infect a diploid cell line developed from the lung of a fetal rhesus monkey (FRhL-2) and the virus was subjected to a total of 12 passages and one cloning step through two limiting dilutions in these cells. The master and secondary Candid #1 vaccine seeds were produced by single amplification in FRhL-2 cells and the secondary seed was used to generate the Candid #1 vaccine stock (Ambrosio et al., 2011). The efficacy and safety of Candid #1 was extensively tested in mice, guinea pigs, and rhesus monkeys (McKee et al., 1992; Medeot et al., 1990) before human clinical trials that involved over 6,500 volunteers were initiated in AHF-endemic regions of Argentina (Maiztegui et al., 1998). These studies demonstrated high immunogenicity and protective efficacy (≥ 84%) of Candid #1 in humans and the absence of serious adverse effects associated with vaccination (Maiztegui et al., 1998). At present, Candid #1 is the only vaccine against AHF that has been fully

licensed in Argentina and used to vaccinate over 250,000 people residing in endemic regions in the last few decades.

Other Vaccine Preparations

Several vaccine preparations including purified viral proteins, inactivated virions and vectored sub-unit vaccines have been evaluated for the ability to induce JUNV-specific immune response and protect experimentally infected animals against lethal challenge. Thus, sub-viral components were extracted from purified JUNV particles by treating with nonionic detergent to disrupt the envelope membrane. Only the soluble fraction that contained viral glycoproteins induced production of neutralizing antibodies in injected laboratory animals that were completely protected against subsequent lethal challenge (Cresta et al., 1980). Inactivated JUNV has also been tested for immunogenicity and protective ability in laboratory animals. Formalin-inactivated preparations of XJCl3 strain of JUNV were used to immunize guinea pigs. Injection of the whole inactivated virions resulted in production of high titers of neutralizing antibodies against homologous virus. However, no protection was achieved against the virulent strain of JUNV (Videla et al., 1989). These data suggests that alternative methods of antigen preparation or vaccine delivery routes are required to elicit fully protective immunity. This hypothesis was later supported by the results from a study that employed an alphavirus-based replicon system expressing the envelop glycoproteins (GPC) of the live-attenuated Candid #1 strain of JUNV. Thus, immunization of guinea pigs with a single dose of the alphavirus-packaged replicon expressing only viral GPC resulted in partial protection against challenge with a lethal dose of the virulent Romero strain of JUNV, whereas animals that received a booster vaccination were completely protected against the challenge (Seregin et al., 2010). Therefore, these results indicate

that GPC is a minimal viral antigen required to induce protective immune response against lethal JUNV infection.

Therapeutics

Immunotherapy with plasma from AHF patients in convalescence is currently the standard treatment available in AHF endemic regions. The use of immune plasma reduced the mortality rate from AHF from historical 15-30% to 1-2% when administered within the first 8 days after the onset of clinical disease. Interestingly, 8-10% of patients develop a late neurologic syndrome (LNS) after treatment with immune therapy. LNS is associated with a number of symptoms including fever, ataxia, nystagmus, cerebellar tremors, cranial nerve palsies, and gait lateralization resulting in abnormal walking patterns, and has never been observed in cases where the infection was resolved naturally (Maiztegui et al., 1979).

Purified IgG from fractions of immune plasma were evaluated for the ability to neutralize JUNV and protect infected guinea pigs. Thus, purified fractions containing IgG1, 2, 4, as well as IgG1, 2, 3, 4 and F(ab')2 were shown to neutralize JUNV. However, treatment with 6,000 therapeutic units (TU) of the F(ab')2 fraction did not provide protection to lethally infected guinea pigs. In contrast, similar doze of IgG1, 2, 4, of IgG1, 2, 3, 4 fraction completely protected all experimental animals (Kenyon et al., 1990). These data suggest that neutralization of infectious JUNV is essential, although, may be not sufficient for *in vivo* protection.

Currently, the only approved drug for therapeutic treatment of arenavirus infections is Ribavirin. This nucleoside analog has been clinically proven effective against several viral diseases (Parker, 2005). Efficacy tests in rhesus macaques demonstrated that disease was prevented when the animals were administered Ribavirin at the time of challenge; however, when the treatment was started 6 days after infection,

only delayed time to death was achieved (Stephen et al., 1980). Similar results were obtained in JUNV-infected guinea pigs. Subcutaneous administration of Ribavirin resulted in inhibited viral replication and increased survival times. Interestingly, no significant differences in survival rates were observed when daily treatment was initiated on the day of challenge or 7 days after. However, all the animals still ultimately succumbed to infection regardless the route of inoculation shortly after the treatment was stopped on day 24 (Kenyon et al., 1986a). Long-term treatment with Ribavirin was demonstrated to statistically increase survival of lethally infected guinea pigs (Salazar et al., 2012). Despite the controversial data from animal experiments, Ribavirin has been successfully used to treat AHF patients when the therapy started shortly after the infection (Weissenbacher et al., 1987).

ANIMAL MODELS OF AHF

Natural Rodent Host

The natural rodent reservoir host of JUNV, *Calomys musculinus*, may develop a lifelong persistent infection, which supports the maintenance of the virus in nature. The chronically infected rodents shed infectious virus through urine, saliva, and feces. Besides its primary host, JUNV has also been occasionally isolated from *Calomys laucha*, *Akodon azarae*, and *Oryzomys flavescens* rodents (Sabattini and Maiztegui, 1970). Interestingly, upon intranasal inoculation at birth, *C. musculinus* animals did not develop any symptoms of neurologic disease; however, 70% of the animals died. In survivors, infectious JUNV was consistently recovered from blood, urine, and oral swab between days 14 and 480 of the observation period. By the end of study, all animals developed viral dissemination to brain, spleen, kidneys, and salivary glands. The persistently infected rodents demonstrated a marked reduction of fertility (13.3% vs. 60% in the control group). These findings suggested that the maintenance of JUNV in its host

rodent population is largely mediated by horizontal rather than vertical transmission mechanisms (Lampuri et al., 1982; Vitullo et al., 1987).

Horizontal transmission is currently considered to be the central mechanism of JUNV dissemination (Sabattini et al., 1977). Analysis of the genetic structure of *C. musculinus* populations in the geographic locations endemic for AHF revealed a high degree of genetic subdivision that indicated that these rodents colonized their current habitat areas fairly recently (Chiappero and Gardenal, 2003). Thus, the observed expansion of AHF-affected areas is possibly due to the spread of *C. musculinus* to new geographic location, which may allow the virus to infect other susceptible rodent species. Another possible reason may be rapid conversion of the humid pampas in the central regions of Argentina to farmlands, which may promote expansion of the rodent population into the developed cornfields and grassy areas surrounding fence lines.

Mice

Recently, mice that have deficiencies in the innate system signaling pathways have been shown to be susceptible to JUNV infection and to develop lethal disease (Kolokoltsova et al., 2010). This report is in line with the experimental data published by other groups showing that the fatal encephalitis in newborn mice after intracranial inoculation with JUNV was not observed in athymic and neonatally thymectomized animals, as well as in mice that were treated with immunosuppressive drugs (Giovanniello et al., 1980; Gómez et al., 2011). These results strongly suggest the involvement of immunological mechanisms in pathogenicity and clearance of JUNV infection in laboratory mice (Weissenbacher et al., 1975).

Intracranially infected, immunocompetent laboratory adult mice do not show any specific disease symptoms despite the development of high titers of JUNV in the brain. However, adult mice of C3H/HeJ strain that lack functional toll-like receptor 4 (TLR-4)

that mediates pathogen recognition and activation of innate immunity developed lethal disease upon intracranial infection with XJ strain of JUNV. Infection resulted in high mortality with undetectable neutralizing antibody response and a delayed-type hypersensitivity reaction. Interestingly, these mice were not susceptible to infection by any other route of virus injection (Campetella et al., 1988).

The use of mouse models allowed to investigate many aspects of protective immunity and pathogenesis associated with JUNV infection. Thus, T lymphocytes were shown to play an important role in the development of neurological symptoms and ultimately lethal outcome. Importantly, fatal encephalitis observed in JUNV-infected mice is of immunopathological nature and is not caused by direct cellular damage from infection, since in mouse brain cells JUNV infection is non-cytophatic. On the other hand, T cells were essential for the stimulation of antibody production and clearance of infectious virus (Nota et al., 1976). T cell-dependent immunopathogenesis shown experimentally was proposed to be specific only to mice and no other species including humans. In humans, the increase in neutralizing antibody titers during viremia is thought to control viral spread and confer protection. JUNV infection in susceptible mice, which can only induce disease development through intracranial inoculation, on the other hand, induces a delayed-type hypersensitivity immune response. In contrast, BALB/c mice that are naturally resistant to JUNV activate contrasuppressor cells that inhibit induction of delayed-type hypersensitivity reaction to infection (Campetella et al., 1990). Therefore, although studies in mice produced very important data, these findings cannot be directly translated to human cases of JUNV infection.

Importantly, JUNV utilizes human transferrin receptor 1 (TfR1) for the entry and the lack of the appropriate receptor in mice might explain its reduced virulence in this species (Radoshitzky et al., 2007). However, JUNV can efficiently infects cells of mouse origin via an TfR-1-independent mechanism and induce induction of innate immune response (Cuevas et al., 2011). These results suggest that the entry mechanism of JUNV

virus into mouse cells differs from the mechanism that the virus utilizes to enter human cells.

Nonhuman Primates

Depending on the species JUNV can induce a disease in NHPs that resembles human AHF. Marmosets are highly susceptible to JUNV and succumb to a disease with hemorrhagic and neurologic manifestations within 3 weeks of infection (Weissenbacher et al., 1979). Similarly to humans, treatment of infected animals with immune serum may cause the LNS (Weissenbacher et al., 1986). Experimental infection of marmosets with TACV induced a cross-reactive immune response against JUNV that protected the challenged animals up to 60 days after TACV infection (Weissenbacher et al., 1982). Similar cross-protection after TACV infection that was mediated by neutralizing antibodies and lasted for at least 16 months was demonstrated using different inoculation routes (Samoilovich et al., 1988; Samoilovich et al., 1984). Live-attenuated Candid #1 strain of JUNV has been demonstrated safe, immunogenic, and protective against lethal challenge with a virulent strain of JUNV in rhesus monkeys (McKee et al., 1992; McKee et al., 1993).

Guinea Pigs

Disease induced by JUNV infection in guinea pigs can vary significantly depending on the virus strain. Two major patterns of disease were described in a study that used JUNV strains that differed in their virulence. One group of JUNV strains was viscerotropic in guinea pigs and predominantly replicated in lymph nodes, spleen, and bone marrow. In most severe cases the animals became viremic, developed necrosis of the spleen, lymph nodes, and bone marrow, showed gastric hemorrhages, and died within the first two week after infection. Second group of virulent strains caused a neurological

Characteristic	Symptom	Human†	Guinea pig
Disease phase			
Acute			
	Fever	+	+
	Myalgia	+	Unknown
	Malaise	+	Unknown
	Dizziness	+	Unknown
	Tremors	+	+
	Petechiae	+	–
Severe			
	Shock	+	+
	Mucosal hemorrhage	+	+
	Coma	+	+
	Convulsion	+	+
	Death	+	+
Hematology			
	Leukopenia	+	+
	Thrombocytopenia	+	+
Clinical biochemistry			
	Proteinuria	+	Unknown
	Elevated AST	+	+
	Hypercholesteremia	Unknown	Unknown

Table 1.1. Comparative Clinical Presentation in Humans with AHF Versus Guinea Pigs Infected with Romero Strain. AST, aspartate aminotransferase. Adapted with permission from (Yun et al., 2008).

disease with only transient replication in spleen and lymph nodes accompanied by lymphocyte depletion in these organs. No viremia or viral replication in bone marrow was detected. However, viral replication in the brain subsequently resulted in polioencephalitis of different severity. Many guinea pigs developed rear leg paralysis before succumbing to disease around day 30 post-infection. Interestingly, one virulent strain induced a disease in inoculated guinea pigs that exhibited signs and manifestations characteristic of both hemorrhagic and neurologic disease patterns (Kenyon et al., 1988).

In contrast with JUNV-infected mice, treatment with immunosuppressive drugs did not improve the survival of guinea pigs infected with a virulent strain of the virus. On the other hand, immunosuppression of guinea pigs infected with an attenuated strain of JUNV resulted in a fatal AHF-like disease. These findings emphasized the importance of the presence of a competent immune response required for the clearance of JUNV infection in guinea pigs (Kenyon et al., 1985).

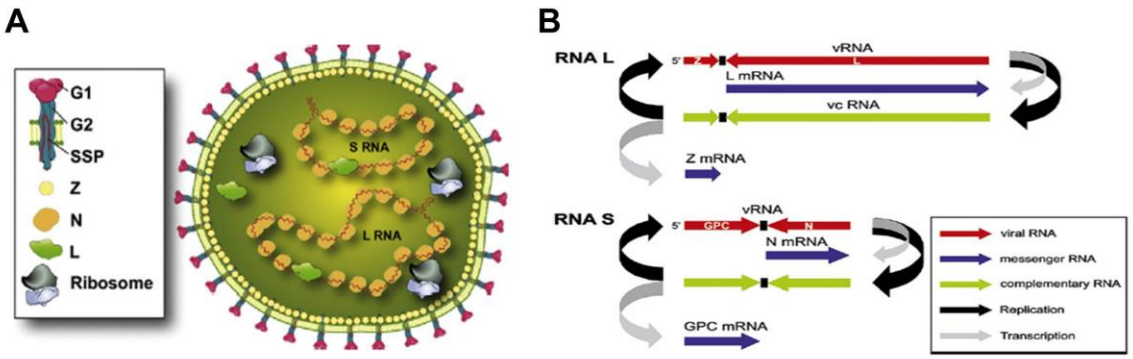

Figure 1.4. Virion structure (A) and genome organization (B) of arenaviruses. G1 and G2, envelope glycoproteins 1 and 2. SSP, stable signal peptide. Z, matrix protein Z. N, nucleoprotein. L, viral polymerase. Adapted with permission from (Gómez et al., 2011).

Romero strain of JUNV is highly virulent in inbred Strain 13 and outbred Hartley guinea pigs, and induces a disease that closely mimics human AHF (Table 1.1). Similarly to infected human patients, Hartley guinea pigs infected with JUNV Romero developed a systemic infection with viremia, thrombocytopenia, leukopenia, elevated concentration of aspartate aminotransferase in serum, and ultimately succumbed to infection between days 13 and 17 post-challenge (Yun et al., 2008). Thus, infection of Hartley guinea pigs with Romero strain of JUNV is a relevant animal model of human AHF that can be used in pathogenesis studies and preclinical development of vaccines and antivirals.

VIRION STRUCTURE AND GENOME ORGANIZATION

Arenaviruses have pleomorphic virions with the diameter ranging from 40 to more than 300 nm (110-130 nm on average) (Murphy and Whitfield, 1975). The arenavirus genome that consists of two single-stranded RNA segments, small (S) and large (L), is enclosed in a nucleocapsid that is coated by a bi-lipid envelope, which includes viral glycoproteins (Fig. 1.4A). The interior of the virions has a granular appearance on electron micrographs due to the presence of cellular ribosomes. It is yet unknown whether incorporation of ribosomes plays any specific role in the arenavirus replication cycle; however, since this phenomenon is highly characteristic for all

arenaviruses, it served as the basis for the virus family name (arenosus = sandy) (Buchmeier, 2013).

Both genomic segments utilize an ambisense coding strategy to encode two genes that are expressed in opposite orientation (Fig. 1.4B). The L RNA segment (~7 kb) encodes the viral RNA-dependent RNA polymerase (LP) that replicates and transcribes viral RNA genome and a small zinc-binding RING finger protein (Z) that the arenavirus analog of the matrix protein of segmented negative-sense RNA viruses and has multiple functions in the viral replication cycle including formation and budding of virions from the plasma membrane, negative regulation of the activity of the viral replication complex, and modulation of the host cell response to infection. The S RNA segment (~3.4 kb) encodes the glycoprotein precursor (GPC) and the nucleoprotein (NP). GPC is co- and post-translationally processed by cellular proteases to yield two glycoproteins GP1 and GP2, and the stable signal peptide (SSP) that form GP1/GP2/SSP glycoprotein complexes on mature virions and mediate virion attachment to target cells and internalization. NP is the most abundantly present viral protein in both infected cells and virions. NP serves as an essential co-factor for LP and blocks recognition of viral RNA replication by the cellular anti-viral defense mechanisms (Buchmeier, 2013).

REPLICATION AND EXPRESSION OF ARENAVIRUS GENOME

Replication and transcription of the arenavirus genome is mediated entirely by a large viral RNA-dependent RNA polymerase (RdRp), L polymerase (LP), that is ~ 250 kDa in size. An active unit of arenavirus RNA synthesis is formed by the L polymerase associated with the viral ribonucleoprotein (RNP) that consists of the viral RNA encapsidated by NP. The catalytic center of the arenavirus polymerase contains the classical SDD motif that is found in all RdRps of segmented negative sense RNA viruses (Buchmeier, 2013).

Synthesis of viral RNA is initiated from a 19-nucleotide promoter sequence located at the 3'-end of genomic (gRNA) and antigenomic (agRNA) L and S segment RNA species. This sequence is required for binding by the viral polymerase and is highly conserved among all arenaviruses, which suggests that the mechanism of viral RNA synthesis initiation is preserved throughout the virus family (Kranzusch et al., 2010). Since the most terminal 19 nucleotides on the 5'- and 3'-ends of both segments exhibit a high degree of complementarity, these sequences were predicted to form panhandle structures (Salvato and Shimomaye, 1989).

Upon infection and delivery of the viral RNP and LP into the cytoplasm, the initial round of transcription results in the synthesis of mRNA for NP and LP from the S and L segments, respectively, that are encoded in antigenomic orientation (Fig. 1.4B). Termination of primary transcription occurs at the stem-loop structures located within the intergenic regions (IGR) of both segments. Theses secondary RNA structures were proposed to stabilize the 3'-termini of the viral mRNAs (Franze-Fernandez et al., 1987; Meyer and Southern, 1993). Arenavirus mRNA is capped and non-polyadenylated. Cap structures are removed from cellular mRNA by a cap snatching mechanism that is mediated by the cap-binding activity of NP and the endonuclease activity of the L polymerase (Lelke et al., 2010; Morin et al., 2010; Qi et al., 2010). To produce full-length agRNA, the polymerase moves across the IGR, by yet unknown mechanism, and proceeds to the 5'-end of gRNA. The S and L agRNA serve as templates for the synthesis of mRNA for GPC and Z, respectively, that are encoded in genomic orientation (Fig. 1.4B) and full-length S and L gRNA (Buchmeier, 2013).

The polymerase of arenaviruses (LP) incorporates a non-template G residue at the 5'-end of gRNA and agRNA species (Garcin and Kolakofsky, 1990). According to the "prime and realign" mechanism of replication initiation that was proposed by Garcin and Kolakofsky for TACV (Garcin and Kolakofsky, 1990), the viral L polymerase first synthesizes a $_{PPP}G_PC_{OH}$ primer from the nucleotides at positions 2 and 3 (CG) of the viral

19-nucleotide promoter sequence at the 3'-end of gRNA and agRNA. Then, the primer is shifted by two nucleotides such that its 3'-terminal C_{OH} aligns with the 1st nucleotide (G) at the 3'end of the viral genome. The realigned $_{PPP}G_PC_{OH}$ then primes the synthesis of a complementary RNA strand (Garcin and Kolakofsky, 1992; Marq et al., 2010).

The (equivalent to) matrix protein Z of arenaviruses is not required for the assembly of the viral replication complex and initiation of RNA synthesis, but rather serves as a potent viral regulator of the L polymerase activity. Thus, Z was demonstrated to inhibit viral RNA synthesis in a dose-dependent manner (Cornu and de la Torre, 2001, 2002; Cornu et al., 2004). Z was shown to bind and lock the viral polymerase in a promoter-bound state, which prevented RNA synthesis initiation. This mechanism was also proposed to be involved in the packaging of the L polymerase into the viral particles (Kranzusch and Whelan, 2011). The dose-dependent inhibitory effect of Z on the catalytic activity of the viral polymerase has been demonstrated for both New World (Lopez et al., 2001) and Old World (Hass et al., 2004) arenaviruses.

GLYCOPROTEINS AND THE ROLE OF ENDOPLASMIC RETICULUM STRESS IN ARENAVIRUS ATTENUATION

Old World arenaviruses and New World Clade C arenaviruses use α-dystroglycan (α-DG) as a receptor for entry into target cells (Cao et al., 1998; Spiropoulou et al., 2002). The function of the transmembrane α-DG in normal cells is to connect the actin cytoskeleton to the extracellular matrix. Although α-DG is considered to be the main receptor for this group of viruses, four alternative receptors including two C-type lectins DC-SIGN and LSECtin, and two membrane tyrosine kinases Tyro3 and Axl have been shown to be utilized by LASV and LCMV for α-DG-independent entry (Shimojima and Kawaoka, 2012; Shimojima et al., 2012). The transferrin receptor 1 (TfR1) that mediates the transport of iron ions into vertebrate cells (Aisen and Listowsky, 1980) has been

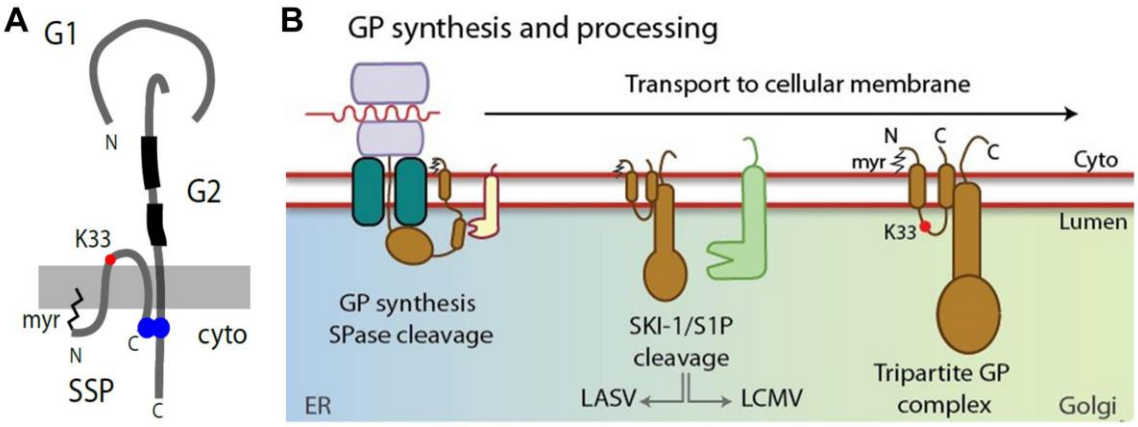

Figure 1.5. Schematic of the envelope glycoprotein complex of arenaviruses (A) and biosynthesis of GPC. A detailed description is provided in the text. Reproduced with permission from (Nunberg and York, 2012) (A) and (Burri et al., 2012) (B).

identified as a primary receptor for the entry of Clade B New World arenaviruses, including JUNV, into mammalian cells (Radoshitzky et al., 2007). Interestingly, all Clade B viruses bind to their host rodent species TfR1 receptors, but only those pathogenic for humans can also efficiently recognize human TfR1 (Abraham et al., 2010; Abraham et al., 2009; Radoshitzky et al., 2008). In addition, previous studies indicate that at least JUNV can also infect cells via a TfR1-independent pathway (Kolokoltsova et al., 2010). The cellular receptor for the Clade A New World arenaviruses has not yet been identified. Upon receptor binding mediated by G1 (Fig. 1.5A), arenaviruses are internalized via endocytosis, which is clathrin-dependent in the case of New World (Martinez et al., 2007) and clathrin-independent in the case of Old World arenaviruses (Borrow and Oldstone, 1994; Kunz, 2009; Quirin et al., 2008). Transmembrane fusion between the viral envelop and the late endosome mediated by G2 (Fig. 1.5A) is strictly dependent on low pH environment. Upon the delivery of viral RNP into the cytoplasm, viral genome replication and gene transcription is initiated by the L polymerase complex in discrete arenavirus-specific cytosolic structures that are associated with cellular membranes (Baird et al., 2012).

The arenavirus GPC consists of three subunits, SSP, G1, and G2 that are co- and post-translationally processed by cellular proteases (Fig. 1.5B) (Buchmeier, 2013). The

SSP of arenaviruses has several properties and features that distinguish it from signal peptides of other viruses. Conventionally, SSP drives the nascent GPC polypeptide into the endoplasmic reticulum (ER) lumen during synthesis on ribosomes. Co-translational cleavage of GPC by cellular signal peptidases results in the production of a 58 amino acid long signal peptide that, in contrast to standard signal peptides, has two transmembrane domains. Therefore, both the N- and C-terminal ends of SSP reside in the cytosol, and the central hydrophilic loop facing the ER lumen/extracellular space (Agnihothram et al., 2007; Eichler et al., 2003; Froeschke et al., 2003; York et al., 2004). The central domain contains a highly conserved lysine residue at position 33 that has been demonstrated to play an important role in pH-mediated fusion of the glycoprotein complex with the cell membrane (York and Nunberg, 2006; York and Nunberg, 2009). The SSP stays associated with the G1-G2 glycoprotein complex on mature virions, which is thought to occur through a zinc-mediated interaction between the C terminus of SSP and the G2 subunit (Agnihothram et al., 2006; York and Nunberg, 2007; York et al., 2004). SSP is myristoylated at the N-terminal glycine that is important for the fusogenic activity but not formation of the glycoprotein complex (York et al., 2004). For JUNV, SSP was shown to trigger export of the G1-G2 precursor from the ER by masking ER-retention signals in the cytoplasmic domain of G2 (Agnihothram et al., 2006). The G1-G2 precursor is cleaved into the G1 and G2 subunits in the Golgi compartment by the cellular proprotein convertase Subtilisin Kexin Isozyme-1 (SKI-1)/Site-1 Protease (S1P) (Beyer et al., 2003; Lenz et al., 2001b; Rojek et al., 2008). This enzyme resides in the early Golgi in uninfected cells and mediates proteolytic processing of the CREB/ATF family of transcription factors, including ATF6, that are involved in the unfolded protein response (UPR) (Elagoz et al., 2002; Schröder, 2008; Ye et al., 2000). The G1-G2 cleavage sites of arenavirus GPCs show a high degree of similarity to the SKI-1/S1P auto-processing motifs (Pasquato et al., 2011). Autologous proteolysis of the inactive zymogen is required for the maturation of SKI-1/S1P (Espenshade et al., 1999). The mimicry of the SKI-

1/S1P auto-processing is thought to allow arenaviruses to minimize interference with the cellular functions of SKI-1/S1P, which, on the other hand, may facilitate the establishment of persistent infection in their natural rodent hosts (Burri et al., 2012). Interestingly, disruption of G1-G2 processing does not abolish the transport of uncleaved GPC to the plasma membrane; however, only correctly processed G1 and G2 subunits are incorporated into the nascent virions (Damonte et al., 1994).

N-linked glycosylation is an essential process that controls correct processing, folding and intracellular transport of viral envelope glycoproteins. To ensure correct folding glycoproteins may undergo multiple glycosylation/deglycosylation events that are followed by folding quality screening by the cellular control mechanisms (Braakman and Van Anken, 2000). Thus, mutation of some glycosylation sites prevented proteolytic processing and maturation of the arenavirus glycoprotein complex (Bonhomme et al., 2011; Eichler et al., 2006). Overloading ER with unfolded protein to the levels that exceed the ER's folding capacity or accumulation of misfolded protein causes a condition that is called "the ER stress". To restore folding processivity a set of intracellular pathways, that are collectively called the unfolded protein response (UPR), is activated to resolve the stress conditions (Schroder and Kaufman, 2005). In mammalian cells, the primary sensor of ER stress conditions is the ER-resident chaperon immunoglobulin heavy chain binding protein BiP/GRP78. In inactive state, BiP forms oligomeric complexes. In the presence of ER stress, BiP complexes dissociate and the monomers bind unfolded or misfolded proteins (Schröder, 2008). Conversion of BiP from oligomeric to monomeric state also triggers expression of its gene (Freiden et al., 1992). In non-stress conditions, BiP also binds and maintains in inactive state the three ER trans-membrane mediators that transduce the UPR activation signal: the kinase/endonuclease inositol-requiring protein 1 (IRE1), the PKR-like ER kinase (PERK), and the activating transcription factor 6 (ATF6). Binding of BiP to unfolded or misfolded proteins triggers the release and activation of these mediators (Schröder, 2008). Upon dissociation of BiP,

PERK undergoes homodimerization and trans-autophosphorylation. The activated PERK then phosphorylates the eukaryotic translation initiation factor 2α (eIF2α), which blocks the assembly of functional ribosomes and inhibits cap-dependent translation of mRNA to prevent further accumulation of nascent proteins in the ER lumen. However, phosphorylation of eIF2α stimulates the expression of certain transcription factors, such as ATF4, that can lead to the activation of apoptosis, which is largely mediated by the pro-apoptotic transcription factor CHOP in cases where ER stress cannot be resolved (Ohoka et al., 2005; Yamaguchi and Wang, 2004). The release of BiP triggers dimerization and autophosphorylation of IRE1 that activates its endoribonuclease activity. Upon activation, IRE1 removes a 26-nucleotide intron from mRNA encoding the X-box-binding protein 1 (XBP1). The spliced form of XBP1 mRNA encodes a transcription factor that activates expression of many UPR target genes (Schröder, 2008). Activation of ATF6 is mediated by translocation to the Golgi apparatus of BiP-free ATF6 where it is first proteolytically processed by the SKI-1/S1P at the luminal side of ER membrane followed by the cleavage by the metalloprotease site 2 protease (S2P) at the cytoplasmic side of ER membrane. This enzymatic reaction releases an N-terminal fragment of ATF6 (ATF6 p50) into the cytosol. ATF6 p50 then translocates to the nucleus and contributes to the activation of UPR genes, including BiP and CHOP (Schröder, 2008; Zhang and Kaufman, 2006). The comparison between acute and persistent infection of cultured cells with LCMV, revealed that during acute infection, expression of the viral glycoproteins selectively activated the ATF6-controlled branch of the UPR, while the PERK and IRE1 pathways remained inactive. During persistent LCMV infection, when expression of the GPC was downregulated, all branches of the UPR were silent. Interestingly, induction of the ATF6 pathway was required for optimal production of infectious LCMV particles during acute but not persistent infection (Pasqual et al., 2011).

MANIPULATION OF ARENAVIRUS GENOME

Segment Reassortment

Since the genome of arenaviruses consists of two segments, simultaneous co-infection of cells with two viruses may lead to the production of progeny virions containing genomes originated from both parental viruses. This methodology has been utilized to generate reassortant viruses between different strains of the same virus, such as PICV and LCMV (Kirk et al., 1980; Riviere et al., 1985; Zhang et al., 2001), as well as between different, though closely related viruses, such as Lassa (LASV) and Mopeia (MOPV) (Lukashevich, 1992). The reassortment approach has been used to define the function of viral proteins in arenavirus pathogenesis (Riviere et al., 1986), arenavirus-induced immunosuppression (Matloubian et al., 1993; Matloubian et al., 1990), and to generate live-attenuated vaccine candidates (Lukashevich et al., 2008; Lukashevich et al., 2005). Although, this technique can be used as a valuable tool to study different aspects of arenavirus biology, it does not allow introduction of specific mutations to alter the function of viral proteins and regulatory genetic factors. In addition, generation of reassortants involves tedious cloning and selection procedures and is often associated with the problem of poor genetic stability and purity of the resulting viruses (Lukashevich, 1992).

Minigenome Systems

To facilitate investigation of the arenavirus replication machinery, minigenome (MG) constructs have been developed based on the S segment of the genome where the viral genes were replaced with reporter genes, often either firefly luciferase (FLuc) or chloramphenicol acetyltransferase (CAT). The first MG system was developed for the prototypic Old World arenavirus LCVM (Lee et al., 2000). Subsequently, MG constructs were generated for other arenaviruses including LASV and JUNV that cause hemorrhagic

fevers in humans (Albariño et al., 2009; Hass et al., 2004; Lan et al., 2009; Lopez et al., 2001; Patterson et al., 2014). The use of MG systems allowed to discover that NP and L polymerase are the minimal trans-acting factors required to initiate RNA synthesis from viral MG templates (Hass et al., 2004; Lee et al., 2000; Lopez et al., 2001). *In vitro* activity assays based on MG systems led to identification of several conserved amino acid residues within the N- and C-terminal domains of LASV polymerase that are essential for viral mRNA synthesis but not replication of genome RNA segments (Hass et al., 2008; Lelke et al., 2010). Analysis of the 5'- and 3'-termini of LASV and LCMV MG constructs by site-directed mutagenesis revealed a sequence specific region from nucleotide 1 to 12 and a variable region from nucleotide 13 to 19 of the viral promoter and that complementarity between the 5'- and 3'-terminal 19 nucleotides of each genome segment is required for viral transcription and replication (Hass et al., 2006; Perez and de la Torre, 2003). In addition, experiments performed using an LCMV MG system provided direct conformation that the intergenic region (IGR) of the S RNA segment serves as a termination signal for viral mRNA transcription (Pinschewer et al., 2005).

Generation of Recombinant Arenaviruses

Reverse genetics systems for the virus rescue from cDNA clones have been developed for several arenaviruses, including LCMV (Flatz et al., 2006), PICV (Lan et al., 2009), LASV (Albariño et al., 2011a), and JUNV (Albariño et al., 2009). All reported rescue systems are either based on the bacteriophage T7 RNA polymerase (T7RP) promoter or the eukaryotic RNA polymerase I (pol-I) promoter to direct the intracellular synthesis of genome RNA segments, S and L, in either genomic or antigenomic orientation. The synthesized segments are subsequently encapsidated by the viral NP and replicated by the viral L polymerase expressed from the RNA polymerase II (pol-II) promoter-driven plasmid constructs (Fig. 1.6). Recombinant arenaviruses rescued using

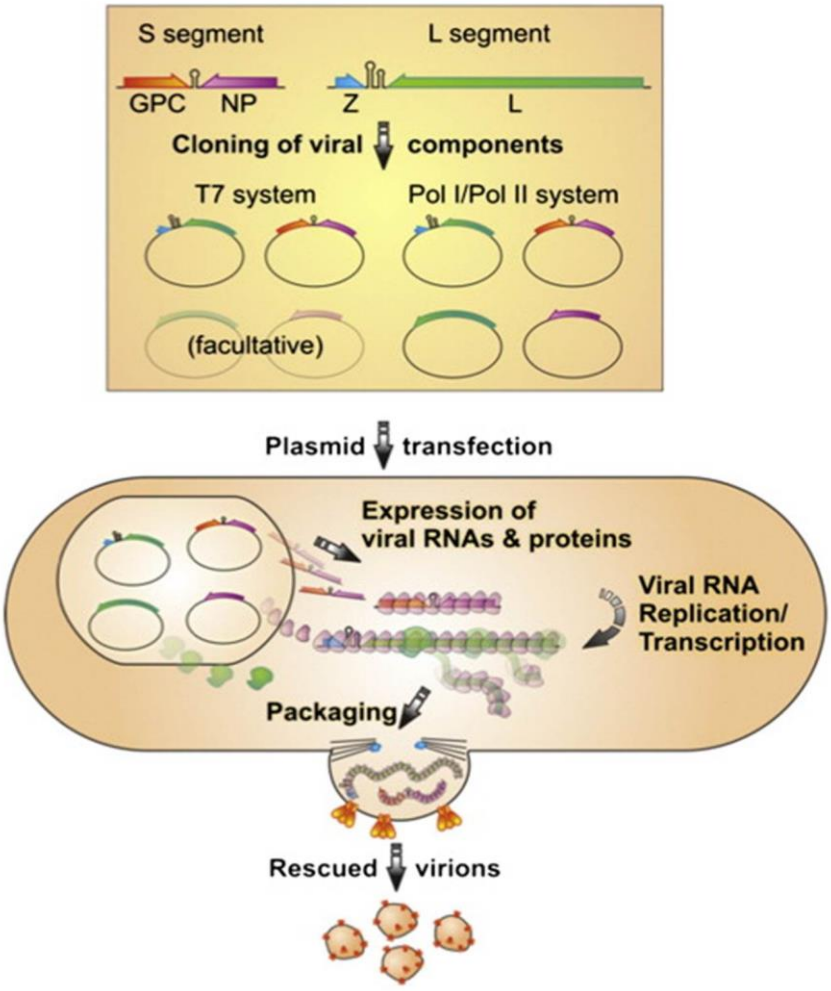

Figure 1.6. Reverse genetics systems for the rescue of arenaviruses from cDNA. A detailed description is provided in the text. Reproduced with permission from (Emonet et al., 2011a)

both T7RP and pol-I systems exhibit similar phenotypic properties both in cultured cells and experimental animals.

Notably, the rescue of arenaviruses from T7RP-based systems does not require co-expression of NP and L polymerase (Albariño et al., 2009; Albariño et al., 2011a), indicating that T7RP-mediated RNA synthesis produces both full-lengh viral segment RNA species and mRNA for NP and L polymerase at the levels sufficient for virus rescue (Fig. 1.6). However, the cells have to be co-transfected with a T7RP expression plasmid or a cell line that stably expresses T7RP has to be used to ensure the synthesis of the genome RNA segments from the T7RP promoter-driven cDNA templates. Since, any

alterations within the viral 19-nucleotide promoter sequence severely affect its activity (Hass et al., 2006; Perez and de la Torre, 2003), the authentic 3'-termini of both genome RNA segments are generated by the hepatitis delta virus (HDV) ribozyme preceding the T7RP termination sequence (Sánchez and de la Torre, 2006). There are several limitations that can negatively affect the efficiency of virus rescue when a T7RP system is used that have to be taken into the account including variability in the ribozyme cleavage efficiency in different cell lines and activation of type I IFN response via intracellular RIG-I-mediated detection of the 5' triphosphate groups of T7RP transcripts that can significantly diminish the efficiency of rescue of recombinant viruses with increased sensitivity to type I IFN (Emonet et al., 2011a; Habjan et al., 2008).

An alternative reverse genetics system to the T7RP system is based on the synthesis of the genome RNAs from plasmid constructs by the RNA pol-I (Fig. 1.6), which is localized in the nucleus of the eukaryotic cell and directs the synthesis of the large ribosomal RNA (rRNA) precursor that is subsequently cleaved into 5.8S, 18S, and 28S rRNA (sizes of human subunits)(Comai, 2004). Arenavirus RNA species synthesized by pol-I are efficiently exported into the cytoplasm and are active in cytoplasmic transcription and replication driven by the viral polymerase complex (Pinschewer et al., 2003). Pol-I promoters are highly species-specific, which limits their use for the purpose of arenavirus rescue to cell lines that were originated from either the same or closely related species of animals. On the other hand, pol-I termination signals terminate transcription very precisely between the last nucleotide of the transcribed construct and the first nucleotide of the terminator sequence that eliminates the need to use ribozymes. Nevertheless, both T7RP and pol-I systems have been successfully used to rescue recombinant arenaviruses with similar efficiencies (Emonet et al., 2011a).

PROJECT AIMS

The live-attenuated Candid #1 strain of JUNV is currently in use to vaccinate human population residing in AHF-endemic regions of Argentina. However, the mechanism of attenuation of this strain still largely remains elusive. Therefore, the identification and functional characterization of viral genetic factors implicated in JUNV pathogenesis or attenuation would significantly improve the understanding of the molecular mechanisms underlying AHF and facilitate the development of novel, effective and safe vaccines.

Specific Aim 1 (Chapters 3 & 4): Develop a reverse genetics system for the rescue of JUNV from cDNA.

1a: Generate cDNA clones for the production of pathogenic Romero and attenuated Candid #1 strains of JUNV.

1b: Generate chimeric JUNV containing different segment or gene combinations between Romero and Candid #1 strains.

An RNA polymerase I/II-based reverse genetics system have been successfully utilized to rescue the prototypic arenavirus LCMV entirely from cDNA (Flatz et al., 2006). Therefore, this approach was used to develop a plasmid-based reverse genetics system for JUNV. This system was further utilized to generate chimeric JUNV variants encoding different gene combinations of pathogenic Romero and attenuated Candid #1 strains of the virus.

Specific Aim 2 (Chapters 3 & 4): Explore the bisegmented genome of JUNV for major pathogenesis factors.

2a: Determine whether the virulence of JUNV has a mono- or polygenetic basis.

2b: Determine the contribution of viral proteins and genetic factors to JUNV pathogenesis.

The G2 subunit of the glycoprotein complex has been identified as an important attenuating factor in a mouse model of lethal intracranial JUNV infection (Albariño et al., 2011b). Using the generated chimeric viruses, the GPC of JUNV was identified as the major pathogenesis and attenuation determinant in a guinea pigs model of lethal infection that closely resembles human AHF (Yun et al., 2008).

Specific Aim 3 (Chapter 5): Investigate the regulation of genome expression and replication during JUNV infection.

3a: Examine the regulation of genome replication by viral genetic factors during JUNV infection.

3b: Determine the role of JUNV genome regulatory elements in the regulation of viral mRNA and protein production in the course of infection.

The transcriptional and protein expression profiles the examined and compared between the chimeric JUNV variants. The GPC of Candid #1 strain of JUNV was demonstrated to undergo abnormal post-translational modification and induce ER stress. The small RING finger protein Z was shown to accumulate in infected cells when it was coexpressed with the GPs of Romero, but not the GPs of Candid #1. Obtained experimental data allowed to propose a model describing a sequence of events that may contribute to the virulent phenotype of Romero and attenuated phenotype of Candid #1 strain of JUNV.

CHAPTER 2: MATERIALS AND METHODS[2]

CELLS, VIRUSES, AND BIOSAFETY

Baby hamster kidney (BHK-21) and Vero cells (American Tissue Culture Collection) were maintained in Dulbecco's modified Eagle's medium supplemented with 10% fetal calf serum and L-glutamine. The wild-type Romero strain of JUNV (GenBank accession no. AY619640 and AY619641) was obtained from Thomas G. Ksiazek (University of Texas Medical Branch [UTMB]). Viral stocks of the Romero and Candid #1 strains were prepared by infecting Vero cells (multiplicity of infection [MOI] 0.01) and collecting virus-containing tissue culture supernatants (TCS) at 72 h postinfection (p.i.), followed by elimination of cell debris by centrifugation (10,000 g for 10 min at 4°C). Work with virulent strains of JUNV and animal experiments were performed in the UTMB biosafety level 4 (BSL-4) facilities in accordance with institutional health and safety guidelines.

SEQUENCING OF FULL-LENGTH S AND L RNA GENOME SEGMENTS FROM ROMERO AND CANDID #1

Sequencing of Candid #1 full-length genome

RNA (0.5 to 1.0 ug) isolated at 72 h p.i. from Candid #1-infected Vero cells was used in two reverse transcription (RT) reactions. One RT reaction was primed with a primer reverse complementary to the conserved 3'-terminal 19 nucleotides (nt) of the S and L genome RNA species, and its cDNA was used to amplify the complete S segment and the 3' half of the L segment. The other RT was primed with a primer reverse

[2] Adapted with permission from Emonet SF*, Seregin AV*, Yun NE, Poussard AL, Walker AG, de la Torre JC, Paessler S. Rescue from cloned cDNAs and in vivo characterization of recombinant pathogenic Romero and live-attenuated Candid #1 strains of Junin virus, the causative agent of Argentine hemorrhagic fever disease. J Virol. 2011 Feb;85(4):1473-83. Epub 2010 Dec 1. (*-equal contribution).

complementary to an internal region of the Candid #1 polymerase gene, and the corresponding cDNA was used for amplification of the 5' half of the L segment. The entire S and L segments were amplified in three and four, respectively, PCRs. PCR products were gel purified using the QIAquick gel extraction kit (Qiagen) and directly sequenced to obtain the corresponding master sequences for the Candid #1 S and L genome RNA species. Sequencing data were analyzed using the program Sequencher 4.9 (Gene Codes).

Sequencing of Romero full-length genome

The complete L and S genome RNA species of Romero were amplified using three and two, respectively, overlapping PCR fragments and procedures similar to those described for Candid #1 and directly sequenced to obtain their corresponding master sequences.

DETERMINATION OF 5' AND 3' TERMINI OF S AND L GENOME RNAS FROM ROMERO AND CANDID #1

To determine the 5' and 3' termini of the S and L RNA segments of Candid #1, total RNA extracted from infected Vero cells was treated with an RNA 5' polyphosphatase (Epicentre), purified using the QIAcube and the RNeasy Minikit procedure, and self-ligated using T4 RNA ligase I. The product of the ligation was purified using the RNeasy Minikit procedure and reverse transcribed using primers JUNGPRev (5'-TCATCAAAGCTGATCTGAAATGAAGCA-3') and JUNZSop (5'-AGCTCTTCGTCATGGTGGTGGTGCTGTTGG-3') for the S and L segments, respectively. The cDNAs were used in PCRs to get products containing the 5' and 3' ends of the S and L segments. The primers for the S segment were JUNGPRev and

JUNNPF1 (5'-CCTCAACTTGTTGAGATCCTCT-3'), and those for the L segment were JUNZSop and XJLR2 (5'-TGGGACATAGTATGCCATGGTCA-3'). Amplified products were cloned into the pCR 2.1 vector using the TA cloning kit (Invitrogen). Multiple individual clones derived from L and S PCR products were sequenced to obtain their corresponding terminal sequences. The 5' and 3' termini of the S and L RNA segments of Romero were determined by 5' and 3' rapid amplification of cDNA ends using the FirstChoice RLM-RACE kit (Ambion) and following the protocol provided by the manufacturer.

PLASMID CONSTRUCTS

Generation of Candid #1 plasmids

The Candid #1 NP was PCR amplified using primers located at the 5' and 3' ends of the open reading frame (ORF) and containing BsmBI restriction sites, gel purified (QIAquick'gel extraction kit; Qiagen), and cloned into pCR2.1 (TA cloning kit; Invitrogen). After sequencing, a clone with the correct insert was digested with BsmBI and the NP gene was introduced into the pCAGGS vector to generate the Candid #1 pC-NP plasmid. Candid #1 pC-L was generated by using a similar strategy but involving a two-step cloning approach in which (i) the first and last thirds of the Candid #1 L polymerase gene were amplified and ligated together via an inserted NotI site and introduced into pCAGGS via BsmBI restriction to generate the intermediate pCAGGS-Candid #1 polymerase vector and (ii) the central part of the L ORF was amplified and inserted into the intermediate pCAGGS-Candid #1 polymerase vector via BstXI restriction sites to create plasmid Candid #1 pC-L. To create a pCAGGS vector expressing the L polymerase of JUNV strain XJ13, six mutations were introduced into the Candid #1 pC-L vector by mutational PCR to recreate the amino acid differences previously reported between the Candid #1 and XJ13 strains (Y76H, A415V, N462D,

P936L, K1156R, and V1883I) (Goni et al., 2006). The NP amino acid sequences of JUNV strains XJ13 and Candid #1 are identical. To generate plasmids containing the full-length S and L genome sequences flanked by the mouse RNA polymerase I (mPol-I) promoter and terminator sequences, the backbones of the Candid #1 S and L segments (5' and 3' untranslated regions, IGR, and cloning sites) were synthesized (Integrated DNA Technologies, San Diego, CA) based on the sequences with GenBank accession numbers AY746353 and AY746354. The extremities were later modified by mutational PCR to reflect either published terminal sequences from XJ13/Romero (NC005081 and AY619641, respectively) or the sequences that were determined in this work. Backbone sequences were introduced into the mPol-I vector pRF42 in antigenomic orientation. Each Candid #1 gene was then introduced after enzymatic restriction to produce the Candid #1 mPol-I-Sag and mPol-I-Lag vectors. For the generation of mPol-I-Sag vectors used for the rescue of r3Candid viruses, genes of interest (the enhanced green fluorescent protein and chloramphenicol acetyltransferase [CAT] genes) were cloned instead of GPC and/or NP into Candid #1 mPol I-Sag as described previously (Emonet et al., 2009).

Generation of Romero plasmids

To generate the Romero mPol-I-Sag and mPol-I-Lag plasmids, the complete S and L segments were amplified in two and three, respectively, PCR fragments. Subsequently, the three L fragments were assembled, using appropriate restriction enzymes, into plasmid pBS-L containing the complete sequence of the L segment that corresponded to the sequence with GenBank accession number AY619640. A similar approach was used to ligate the two S fragments to generate plasmid pBS-S containing the complete sequence of the S segment that corresponded to the sequence with GenBank accession number AY619641. To generate plasmids containing the full-length S and L genome sequences of Romero flanked, in antigenomic orientation, by the mPol-I

promoter and terminator sequences, fragments containing full-length L and S segments were cut out of pBS-L and pBS-S, respectively, and inserted into pRF42 to generate Romero mPol-I-Sag and mPol-I-Lag. Plasmids expressing the NP and L polymerase of the Romero strain of JUNV were generated similarly to the corresponding plasmids of the Candid #1 strain.

ESTABLISHMENT OF AN MG RESCUE ASSAY FOR JUNV

BHK-21 cells (seeded at 3 x 10^5/well of an M12 plate) were transfected with 0.4 ug of pC-NP, 0.6 ug of pC-L, and 0.5 ug of the indicated Candid #1 mPol-I-S to direct intracellular synthesis of the minigenome (MG) RNA of interest. Three days later, assays for either CAT reporter gene expression using cell lysates and the CAT enzymelinked immunosorbent assay kit (Roche) or for Gaussia luciferase expression using the cell supernatant and the Biolux Gaussia kit (New England Biolabs) were performed.

RESCUE OF RROMERO AND RCANDID #1

To rescue rRomero, BHK-21 cells were seeded into 12-well plates at 6 x 10^4/well 1 day prior transfection. Each well was transfected with equimolar amounts of mPol-I-Lag, mPol-I-Sag, pC-LP, and pC-NP, resulting in a total amount of 2 ug of plasmid DNA. Transfections were done using FuGene HD transfection reagent (Roche) by following the standard protocol. The next day, transfected cells were trypsinized and transferred into T75 tissue culture flasks, and 72 later, TCS were harvested. To rescue rCandid #1, subconfluent monolayers of BHK-21 cells (2 x 10^6/well of an M6 plate) were transfected for 5 h by using 2.5 ul of Lipofectamine 2000 (Invitrogen)/ug of plasmid DNA. The plasmid mixture included 1.2 ug of pC-NP and 1.5 ug of pC-L, together with plasmids mPol-I-Lag (2.1 ug) and mPol-I-Sag (1.2 ug). At 3 days posttransfection, cells

in each transfected M6 well were trypsinized and passed into a T75 flask, and 72 h later, virus-containing TCS were collected.

To prepare rRomero and rCandid #1 virion samples for Western blot analysis, aliquots of the viral stocks containing equal amounts of PFU were passed through 0.45 μm pore-size filters (Fisher) to remove cell debris and then purified on the Amicon Ultracel 100K filtering devices (Millipore) with the molecular weight cutoff of 100,000 Da by centrifugation at 4,000g for 20 min at room temperature.

IDENTIFICATION OF GENETIC TAGS INCORPORATED INTO THE GENOMES OF RROMERO AND RCANDID #1

Total RNA isolated from infected Vero cells or brain tissue from inoculated guinea pigs was reverse transcribed, and cDNAs were subjected to PCR using specific primers to amplify fragments of 822 bp (within the L polymerase gene of Romero and rRomero) or 664 bp (within the NP gene of Candid #1 and rCandid #1). The genetic tag in the rRomero genome consisted of a silent change from C to U at nucleotide position 715 within the L segment that was confirmed by sequencing of the 822-bp PCR fragment. The genetic tag in the rCandid #1 genome consisted of two silent mutations within the NP gene (U1263C and C1266U) that created a second NcoI restriction site within the 664-bp PCR fragment of the virus NP. To confirm this genetic tag, the 664-bp PCR product was digested with NcoI and analyzed by agarose gel electrophoresis to reveal one (Candid #1, bands of 308 and 356 bp) or two (rCandid #1, bands of 308, 227, and 129 bp) NcoI restriction sites. The sequences of the primers and detailed PCR protocols are available upon request.

RESCUE OF CHIMERIC JUNV VARIANTS

The mPol-I-Sag and mPol-I-Lag plasmids encoding chimeric S and L segments, respectively, were generated by genetically engineering the open reading frames (ORF) of Candid #1 genes into the Romero genome using appropriate restriction enzymes. Chimeric JUNV variants were rescued in BHK21 cells as described for rRomero and rCandid. To rescue intersegment chimeric viruses containing one RNA segment originated from the genome of Romero and the other from the genome of Candid #1, the corresponding mPol-I-Sag and mPol-I-Lag plasmids were used in combination with the pC-NP and pC-LP plasmids expressing the NP and L polymerase of JUNV Romero.

VIRUS PROPAGATION, GROWTH KINETICS, AND TITRATION

Virus propagation and growth kinetics in cultured cells were done by infecting (MOI = 0.01) Vero cells and collecting TCS at the indicated times. Virus titers in TCS and infected tissues were determined by either plaque assay (Romero and rRomero) or determination of 50% tissue culture infective doses (TCID50; Candid #1 and rCandid #1). For the plaque assay 10-fold dilutions of TCS specimens were added to Vero cell monolayers in six-well culture plates for 1 h at 37°C in an atmosphere of 5% CO2 and then overlaid with minimum essential medium (MEM) containing 5% fetal bovine serum, 1% penicillin-streptomycin (P/E) solution, and 0.5% agarose. Plates were then incubated for 7 days at 37°C, and plaques were revealed by fixation of cell monolayers with formaldehyde, followed by crystal violet staining. Infected tissues were dissected at necropsy and homogenized in MEM containing 1% P/E. Homogenates were clarified by centrifugation, and the supernatants were used for plaque assays as described for TCS specimens. Virus TCID50 were determined using the endpoint dilution assay and the Reed-Muench calculation method. Briefly, 10-fold virus dilutions were used to infect Vero cell monolayers in quadruplicate in a 96-well plate. At 3 days p.i., cells were fixed with 4% formaldehyde in phosphate-buffered saline (PBS) and permeabilized in a 0.3%

Triton X-100–3% bovine serum albumin-PBS solution. The cells were then stained using a mouse monoclonal antibody to NP (IC06-BE10) and an Alexa Fluor 568-labeled anti-mouse second-stage antibody (Molecular Probes). Similar procedures were used to detect viral antigen in infected cells using a mouse monoclonal antibody to either JUNV G1 (GB03-BE08) or NP (IC06-BE10). The following reagents were obtained through the NIH Biodefense and Emerging Infections Research Resources Repository, NIAID, NIH: monoclonal anti-JUNV antibody (clone IC06-BE10; immunoglobulin G, mouse) and monoclonal anti-JUNV antibody (clone GB03-BE08; immunoglobulin G, mouse).

ANIMAL EXPERIMENTS

Ten-week-old female Hartley guinea pigs were purchased from The Charles River Laboratory and housed for at least 7 days in a specific-pathogen-free environment before being used in any experimental procedure. All virus inoculations, including vaccination with rCandid #1, were conducted under BSL-4 conditions in the Robert E. Shope BSL-4 Laboratory, UTMB. All animal studies were reviewed and approved by the Institutional Animal Care and Use Committee at the UTMB and were carried out according to the National Institutes of Health guidelines. Guinea pigs were anesthetized using an isoflurane precision variable-bypass vaporizer prior to virus inoculation by the intraperitoneal route with 10^3 PFU. Standardized recording of death and disease symptoms was performed using the following definitions: encephalitis; development of discoordination, ataxia, or transient seizures with retention of the ability to drink and feed; paralysis; and hind limb (hemiplegic) or quadriplegic paralysis with the inability to reach the feeder or water bottle. The experimental endpoint was set at 21 days, when animals that survived infection were humanely euthanized. Telemetric monitoring of body temperature and measurement of body weight were performed during the course of study. For telemetry, animals were anesthetized and implanted subcutaneously with

BMDS IPTT-300 transponders (chips) obtained from Bio Medic Data Systems, Inc. (Seaford, DE), using a trocar needle assembly. Animals were monitored for signs of infection or transponder migration for 2 days prior to transfer to the BSL-4 facility. Chips were scanned using a DAS-6007 transponder reader (Bio Medic Data Systems, Inc.). Downloading of digital temperature data was performed in accordance with the manufacturer's protocol.

HEMATOLOGIC AND CLINICAL CHEMICAL ANALYSES

Blood was collected from guinea pigs into tubes containing EDTA, and a standard hematologic analysis was performed using the HEMAVET 1700 (Drew Scientific, Inc.) on whole-blood specimens to determine platelet and differential counts, in accordance with the manufacturer's recommendation. Clinical chemical analysis was performed using the ACE Alera Clinical Chemistry System (Alfa Wassermann) according to the manufacturer's instructions.

HISTOPATHOLOGICAL AND IMMUNOHISTOCHEMICAL ANALYSIS

Tissue samples were fixed in 4% buffered formalin for a minimum of 7 days and stored in 70% ethanol for 12 h. The samples were then embedded in paraffin. For histopathology, sections (4 um) were mounted on slides and subjected to standard hematoxylin and eosin (H&E) staining. For immunohistochemical analysis, tissue sections were deparaffinized and rehydrated through xylene and graded ethanol solutions. To block endogenous peroxidase activity, slides were then treated with a solution of Tris-buffered saline containing 0.1% Tween 20, 3% hydrogen peroxide, and 0.03% sodium azide for 15 min, followed by heat antigen retrieval in a water bath at 95°C for 40 min in Dako Target Retrieval Solution, pH 6.1 (Dako Corporation). To block endogenous biotin

reactivity, sequential 15-min incubations with avidin D and biotin solutions (Vector Laboratories) were performed. Subsequently, to prevent nonspecific protein binding, sections were incubated in blocking solution according to the manufacturer's instructions (Histomouse-SP kit; Zymed). For detection of viral antigen in tissue sections, a LASV group hyperimmune ascitic fluid (HIAF) prepared in adult ICR mice was used. This HIAF was provided by Robert Tesh, World Reference Center of Emerging Viruses and Arboviruses at UTMB. This HIAF contained cross-reacting antibodies to JUNV and recognized viral antigens in sections from paraffin-embedded tissue. Tissue sections were incubated for 60 min with HIAF at a 1:500 dilution in antibody diluent solution (BD Pharmingen). Tissue sections from uninfected guinea pigs were used as a negative control for immunostaining. As an additional negative control, tissue sections from Junin-infected guinea pigs were incubated with diluent alone. To detect HIAF bound to Junin antigen in guinea pig tissue, the Histomouse-SP kit (Zymed) biotinylated secondary antibody was used, followed by streptavidinperoxidase. Color development was achieved by using the chromogenic substrate according to the manufacturer's instructions. Slides were counterstained with Mayer's modified hematoxylin for microscopy.

WESTERN BLOTTING

Infected or transfected cells were harvested in the Laemmli's SDS loading buffer (65.8 mM Tris-HCl, pH 6.8, 2.1% SDS, 26.3% (w/v) glycerol, 0.01% bromophenol blue, 10% β-mercaptoethanol) (Bio-Rad). The samples were boiled at 95 ^{0}C for 5 min prior to fractionation by SDS-PAGE in 4-15% Mini-Protean TGX gels (Bio-Rad). Proteins were transferred to polyvinyl difluoride (PVDF) membranes using the Trans-Blot Turbo electrotransfer system (Bio-Rad) according to the manufacturer's protocol. After transfer, the membranes were washed ones in distilled water and blocked in PBS-T (10mM sodium phosphate, 0.15M NaCl, 0.1% Tween-20, pH 7.5) containing 5% non-fat dried

milk for 1 h at room temperature. Then, the membranes were probed with primary antibodies diluted in blocking buffer (1:1,000) at 4^{o} C overnight, washed three times for 15 min with PBS-T, and incubated with a secondary antibody conjugated with the horse radish peroxidase (HRP) (Cell Signalling) in PBS-T (1:1,000) for 1 h at room temperature. After another wash in PBS-T, the HRP signal was visualized by enhanced chemoluminescence (ECL) (ECL Western Blotting System, Amersham). The primary polyclonal antibodies targeting JUNV G2 and Z were raised in rabbits against synthetic peptides corresponding to amino acid sequences GKYPNLKKPTVWRR and GASKSNQPDSSRAT (ProSci), respectively, that are completely conserved between Romero and Candid #1. The anti-NP monoclonal antibody NA05-AG12 was obtained from the Biodefense and Emerging Infections Research Resources Repository (BEI Resources). The antibodies against BiP and β-actin were purchased from Cell Signaling Technology, Inc.

NORTHERN BLOTTING

Total RNA from infected cells lysed in TRIzol Reagent (Invitrogen) was isolated using the Direct-zol RNA MiniPrep kit (Zymo Research) following the manufacturer's protocol. The Northern blot analysis was performed using the NorthernMax-Gly kit (Ambion). Briefly, 1 μg of total RNA was denatured in glyoxal loading buffer containing EtBr at 50^{o} C for 30 min. RNA was separated by electrophoresis in 1% low electroendosmosis (LE) agarose gel and transferred onto the BrightStar-Plus positevily charged nylon membrane (Ambion) by downward passive transfer for 2 h. Before hybridization with RNA probes, EtBr-stained 18S rRNA was visualized under long-waive UV light and photographed to assess the quality of RNA and to ensure equal sample loading. To prepare the RNA probe for the detection of S gRNA and GPC mRNA species, a 590 nt PCR fragment was amplified from Romero mPol-I-Sag spanning

positions 743 to 1333 of the S segment. The probe was *in vitro* transcribed using the MAXIscript T7 kit (Ambion) from the T7 promoter included in the primer annealing at position 743 and biotinylated using the BrightStar Psoralen-Biotin Kit (Ambion) according to the protocols provided by the manufacturer. The RNA probe targeting the S agRNA and NP mRNA species was synthesized from a 544 nt PCR fragment spanning positions 1870 to 2414 of the S segment of Romero genome (T7 promoter was included in the primer annealing at position 2414). Blots were hybridized with biotinylated RNA probes at 0.1 nM overnight at 68^{o} C followed by one low-stringency wash for 10 min at room temperature and two high-stringency washes for 15 min at 68^{o} C. Hybridization signals were detected using the BrightStar BioDetect Nonisotopic Detection Kit (Ambion).

QUANTITATIVE REAL-TIME PCR

Total RNA from JUNV-infected cells was isolated as described for Northern blot experiments. Viral RNA quantification was performed in triplicates using the iScript One-Step RT-PCR Kit with SYBR Green (Bio-Rad) with 100 ng of total RNA. The following primers were used for detection: NP direct, GGTCCTTCAATGTCGAGCCA; NP reverse, AATCACAGGCAGGTCATGGG; Z direct, AAGTGCTGCTGGTTTGC TGA; Z reverse, TCCACCGGTACTGTGATTGTG, GAPDH-Vero direct, AGTCAA CGGATTTGTCGTA; GAPDH-Vero reverse, GGGTGGAATCATACTGGAAC; GAPDH-guinea pig direct, TACGACAAGTCCCTCAAGATTG; GAPDH-guinea pig reverse, TCTGGGTGGCAGTGATGG. Melt curve analysis was performed to confirm PCR fragment specificity. Sample cycle thresholds (Ct) were normalized to the Ct values of GAPDH. Relative amounts of viral RNA in infected cells and tissues were calculated against rRomero RNA using the equation $2^{-\Delta Ct}$, where $\Delta Ct^{sample} = (Ct^{sample} - Ct^{GAPDH/sample}) - (Ct^{rRomero} - Ct^{GAPDH/rRomero})$ (Pfaffl, 2001).

CHAPTER 3: RESCUE FROM CLONED CDNAS AND *IN VIVO* CHARACTERIZATION OF RECOMBINANT PATHOGENIC ROMERO AND LIVE-ATTENUATED CANDID #1 STRAINS OF JUNIN VIRUS[3]

INTRODUCTION

Arenaviruses are enveloped viruses with a bisegmented negative-strand (NS) RNA genome. Each genomic RNA segment, L (ca. 7.3 kb) or S (ca. 3.5 kb), uses an ambisense coding strategy to direct the synthesis of two polypeptides in opposite orientations and separated by a noncoding intergenic region (IGR) that acts as a transcription termination signal for the virus polymerase (Meyer and Southern, 1994; Tortorici et al., 2001). The S RNA encodes the viral glycoprotein precursor (GPC) and the nucleoprotein (NP). The GPC is posttranslationally cleaved by the cellular site 1 protease to yield the two glycoproteins GP1 and GP2, which, embedded in the lipid bilayer, form the viral spikes in the mature virion that are crucial for receptor recognition and cell entry. The L RNA encodes the viral RNA-dependent RNA polymerase (or L polymerase) and the small (ca. 11-kDa) RING finger protein Z that is the arenavirus counterpart of the matrix protein found in many other NS RNA viruses (Perez et al., 2003; Strecker et al., 2003; Urata et al., 2006).

Arenaviruses cause chronic infections in rodents with a worldwide distribution (Buchmeier, 2013). Infection of humans usually occurs through mucosal exposure to aerosols or by direct contact of abraded skin with infectious materials and may result in severe disease. Thus, the Old World LASV and several New World (NW) arenaviruses

[3] Adapted with permission from Emonet SF*, Seregin AV*, Yun NE, Poussard AL, Walker AG, de la Torre JC, Paessler S. Rescue from cloned cDNAs and in vivo characterization of recombinant pathogenic Romero and live-attenuated Candid #1 strains of Junin virus, the causative agent of Argentine hemorrhagic fever disease. J Virol. 2011 Feb;85(4):1473-83. Epub 2010 Dec 1. (*-equal contribution).

cause hemorrhagic fevers (HF), posing a serious public health problem in the regions where they are endemic (McCormick and Fisher-Hoch, 2002; Peters, 2002).

The NW arenavirus JUNV causes AHF, a disease mostly endemic to the Pampas region of Argentina. AHF is a severe illness with hemorrhagic and neurological manifestations and a case fatality rate of 15 to 30% (Harrison et al., 1999; Peters, 2002; Weissenbacher et al., 1987). In addition to its impact on public health, JUNV possesses features that make it suitable as a potential biological weapon. JUNV is very stable, is highly infectious by aerosol, and produces high morbidity and significant mortality at low doses. Accordingly, the development of antiviral strategies against JUNV is one of the top priorities within the Implementation Plan of the HHS Public Health Emergency Medical Countermeasures Enterprise. Immune plasma therapy can ameliorate AHF symptoms and reduce mortality if administered during the prodromal phase. However, 10% of patients still present with late neurologic syndrome due to unknown mechanisms (Enria and Barrera Oro, 2002; Peters, 2002). Further limitations of this treatment are dictated by a short supply of plasma and the risk of transmission of blood-borne pathogens (Enria et al., 2008). Therapeutic efficacy of the nucleoside analogue ribavirin (Rib) has been demonstrated in both *in vitro* and *in vivo* studies against several arenaviruses, including JUNV (Andrei and De Clercq, 1993; Damonte and Coto, 2002). However, Rib is only partially effective and causes significant side effects, including anemia and congenital disorders, which, together with the need for its intravenous administration for optimal efficacy, underscores the need for the development of novel antiarenaviral drugs. The JUNV live-attenuated Candid #1 strain, derived from the 44th mouse brain passage of the prototype XJ strain of JUNV, was found to be attenuated in guinea pigs, and preclinical studies at USAMRIID supported the safety, immunogenicity, and protective efficacy of Candid #1 in both guinea pigs and rhesus macaques (McKee et al., 1992). Moreover, a TC83 replicon vectored vaccine expressing GPC of Candid #1 has been shown to be sufficient to induce a protective immune response against virulent

JUNV in guinea pigs (Seregin et al., 2010). More importantly, clinical studies involving agricultural workers in the area where JUNV is endemic have shown Candid #1 to be an effective and safe vaccine in humans (Maiztegui et al., 1998). This vaccine was licensed in 2006 for use exclusively in Argentina, whereas in the United States, Candid #1 remains only an investigational new drug and studies addressing long-term immunity and safety have not been conducted. The current availability within the United States of a Candid #1 master virus seed (MVS) is uncertain, and reimportation of Candid #1 vaccine from Argentina is likely to meet unsolvable obstacles due to foot-andmouth- disease virus activity in several geographic regions of Argentina and the potential lack of FDA-compliant documentation. In addition, a detailed genetic composition and the bases for the attenuated phenotype of Candid #1 have not been documented. Therefore, the development of a vaccine against AHF for licensure in the United States will be facilitated by the generation of a genetically well-characterized MVS from a source that has not been in Argentina and the identification of the viral genetic determinants and virus-host interactions underlying JUNV pathogenesis.

The rescue of the XJ13 strain of JUNV from cloned cDNAs using a T7-based system has recently been documented (Albariño et al., 2009). XJ13 was derived by carrying out two passages in guinea pigs and 13 passages in mouse brain of the XJ strain originally isolated from a case of AHF in Junin City (Buenos Aires, Argentina) (Parodi et al., 1958). During these passages, XJ acquired several mutations, and therefore its derivative XJ13 may not accurately reflect the pathogenicity of JUNV in humans. In addition, the ability of the rescued XJ13 virus to induce AHF-like disease in guinea pigs has not been demonstrated (Albariño et al., 2009). In contrast, the Romero strain, also isolated from a patient with AHF, has not been subjected to multiple passages in cultured cells or animals in the laboratory and therefore it is expected to represent a truly human pathogenic JUNV. In addition, over the years, a large body of data has been accumulated regarding the parameters associated with Romero-induced AHF-like disease in guinea

pigs (Yun et al., 2008), which would facilitate the use of rRomero for the investigation of viral determinants of JUNV pathogenesis.

In this chapter, I describe the use of reverse genetics to rescue from cloned cDNAs infectious, live-attenuated Candid #1 and pathogenic Romero strains of JUNV with well-defined genetic compositions. The recombinant Candid #1 (rCandid #1) and Romero (rRomero) viruses were genetically identical to their parent viruses and grew to high titers in cultured cells without a need for cell culture adaptation. Moreover, guinea pigs infected with rRomero or the parental Romero field isolate succumbed with the same kinetics and symptoms. Likewise, guinea pigs infected with rCandid #1 did not exhibit clinical symptoms and were protected against a subsequent challenge with the pathogenic Romero strain.

RESULTS

Identification of viral cis-acting sequences and trans-acting factors required for efficient RNA replication and gene transcription of live-attenuated Candid #1 and pathogenic Romero strains of JUNV

The first step to rescue infectious Candid #1 and Romero from cloned cDNAs was to develop a MG rescue system for JUNV to identify functional clones for the minimal viral trans-acting factors, NP and L, required for RNA replication and transcription by the JUNV polymerase complex. For this, a polymerase I-based plasmid was generated that directs the intracellular synthesis of an S-based RNA MG containing the 5' and 3' noncoding regions and IGR corresponding to published Candid #1 sequences and where the ORF of the CAT or Gaussia luciferase (Gluc) reporter gene substituted for the ORF of the viral NP. Intriguingly, the highly conserved 19 nt characteristically observed at the 5' end of all other arenaviruses so far examined appeared to contain significant

A

S segment

Virus	Strain	Accession number	5 ' end	3 ' end
LCMV	Armstrong	AY847350	---CGCACCGGGGATCCTAGGC	GCCTAGGATCCACTGTGCG
JUNV	Candid #1	AY746353	GTGCAGTAAGGGGATCCTAGGC	GCCTAGGATCCACTGTGCG
		Exp.	---CGCACCGGGGATCCTAGGC	GCCTAGGATCCACTGTGCG
	Romero	AY619641	---CGCACAGTGGATCCTAGGC	GCCTAGGATCCACTGTGCG
		Exp.	---CGCACCGGGGATCCTAGGC	GCCTAGGATCCACTGTGCG

L segment

Virus	Strain	Accession number	5 ' end	3 ' end
LCMV	Armstrong	AY847351	CGCACCGGGGATCCTAGGC	GCCTAGGATCCTCGGTGCG
JUNV	Candid #1	AY819707	CGCACAGTGGATCCTAGGC	GCCTAGGATCCACTGTGCG
		AY746354	CGCACCGGGGATCCTAGGC	GCCTAGGATCCCCGGTGCG
		Exp.	CGCACCGGGGATCCTAGGC	GCCTAGGATCCTCGGTGCG
	Romero	AY619640	CGCACAGTGGATCCTAGGC	GCCTAGGATCCACTGTGCG
		Exp.	CGCACCGGGGATCCTAGGC	GCCTAGGATCCTCGGTGCG

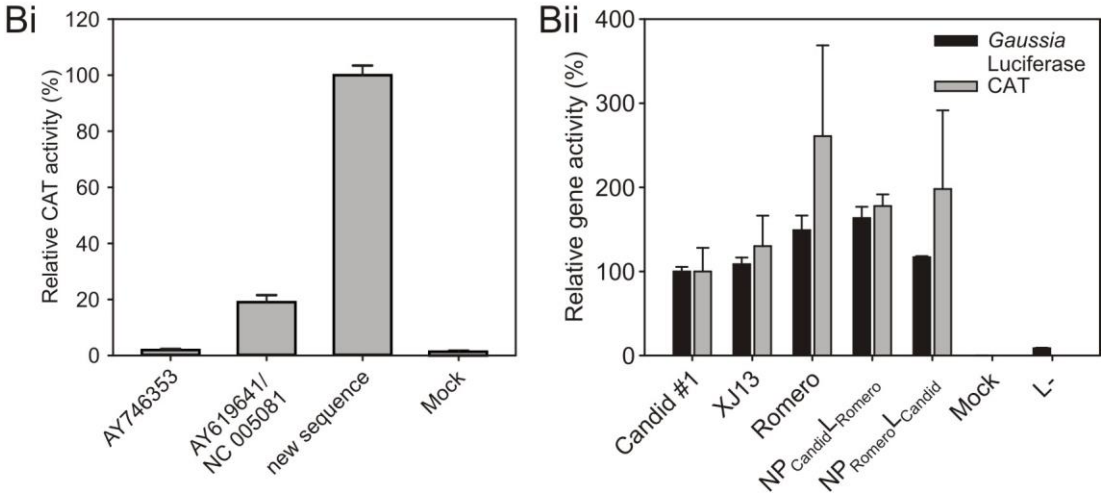

Figure 3.1. (A) Comparison of the 5'- and 3'-terminal sequences of the S and L segments of previously published JUNV sequences and the sequences determined in this study. Comparison of the 5'- and 3'-most terminal 19 nt of the S and L segments of the previously published Candid #1 (accession no. AY746353 and AY819707) and Romero (accession no. AY619641) sequences and the corresponding sequences determined in this study (Exp.). Not indicated is the nontemplated G characteristically found at the 5' end of arenavirus genome and antigenome RNA species. **(B) Establishment of a JUNV MG rescue system and identification of functional L and NP viral trans-acting factors for the Romero and Candid #1 strains of JUNV. (Bi)** Comparison of CAT expression by an MG with Candid #1 or Romero previously published or newly determined 5'/3' termini. BHK-21 cells were transfected with Candid #1 pC-NP and pC-L and three different mPol-I-S vectors expressing the Candid #1 S segment with the CAT gene instead of the NP gene. The mPol-I-S vectors differed only in the 3' and 5' termini of the expressed MG RNA, reproducing the published Candid #1 termini (accession no. Y746353), the Romero and XJ13 termini (accession no. AY619641 and NC005081), or the 5'/3' termini determined in this study for both the Candid #1 and Romero strains of JUNV. At 3 days posttransfection, cells were harvested

and CAT expression was determined. CAT expression was set to 100% for the sample corresponding to the mPol-I-S MG containing the 5'/3' termini determined in this study, and values obtained for the other MG constructs were normalized accordingly. **(Bii)** Comparison of the levels of efficiency with which NP-L combinations from different JUNV strains replicate and express a Candid #1 MG expressing either the CAT or the Gaussia luciferase (Gluc) gene instead of the NP gene. BHK-21 cells were transfected with pC-NP, pC-L, and the mPol-I-S vector. At 3 days posttransfection, cells and TCS were harvested and assessed for CAT expression and Gluc activity, respectively. The value obtained with the Candid #1 NP-L combination was set to 100% activity, and the other values were normalized accordingly. Reproduced with permission from (Emonet et al., 2011b).

differences in the S genome RNA of Candid #1 deposited in GenBank (accession number AY746353), including the presence of an extra 3 nt (Fig. 3.1A). Therefore, the 5'/3' termini were revisited for both the S and L RNA genome species of Candid #1, as well as the Romero strain. For this, a comprehensive analysis of the Candid #1 and Romero 5'- and 3'-end genomic sequences was conducted by using viral genome RNA isolated at 72 h p.i. Results from these studies clearly indicated differences from previously published 5'- and 3'-end sequences of the Candid #1 and Romero genome RNA species (Fig. 3.1A). Thus, the next step was to investigate whether previously published sequences (i) reflected genetic differences within the S and L termini of Candid #1 and Romero potentially associated with phenotypic differences or (ii) were artifacts caused by the experimental procedures associated with the sequencing strategy used. To this end, three mPol-I-S vectors expressing CAT instead of NP were generated that differed only in their 5' and 3' termini. One vector had 5' and 3' termini from the published Candid #1 sequence (accession number AY746353), another had 5' and 3' termini from previously published XJ13 and Romero sequences (accession numbers NC005081 and AY619641, respectively), and the last one had 5' and 3' termini from the newly determined Candid #1 and Romero sequences. To provide the minimal viral trans-active factors required for RNA replication and expression of the virus MG, expression constructs for the NP and L of Candid #1 and Romero were generated using a Pol-II-based expression vector (pCAGGS). Previous report describing the rescue of infectious LCMV from cloned

cDNAs demonstrated that single amino acid differences, including those highly conserved with respect to the virus master sequence present in L and NP expression clones, can significantly affect the activity of a virus polymerase complex (Flatz et al., 2006; Sánchez and de la Torre, 2006). Therefore, the sequences of the L and NP ORFs cloned into pCAGGS were confirmed to be identical to the corresponding master sequences determined for Candid #1 and Romero before the MG assays were performed. Results from the MG experiment clearly demonstrated that only the newly determined 5/3-terminal sequences were fully functional, whereas 5'/3'-termini from the published Candid #1 sequence completely abolished MG expression (Fig. 3.1Bi). Next, the relative efficiencies with which different combinations of L and NP derived from Romero and Candid #1 promoted RNA replication and expression of the Candid #1 S-based MG were determined (Fig. 3.1Bii). As a control, an L polymerase clone derived from the JUNV XJ13 strain, the parental strain of Candid #1 was included in these studies. The MG activity of the L/NP combination of Candid #1 origin was assigned a value of 100% in order to evaluate the activities of other L/NP combinations. Our results indicated that the Romero L-NP combination was more active than the Candid #1 or XJ13 L-NP combination in the MG rescue assay. These results confirmed that we had obtained functional L and NP clones from both Romero and Candid #1 that are required for virus rescue. In addition, that combinations of L and NP derived from Romero and Candid #1 exhibited similar levels of activity in this assay indicated the feasibility, as predicted based on their genetic proximity, of generating chimeric viruses based on Candid #1 and Romero.

Rescue of live-attenuated Candid #1 and pathogenic Romero strains of JUNV from cloned cDNAs

To rescue infectious rRomero and rCandid #1 from cloned cDNAs, BHK-21 cells were transfected with mPol-I-Sag and mPol-I-Lag for either Romero or Candid #1,

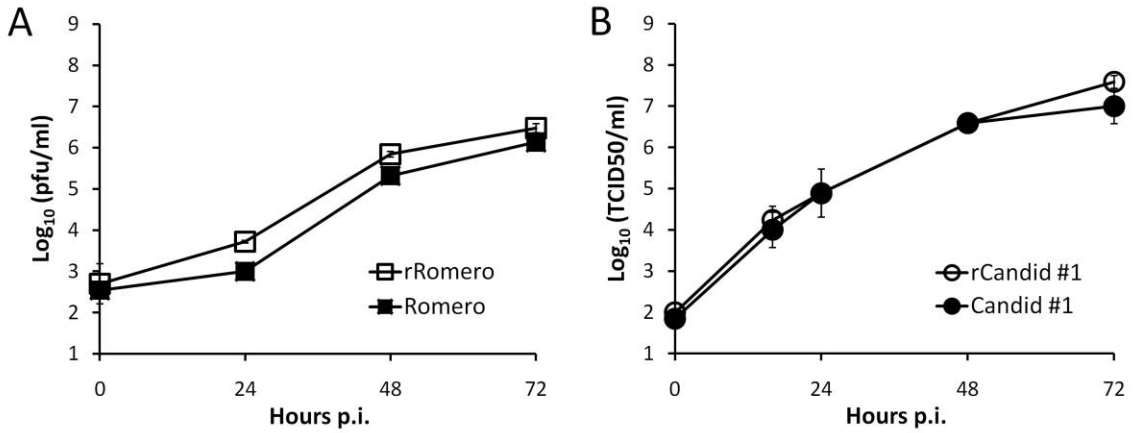

Figure 3.2. Characterization of rRomero and rCandid #1 in cultured cells. (A) Comparison of the growth properties of Romero and rRomero in Vero cells. Cells were infected at an MOI of 0.01, TCS were collected at the indicated time points, and virus titers were determined by plaque assay. **(B)** Comparison of the growth kinetics of the Candid #1 and rCandid #1 viruses in Vero cells. Cells were infected at a low MOI (0.01), and at the indicated time points, TCS were harvested and viral titers were determined. Reproduced with permission from (Emonet et al., 2011b).

together with Pol-II expression plasmids for the minimal corresponding viral trans-acting factors, L and NP, derived from each one of the two viral strains. For rRomero, TCS collected at 96 h posttransfection consistently had titers in the range of 10^4 to 10^5 PFU/ml. For rCandid #1 at 72 h posttransfection, cells were transferred to a T75 flask, and 72 h later, TCS were collected and used to infect a fresh monolayer of Vero cells. The rationale for this was to demonstrate that the rescued Candid #1 vaccine strain could be grown to high titers in Vero cells, an approved cell substrate for vaccine production, without requiring adaptation. Vero cell TCS were collected at 72 h p.i., and they consistently had titers in the range of 10^6 to 10^7 TCID50/ml. Both rRomero and rCandid #1 were unequivocally identified based on genetic tags introduced into the recombinant L and S segments, respectively, as described in Materials and Methods. To assess the growth kinetics, Vero cells were infected at an MOI of 0.01 with each of the parental or recombinant viruses and at the indicated times after infection determined infectious virus titers in TCS. The rescued rRomero (Fig. 3.2A) and rCandid #1 (Fig. 3.2B) displayed growth properties similar to those of Romero and Candid #1, respectively, the parental

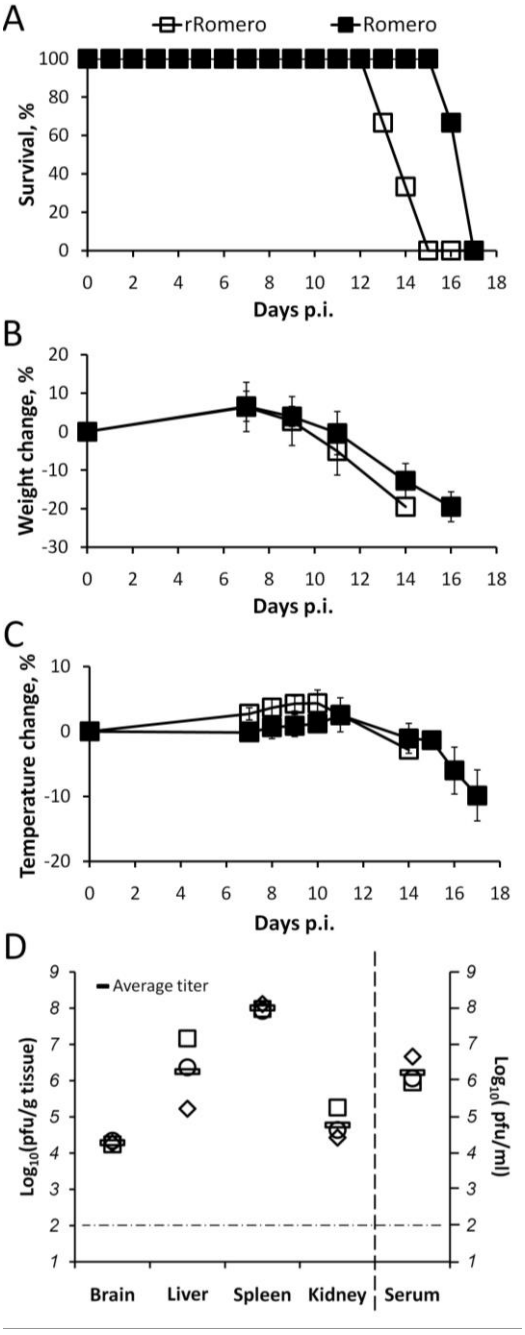

isolates. In addition, rRomero and rCandid #1 exhibited plaque-forming efficiencies, as well as plaque sizes and morphologies, similar to those of their respective counterparts, Romero and Candid #1.

In vivo biological properties of rRomero and rCandid #1

To confirm that the experimental procedures used for the rescue of rRomero and rCandid #1 did not result in unexpected changes in their phenotypic properties, rRomero and rCandid #1 were compared to Romero and Candid #1 with respect to their abilities to induce an AHF-like disease in guinea pigs. As with strain Romero (Seregin et al., 2010; Yun et al., 2008), infection with strain rRomero was 100% lethal in Hartley guinea pigs by 17 days p.i. (Fig. 3.3A). We observed a steady decrease in body weight after 7 days p.i. (Fig. 3.3B), and all infected

Figure 3.3. Induction of lethal disease and viral loads in guinea pigs infected with rRomero. (A) Female Hartley guinea pigs were inoculated i.p. with 10^3 PFU of either Romero (n = 3) or rRomero (n = 3) and monitored for 21 days for survival. **(B and C)** Body temperatures and weight changes were recorded throughout the course of the study. Shown are average values and standard deviations. **(D)** Virus titers in organs of rRomero-infected guinea pigs. Necropsies were performed on three rRomero-infected guinea pigs euthanized at 12 days p.i. Organs were homogenized, and virus titers in the organ samples and sera were determined by plaque assay. Reproduced with permission from (Emonet et al., 2011b).

Animal[b]	Preinoculation/postinoculation values[a]							
	Platelet count (10^3/ml)	Mean platelet volume (fl)	Albumin (g/dl)	Alkaline phosphatase (U/liter)	Alanine aminotransferase (U/liter)	Amylase (U/liter)	Calcium (mM)	Globulin (g/dl)
GPrR1	470/214	5.3/2.6	4.30/2.50	119/1,041	23/87	1,712/864	3.03/10.5	1.3/3.5
GPrR2	548/217	5.8/3.2	4.30/2.00	112/683	26/119	1,541/1,353	2.94/8.4	1.7/2.7
GPrR3	486/233	5.5/2.9	4.30/2.10	102/688	24/136	1,292/721	11.6/8.9	1.6/3.1

Table 3.1. Hematology and blood chemistry parameters in guinea pigs infected with rRomero. [a] Blood was collected preinfection (day -6) and postinfection (day +11), and hematology and blood chemistry parameters were analyzed. [b] Three guinea pigs were euthanized 12 days after inoculation with rRomero. Reproduced with permission from (Emonet et al., 2011b).

guinea pigs became febrile (body temperature, ≥39.5 ^{o}C) at 10 days p.i., which was followed by a rapid decline in body temperature between 12 and 14 days p.i. (Fig. 3.3C). Clinical signs of infection were first observed at 12 to 13 days p.i., with 50% (2/4) of the guinea pigs developing clinical encephalitis and 25% (1/4) developing paralysis at 17 days p.i. (data not shown). Infected guinea pigs developed high levels of viremia (in the range of 10^6 PFU/ml) and had high titers of infectious virus in the spleen, liver, kidneys, and brain (Fig. 3.3D). More importantly, the infection with rRomero caused thrombocytopenia, as previously reported from studies with Romero. In addition, increased levels of liver enzymes and reduced production of albumin correlate with the histopathology reported for Romero infection and indicate mild liver damage (Table 3.1). Next, the histopathology associated with rRomero infection of guinea pigs was assessed. Representative H&E-stained sections of brains, including the cerebrum, cerebellum, and hippocampus, from rRomero-infected and mock-infected control guinea pigs did not reveal significant inflammation or necrosis in the brains of rRomero-infected guinea pigs (Fig. 3.4A). However, vascular cuffs of mononuclear cells in the cortexes of rRomero-infected animals were occasionally observed. This finding correlates with the detection of viral antigen in neurons in small foci located mostly in the cortex (Fig. 3.4B). These results indicated that, as reported for Romero, the rRomero virus was also able to penetrate the central nervous system and cause mild inflammatory changes in the brain. In addition, pathological changes in the spleens and livers of rRomero-

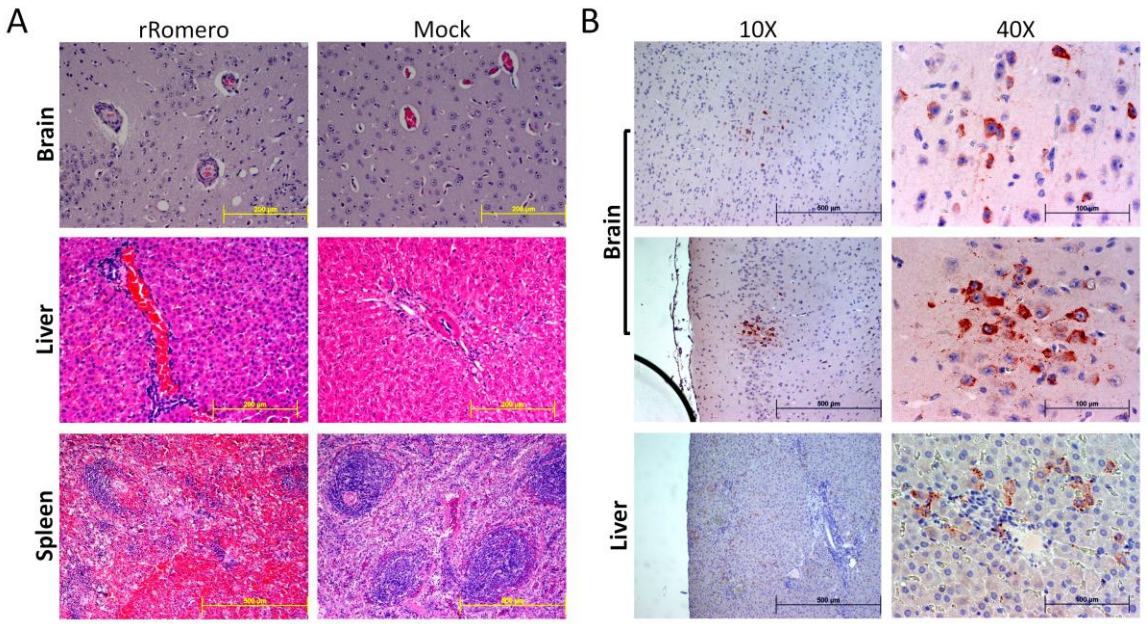

Figure 3.4. Histopathology and tissue viral antigen distribution in rRomero-infected guinea pigs. (A) Histopathologic analysis. Tissue sections from guinea pigs infected with rRomero or mock infected were subjected to standard H&E staining. Magnification, ×20. **(B)** Dissemination of rRomero in the brains and livers of infected guinea pigs. Tissue sections were probed with an LASV group HIAF and a biotinylated secondary antibody. Color development was performed by using streptavidin-peroxidase, followed by the addition of a chromogenic substrate (brown-red). Reproduced with permission from (Emonet et al., 2011b).

infected guinea pigs similar to those previously reported for Romero-infected guinea pigs (Yun et al., 2008) were consistently observed at 12 days p.i. (Fig. 3.4A). Compared to those of mock-infected controls, the spleens from rRomero-infected guinea pigs showed a "motheaten" appearance of the white pulp with apparently numerous macrophages. The red pulp contained clusters of neutrophils, particularly in the marginal zones. Severely affected animals showed generalized cellular depletion within the red pulp. Liver pathology was characterized by the presence of diffuse microvesicular steatosis, mild portal inflammation, and mild lobular inflammation. Additionally, steatosis was more pronounced, predominantly macrovesicular. Scattered foci of nuclear debris were present in portal triads and in lobular foci, suggesting leukocyte degeneration. In contrast to the findings with rRomero, guinea pigs infected with rCandid #1 did not exhibit noticeable clinical symptoms throughout an observation period of 21 days. During this time,

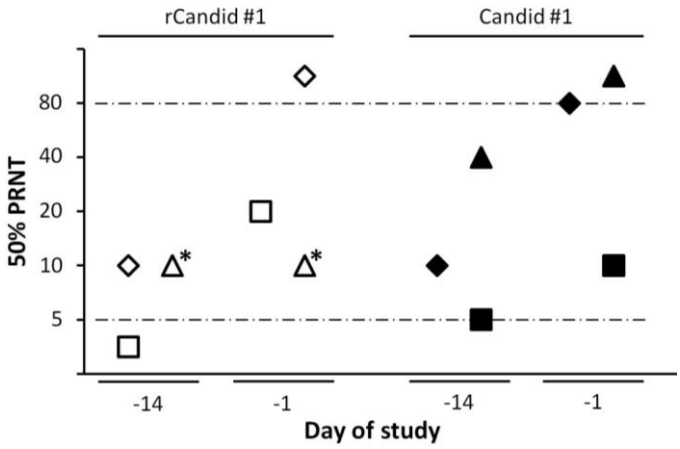

Figure 3.5. Immunogenicity of rCandid #1 in guinea pigs. Serum samples were collected at the indicated time points (14 and 1 day prior to challenge with rRomero) from guinea pigs immunized with either Candid #1 or rCandid #1, and the titers of Candid #1-specific neutralizing antibodies were determined by 50% plaque reduction neutralization test (PRNT). The detection range of the assay is flanked by dashed lines. Asterisks indicate the serum virus titers of the guinea pig that did not recover from anesthesia after blood collection performed on day 11 after a challenge with rRomero. Reproduced with permission from (Emonet et al., 2011b).

rCandid #1 and Candid #1 induced similar neutralizing antibody titers (Fig. 3.5). At day 21 p.i., rCandid #1-infected guinea pigs were challenged with a lethal dose of rRomero and monitored for the development of clinical symptoms to determine whether infection with rCandid #1 had endowed the guinea pigs with protective immunity against a pathogenic JUNV (Fig. 3.6). All (n = 3) mock-immunized guinea pigs showed a steady decrease in body weight starting at day 8 postchallenge, and all of them succumbed by day 17 postchallenge. In contrast, immunization with Candid #1 or rCandid #1 provided protection against the development of disease symptoms and death following a challenge with a lethal dose of rRomero. One guinea pig immunized with rCandid #1 did not recover from anesthesia procedure done to collect blood on day 8 post-challenge with rRomero, which resulted in 66% instead of the expected 100% survival in the group immunized with rCandid #1 and challenged with rRomero.

DISCUSSION

In this chapter, I have described the rescue of the pathogenic Romero and attenuated Candid #1 strains of JUNV from cloned cDNAs. To this end, a rescue system was employed that is based on the use of Pol-I vectors to drive intracellular synthesis of the virus S and L genome RNA species and Pol-II expression plasmids to initially provide the minimal viral trans-acting factors, L and NP, required for RNA replication and gene transcription directed by the virus polymerase complex. The characterization of rRomero and rCandid #1, both in cultured cells and in a guinea pig model of JUNV infection, demonstrated that rRomero and rCandid #1 were genetically and phenotypically indistinguishable from the corresponding parental Romero and Candid #1 viruses.

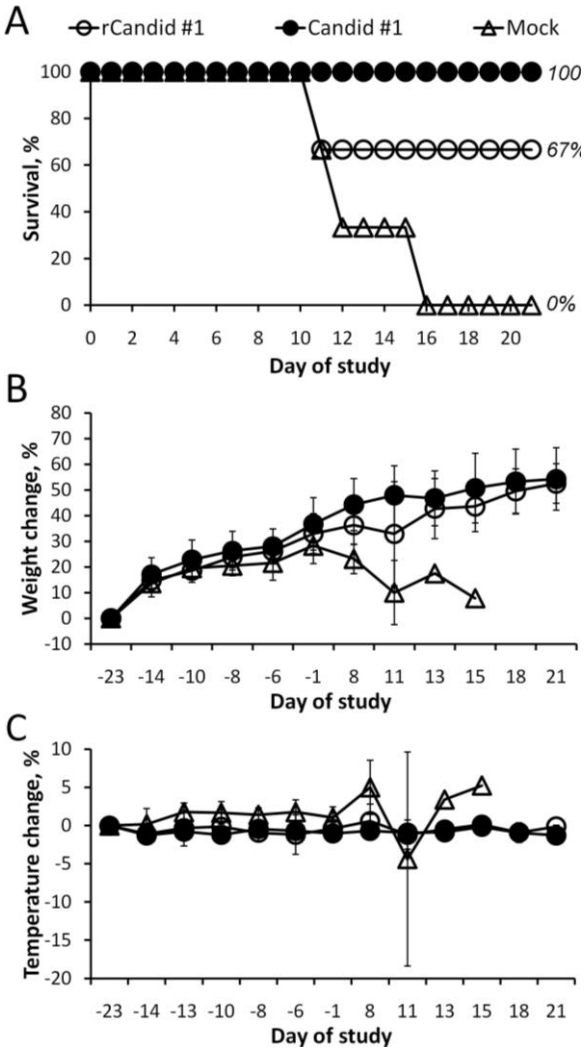

A first and necessary step to accomplish this goal was to accurately determine the complete master genome sequences for Romero and Candid #1,

Figure 3.6. Protection of rCandid #1-infected guinea pigs against a lethal challenge with rRomero. (A) Comparison of guinea pig survival after immunization with Candid #1 or rCandid #1 and a challenge with rRomero. Female Hartley guinea pigs (three per group) were inoculated i.p. with 103 PFU of either Candid #1 or rCandid #1 or mock immunized. At 21 days after immunization, all of the guinea pigs were challenged by the i.p. route with 103 PFU of rRomero and monitored for survival. **(B and C)** Body weight **(B)** and temperature **(C)** changes were recorded at the indicated time points pre- and postchallenge. Average values and standard deviations are shown. Reproduced with permission from (Emonet et al., 2011b).

including the precise L and S 5'/3' termini that have been shown to play critical roles in the control of arenavirus RNA synthesis. Then, this information was used to generate Pol-II expression plasmids for the corresponding L and NP ORFs, whose functionality was assessed in an MG rescue assay based on the S segment of Candid #1. The newly obtained sequencing data revealed several differences within the 5'/3' termini between previously published Romero and Candid #1 sequences and the ones that were determined (Fig. 3.1A). More intriguingly, the obtained sequence for the 5' end of the Candid #1 S segment was identical to that of LCMV, whereas the sequence published for the 5' end of the S segment of Candid #1 appeared to be extended by 3 nt and contained five nucleotide differences within the 5'-end 19 nt that are highly conserved among arenaviruses. Because the role played by the 5'/3' termini in the regulation of viral RNA synthesis, the unique sequence features of the 5' end of the Candid #1 S segment might have a role in attenuation. Results from MG rescue assays clearly indicated that the previously published 5'-end sequence of the Candid #1 S segment was not compatible with virus RNA replication and gene expression (Fig. 3.1B).

Romero and rRomero exhibited similar growth kinetics and peak titers in cultured cells (Fig. 3.2A). More importantly, guinea pigs infected with rRomero or Romero were similar in temporal development and the magnitude of their clinical symptoms, as well as in mortality. All animals that were inoculated with Romero and rRomero developed a systemic febrile illness that led to characteristic hematologic and neurologic manifestations associated with typical histopathological changes in organs such as the liver, spleen, and brain. In this particular study, animals infected with rRomero succumbed to the diseases insignificantly faster but within the normal time range (Yun et al., 2008).

As predicted, guinea pigs infected with either Candid #1 or rCandid #1 did not develop noticeable clinical symptoms, and the two viruses induced similar levels of neutralizing antibodies against JUNV (Fig. 3.5). Consistent with these results, two of the

three rCandid #1-infected guinea pigs were totally resistant to a lethal challenge with Romero (Fig. 3.6). One rCandid #1-immunized guinea pig developed some fever and lost some weight upon the lethal challenge with Romero. This animal did not recover from anesthesia during a blood collection procedure, and therefore it is unknown whether it would have survived the challenge as the other animals in the same group did.

Different reasons could account for this unexpected finding. First, most protocols allow 6 to 8 weeks between Candid #1 immunization and a lethal challenge with pathogenic JUNV. In contrast, in our protocol, rCandid #1-immunized guinea pigs were subjected to a lethal challenge with Romero only 21 days after immunization. This significantly shorter time between immunization and challenge may result in some guinea pigs having suboptimal neutralizing antibody titers at the time of the challenge. In addition, in this study, outbred Hartley guinea pigs were used instead of Strain 13 inbred guinea pigs, which are commonly used for vaccination studies with Candid #1. Therefore, a higher degree of genetic heterogeneity within outbred Hartley guinea pigs may have contributed to the higher levels of variation in the immune responses seen following immunization with rCandid #1. Likewise, a very large challenge dose (1,000 50% lethal doses) and potential genetic differences could influence guinea pig susceptibility to Romero, and therefore, even restricted Romero multiplication due to vaccination could result in the development of clinical symptoms. Although more detailed studies are required to conclusively establish the safety and efficacy of rCandid #1 in guinea pigs and nonhuman primates, our results have documented, for the first time, the generation of a genetically defined molecular clone of strain Candid #1 that was able to induce protective immunity against a pathogenic strain of JUNV in guinea pigs, which are a well-established model of JUNV infection and pathogenesis.

Previous studies, including the comparison of LCMV Docile and Aggressive strains (Chen et al., 2008) or PICV nonpathogenic P2 and pathogenic P18 strains (Lan et al., 2009), have examined the relationship between genetic changes within the arenavirus

genome and virus pathogenic potential. However, the implementation of these studies for JUNV would, for the first time, involve an arenavirus highly significant to human health. Romero was isolated from a severe, nonfatal human infection, whereas Candid #1 has been used in Argentina since 1991 to vaccinate individuals at high risk of infection with JUNV (Enria and Barrera Oro, 2002). Moreover, Candid #1 was derived from the prototype XJ strain originally isolated from a human with a fatal case of AHF (Peters et al., 1987). Therefore, some of the genetic differences between Candid #1 and Romero are likely to be related to the acquisition of attenuation in humans, nonhuman primates, and guinea pigs. In contrast, genetic differences between the nonpathogenic P2 and pathogenic P18 strains of PICV are likely related to the acquisition of virulence factors in guinea pigs whose relevance to arenavirus-induced disease in humans remains to be determined.

Importantly, the NP and L proteins of Romero and Candid #1 were exchangeable in an MG rescue system. This finding supports the idea that it would be feasible to rescue rCandid #1 and rRomero with an exchanged gene or RNA segment(s), which would facilitate the identification of viral genes associated with pathogenicity.

The precise genetic characterization of Candid #1 vaccine remains uncertain. Several Candid #1 sequences have been deposited in GenBank, and their comparison shows several mutations among them. For example, a recent report (Goñi et al., 2010) documented five amino acid differences in NP with respect to previously reported Candid #1 (AY746353) and XJ13 (NC005081) NP sequences. This lack of a precise genetic identity for Candid #1 not only complicates the identification of amino acid changes potentially responsible for the virus's attenuation but also raises some questions about the safety of the vaccine. The use of reverse genetics to generate a Candid #1 strain with a well-defined genotype should help to develop a well-characterized Candid #1 MVS for the development of a vaccine against JUNV that would be able to meet FDA requirements for licensure in the United States. The ability to manipulate the genomes of

two genetically well-defined and closely related strains of JUNV, one pathogenic (rRomero) and the other attenuated (Candid #1), in a well-established guinea pig model of JUNV infection should facilitate studies aimed at identifying viral genetic determinants associated with virulent and attenuated phenotypes, as well as the mechanisms by which different viral genes contribute to virus-host interactions underlying the development of HF arenaviral disease.

CHAPTER 4: THE GLYCOPROTEIN PRECURSOR GENE IS THE MAIN VIRULENCE FACTOR AND DETERMINES THE PATHOGENESIS OF ROMERO STRAIN AND ATTENUATION OF CANDID #1 STRAIN OF JUNIN VIRUS

INTRODUCTION

The main clinical features of human AHF are central nervous system (CNS) involvement and hemorrhagic manifestations (Elsner et al., 1973). The incubation period of AHF is usually from 6 to 14 days, which is followed by the onset of fever with a flu-like syndrome that is considered the first day of illness. Based on the final course of the clinical picture, disease outcome, and the severity of the neurological involvement, patients are grouped into mild, moderate, and severe clinical forms (Molinas et al., 1987). Patients with the mild form have fever during the first week of disease and tongue tremor is the only neurological manifestation observed. Fever persists during the second week in patients with the moderate form of disease that show more pronounced CNS alterations such as hyporeflexia or areflexia and mental confusion. Patients with severe forms of AHF present with marked CNS manifestations including areflexia, muscular hypotonia, ataxia, seizures and coma. Fatal cases are commonly associated with a terminal shock syndrome; superimposed bacterial infections can also be observed (Marta et al., 1998). Leucopenia and thrombocytopenia are detected during the first and second week after onset of symptoms. The most frequent hemorrhagic manifestations are petechiae in the mouth and the axillary region and bleeding of the gums. Less common manifestations are epistaxis, hematuria, metrorrhagia, hemoptysis and gastrointestinal hemorrhages (Molinas et al., 1981). The mortality rates can be up to 30% in cases without specific treatment.

Guinea pigs reproduce most of the human lesions, with increased viremia from day 7 post-infection until death around day 14 (Yun et al., 2008). Infected guinea pigs develop leucopenia and thrombocytopenia, reproduce the characteristic hemorrhagic manifestations of AHF, and die without detectable antibodies (Enria et al., 2008; Laguens et al., 1983). The development of hyperthermia and a rapid weight loss are highly predictive of a lethal outcome in infected animals (Yun et al., 2008). Intriguingly, the treatment of infected guinea pigs with immune sera results in the development of a late neurological syndrome with prominent rear-limb paralysis (Kenyon et al., 1986b). A late neurological syndrome is also observed in approximately 10% of patients treated with immune plasma from convalescent patients (Enria et al., 1985; Maiztegui et al., 1979).

Arenaviruses have evolved the ability to modulate the cellular responses to infection, which requires the involvement of at least two viral proteins, NP and Z. NP is most abundantly expressed in infected cells, comprises the main structural element of the viral RNP, and is essential for the activity of the viral polymerase complex (Buchmeier, 2013). In addition, NP has been shown to inhibit type I IFN signaling (Martínez-Sobrido et al., 2009; Martinez-Sobrido et al., 2007; Martinez-Sobrido et al., 2006). This function of NP is dependent on the exonuclease activity that has been mapped to the C-terminal domain that structurally resembles the active center of exonucleases belonging to the DEDDh exonuclease family (Eckerle et al., 2010; Qi et al., 2010). The small protein Z that contains a zinc-binding RING finger domain is the arenavirus analog of the matrix proteins of the negative strand RNA viruses (Buchmeier, 2013). The noncytophatic cell culture phenotype of the prototypic arenavirus LCMV has been proposed to be associated with the ability of its Z to interact with the promyelocytic leukemia (PML) protein in infected cells and trigger its relocation from the nucleus to the cytoplasm (Borden et al., 1998; Djavani et al., 2001). Z has also been proposed to inhibit cellular cap-dependent translation by binding to the eukaryotic translation initiation factor 4E (eIF4E) (Campbell Dwyer et al., 2000; Volpon et al., 2010). In addition to NP and Z, the viral glycoproteins

have also been proposed to contribute to the virulence of JUNV. The transferrin receptor 1 (TfR1) is the primary receptor for the Clade B New World arenaviruses, including JUNV, for the entry into the host cell (Radoshitzky et al., 2007). However, the human TfR1 can only be efficiently utilized by the GPs of pathogenic viruses and the entry of nonpathogenic viruses into cells of human origin is directed via TfR1-independent pathways. Pathogenic New World arenaviruses can also infect cells via TfR1-independent pathways, albeit less efficiently (Flanagan et al., 2008). Interestingly, F427I substitution found in the transmembrane region of GP2 of attenuated Candid #1 strain of JUNV was demonstrated to significantly attenuate the parental pathogenic virus in mice inoculated intracranially (Albariño et al., 2011b). Further analysis revealed that this mutation was responsible for decreased infectivity of Candid #1 virus in human cells (Droniou-Bonzom et al., 2011).

Here, I describe generation of a set of chimeric viruses where either the entire RNA segments or individual viral genes were exchanged between the attenuated Candid #1 and the pathogenic Romero strains of JUNV. Analysis of the *in vitro* growth properties of these viruses demonstrated that with the exception of the Romero LP and Candid #1 Z, all other viral proteins exhibited a high degree of compatibility between the two viral strains. Therefore, the chimeric JUNV encoding the combination of Romero LP and Candid #1 Z showed a delayed growth in tissue culture; however, the growth properties of the virus variant containing the LP of Candid #1 and the Z of Romero were not affected, suggesting a specific incompatibility between LP of the pathogenic and Z of the attenuated parental strain. Analysis of the *in vivo* biological properties of the chimeric JUNVs revealed that the amino acid changes in the GPC determine the pathogenicity and virulence of Romero and the attenuated state of Candid #1. Importantly, the F427I mutation in the G2 of Candid #1 that has recently been demonstrated to attenuate the neurovirulence of JUNV in mice, also significantly attenuated Romero in a guinea pig model of lethal infection. However, incorporation of this mutation in the genome of

rRomeo was not sufficient to eliminate disease development and other mutations in the GPC were required for complete *in vivo* attenuation of the virus.

RESULTS

Rescue and *in vitro* growth properties of inter- and intrasegment chimeric viruses between Romero and Candid #1 strains of JUNV

In the previous chapter, I described the results from an *in vitro* MG assay that demonstrated that the L polymerase of the highly pathogenic Romero strain of JUNV exhibits similar ability to replicate the S segment of the attenuated Candid #1 strain to the L polymerase of Candid #1 (Chapter 3 and (Emonet et al., 2011b)). This allowed to hypothesize that the components of the viral polymerase complex are interchangeable between Romero and Candid #1 and both complexes can efficiently utilize the genome RNA segments of both strains as templates for viral RNA synthesis and gene expression, thereby making possible the generation of chimeric viruses with genetic information exchanged between Romero and Candid #1. The first logical step was to attempt to generate intersegment chimeric viruses that would have one genome RNA segment originated from Romero and the other segment originated from Candid #1 (rRomL/CanS and rCanL/RomS, Fig. 4.1A). For this, the pol-I plasmids containing the full-length sequences of the L and S RNA segments were reciprocally exchanged between the Romero and Candid #1 reverse genetics systems in rescue experiments (see Materials and Methods). Next, the efficiency of plaque formation in Vero cells was assessed for both viruses and compared with that of rRomero and rCandid #1. The results demonstrated that the chimeric virus that had the S segment originated from Romero, rCanL/RomS produced large plaques similar in size and morphological appearance to those of rRomero (Fig. 4.1B). On the other hand, the rRomL/CanS virus that had the S segment originated

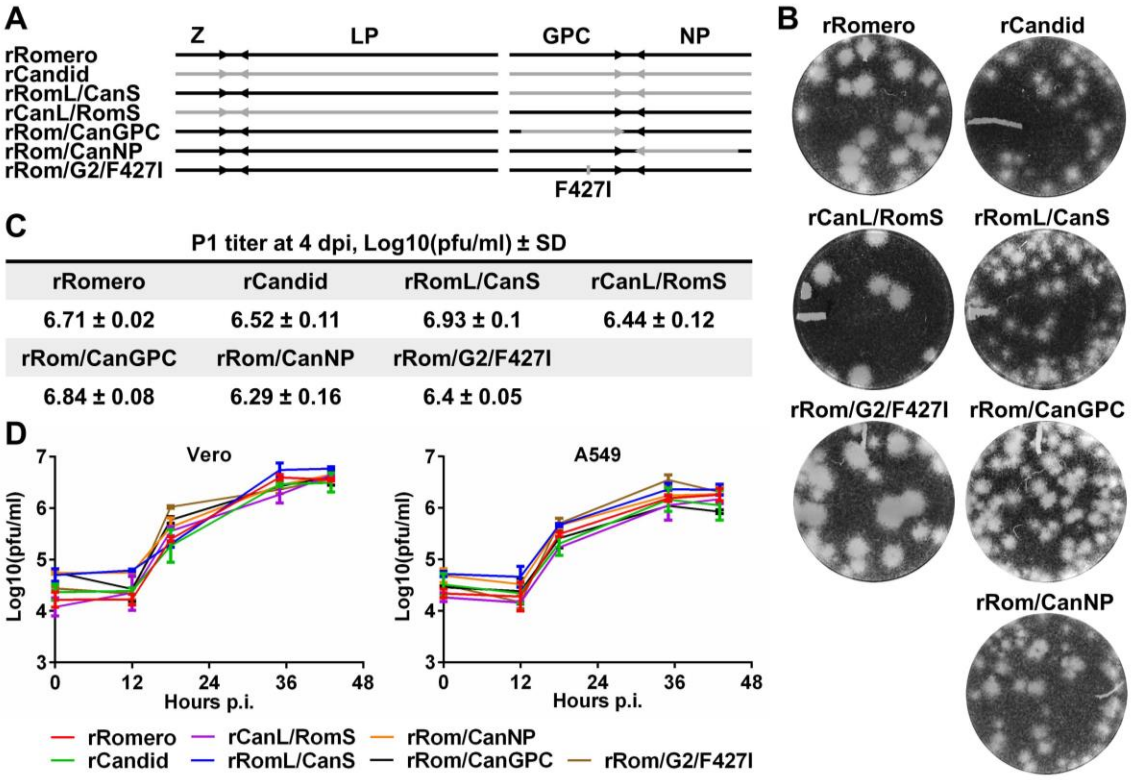

Figure 4.1. Rescue and characterization of *in vitro* growth properties of inter- and interasegment chimeric viruses between Romero and Candid #1 strains of JUNV. **(A)** Schematic representation of rJUNV genomes. Black and grey colors indicate the genetic material of Romero and Candid #1 strains of JUNV, respectively. **(B)** Morphological appearance of plaques on Vero cells. Infected cell monolayers were overlayed with growth medium containing 0.5% agarose and incubated for 7 days. Cells were stained with crystal violet to visualize plaques. **(C)** Passage one (P1) titers on Vero cells were determined by plaque assay at 4 days post-inoculation (dpi). **(D)** One-step growth curves of rJUNVs on Vero (left) and A549 (right) cells. TSCs of cells infected at an MOI of 5 were collected at the indicated times, and titers were determined by plaque assay.

from Candid #1 produced small plaques similar to those of Candid #1 (Fig. 4.1B). These results suggested that the genetic factors that determine the phenotype of plaques produced by JUNV are encoded by S genome segment.

To further determine which viral gene encoded by the S segment was responsible for the plaque phenotypes observed for the intersegment chimeric viruses, two intrasegment chimeric viruses, rRom/CanGPC and rRom/CanNP, were genetically engineered to express the GPC and NP genes of Candid #1 origin in the backbone of Romero genome (Fig. 4.1A). Interestingly, both viruses produced plaques of intermediate

size on Vero cell monolayers, between those of Romero and Candid #1 (Fig. 4.1B). This result indicated that both viral genes encoded by the S segment of JUNV genome play a role in the formation of plaques when the virus is cultivated on cell monolayers. Of note, all JUNV clones produced similar titers of infectious virus in the range of 10^6 to 10^7 PFU/ml (Fig. 4.1C) after the firs passage in Vero cells.

Next, to investigate whether the observed plaque phenotypes were associated with impaired ability of recombinant viruses that produce small and medium size plaques to replicate in cultured cells, the growth kinetics of the recombinant chimeric viruses were investigated in IFN-deficient (Vero) and IFN-competent (A549) cells. For this, cells were infected at an MOI of 5 to achieve the infection of > 90% of cells (Condit, 2013) and accumulation of infectious virus in TSC was analyzed to establish the one-step growth curve for each rJUNV and compare to those of the parental rRomero and rCandid #1. The results demonstrated that all rescued inter- and intra-S segment chimeric viruses exhibited similar kinetics of infectious virus production in both Vero and A549 cells (Fig. 4.1D). Thus, it can be concluded that the growth properties of the rescued chimeric viruses in cultured cells cannot account for the differences observed in plaque formation.

Recently, a single amino acid substitution in the transmembrane region of GP2 of XJ13 strain of JUNV has been demonstrated to significantly attenuate its neurovirulence in mice and was proposed as a major attenuating mutation (Albariño et al., 2011b). To evaluate the effect of this mutation in *in vitro* growth and, later, on *in vivo* virulence of JUNV, a version of rRomero was generated where phenylalanine at position 427 of the GPC was substituted for isoleucine (F427I) that is found at this position in the GPC of Candid #1 (Fig. 4.1A). This virus, rRom/G2/F427I, exhibited similar growth properties in Vero and A549 cells to rRomero, rCandid #1, and all rescued chimeric viruses (Fig. 4.1C and D). Interestingly, rRom/G2/F427I produced large plaques in Vero cells that were similar in size and morphology to those of rRomero (Fig. 4.1B), indicating that the F427I

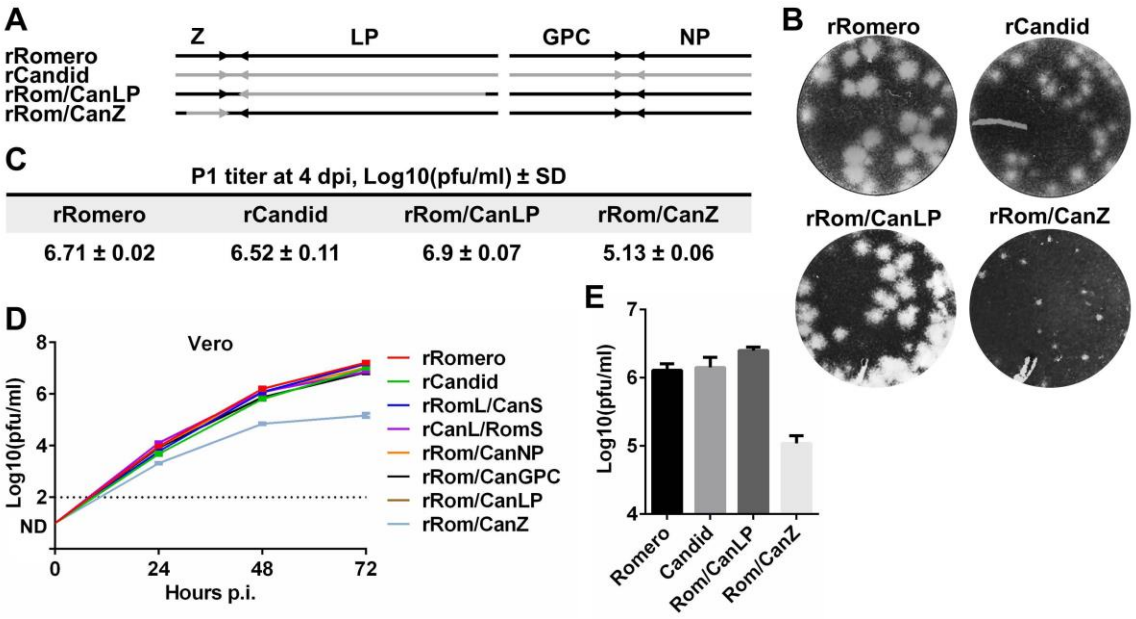

Figure 4.2. Rescue and characterization of *in vitro* growth properties of intra-L segment chimeric viruses between Romero and Candid #1 strains of JUNV. (A) Schematic representation of rJUNV genomes. Black and grey colors indicate the genetic material of Romero and Candid #1 strains of JUNV, respectively. (B) Morphological appearance of plaques on Vero cells. Infected cell monolayers were overlayed with growth medium containing 0.5% agarose and incubated for 7 days. Cells were stained with crystal violet to visualize plaques. (C) Passage one (P1) titers on Vero cells were determined by plaque assay at 4 days post-inoculation (dpi). (D) Growth properties of rJUNVs on Vero cells. TSCs of Vero cells infected at an MOI of 0.01 were collected at the indicated times, and titers were determined by plaque assay. (E) Virus titers in TCS of Vero cells infected with rJUNVs at an MOI of 5 at 48 hours p.i.

substitution in the GPC of Candid #1 was not responsible for the small plaque phenotype exhibited by the attenuated strain of JUNV.

To evaluate the compatibility between the viral genes encoded by the L segment of the JUNV genome, two intra-L segment chimeric viruses, rRom/CanLP and rRom/CanZ, were constructed by replacing the LP and Z genes in the genome of Romero with the corresponding genes of Candid #1 origin (Fig. 4.2A). Surprisingly, the chimeric virus expressing the LP of Romero and the Z protein of Candid #1, rRom/CanZ, produced plaques in Vero cells that were smaller than plaques produced by both parental viruses, rRomero and rCandid #1 (Fig. 4.2B). In contrast, the virus expressing the LP of Candid #1 in combination with the Z protein of Romero produced large plaques similar to those of rRomero (Fig. 4.2B). This unexpected result correlated with the reduction of

virus titer produced by rRom/CanZ after the first passage in Vero cells by more than one log10 when compared to rRomero and rCandid #1 (Fig. 4.2C), which could indicate inhibited growth of rRom/CanZ in cultured cells. Interestingly, rRom/CanLP produced similar P1 titer to those of both rRomero and rCandid #1 (Fig. 4.2C).

Next, the growth properties of both intra-L segment chimeric viruses were assessed in Vero cells and compared to those of parental rRomero and rCandid #1. To ensure detection of even minimal differences in growth kinetics, Vero cells were infected at a low MOI of 0.01 PFU/ml. rRom/CanZ exhibited a delayed growth in Vero cells, whereas rRom/CanLP exhibited growth properties highly similar to both parental viruses (Fig. 4.2D). These results correlated with impaired accumulation of infectious rRom/CanZ virion in TSC of Vero cells, infected at an MOI of 5, collected at 48 hours post-infection (Fig. 4.2E). The obtained data demonstrate that, most likely due to coevolution with its homologous polymerase, the Z protein of Candid #1 has a significantly diminished compatibility with the LP of wild-type Romero. However, on the other hand, the Z of Romero is still able to sufficiently support the replication of rRomero/CanLP that expresses the LP of Candid #1.

In vivo biological properties of inter- and intrasegment chimeric viruses between pathogenic Romero and attenuated Candid #1 strains of JUNV

In a previously published study the neurovirulence of JUNV for mice was found to be associated with the genetic factors, in particular the GPC gene, encoded by the S segment of the viral genome (Albariño et al., 2011b). To investigate whether the S segment contained genetic factors important for the pathogenicity and virulence of JUNV in an animal model that closely mimics the pathological features of human AHF (Emonet et al., 2011b), outbred Hartley guinea pigs were infected via the i.p. route with 10^3 PFU of either rRomL/CanS or rCanL/RomS (Fig. 4.1A). The rRomero virus expressing the

F427I mutation in the transmembrane domain of GP2, rRom/G2/F427I, was also included in this animal experiment to investigate whether this single mutation would attenuate Romero in a guinea pig model of lethal JUNV infection. The survival and disease characteristics of the animals infected with the chimeric viruses were compared to those of guinea pigs infected with the parental viruses, rRomero and rCandid #1 (Fig. 4.1A). Guinea pigs infected with rCanL/RomS experienced a steady weight loss starting at 7 days p.i. that was followed by rapid deterioration of animals' condition around 11 days p.i., development of fever, rapid weight loss, and uniformly lethal outcome between days 17 and 19 p.i. (Fig. 4.3A, B, and C). These data were in good agreement with the results obtained in the animal experiment with rRomero described in the previous chapter (Fig. 3.3). In contrast, none of the guinea pigs inoculated with rRomL/CanS developed any clinical symptoms (Fig. 4.3A) and all infected

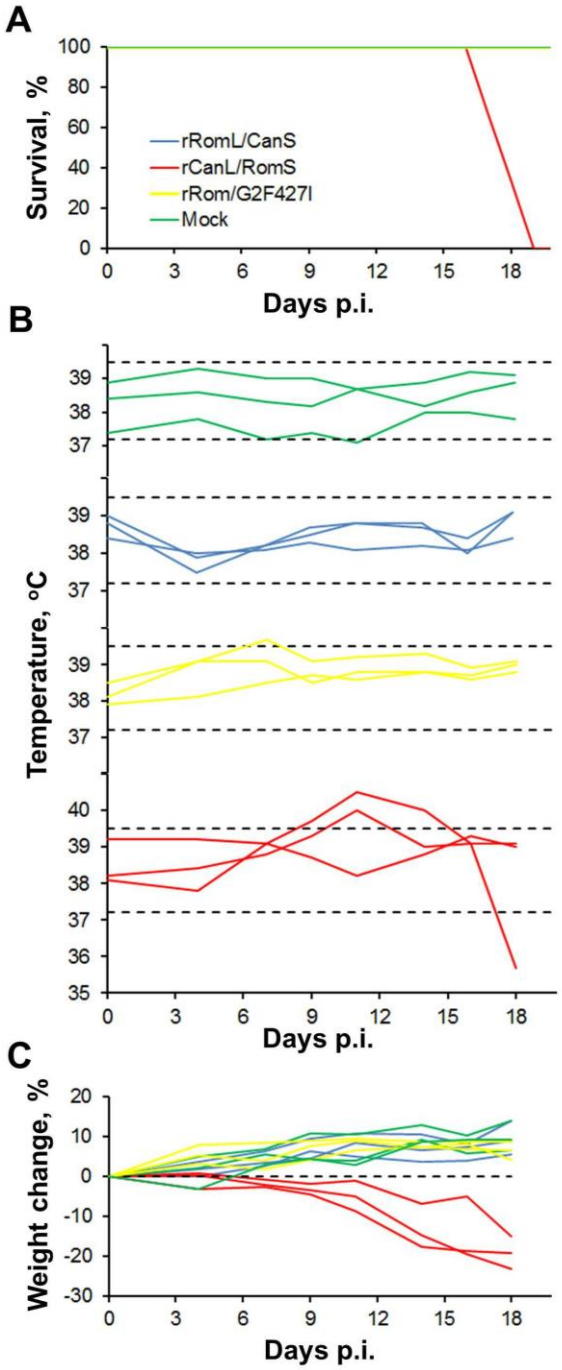

Figure 4.3. Survival and disease characteristics of guinea pigs infected with intersegment chimeric viruses and rRomero expressing the F427I mutation in G2. **(A)** Hartley guinea pigs were inoculated i.p. with 10^3 PFU of rJUNVs (n = 3) and monitored for 21 days for survival. **(B and C)** Body temperatures and weight changes were recorded throughout the course of the study. The range of normal guinea pig body temperature (37.2 -39.5 C^o) is flanked by dashed lines on temperature graphs.

animals gained weight during the observation period (Fig. 4.3C). Likewise, the body temperature of these animals stayed within the normal range (37 - 39.7 ^{o}C) without exhibiting any significant temperature fluctuations (Fig. 4.3B). Interestingly, all guinea pigs inoculated i.p. with rRom/G2/F427 survived the infection (Fig. 4.3A). However, two out three experimental animals experienced a mild weight loss between days 4 and 8 p.i. (Fig. 4.3B), one of which also developed a transient fever that fully resolved by day 10 p.i. (Fig. 4.3C). Analysis of clinical hematology and blood chemistry parameters of the infected guinea pigs revealed that infection with rCanL/RomS, similarly to rRomero infection, caused thrombocytopenia and general immunosuppression indicated by the reduction of platelet, lymphocyte, and total white blood cell counts, as well as decrease in albumin production and release of liver enzymes, most likely associated with liver damage (Table 4.1) (Yun et al., 2008). In contrast, the hematological and blood chemistry values of rRom/CanS- and rRom/G2/F427I-infected animals were highly similar to those of rCandid #1-infected animals (Table 4.1). To further evaluate and compare the degree of *in vivo* attenuation between rRomL/CanS and rRom/G2/F427I, the kinetics of serum neutralizing antibody production were determined by the PRNT assay using rCandid #1 as the test virus (Fig. 4.4). Infection with rRomL/CanS induced neutralizing antibody titers (Fig. 4.4) comparable to the titers detected in sera of rCandid #1- and Candid #1-

Group[b]	Preinoculation/postinoculation values[a]				
	Platelet count (10^3/ml)	White blood cell count (K/μL)	Lymphocyte count (K/μL)	Albumin (g/dl)	Alanine aminotransferase (U/liter)
rRomero	463±122/40±15	5.86±1.7/1.82±0.91	3.69±0.76/0.75±0.37	4.0±0.1/3.0±1.1	34±9/79±25
rCanL/RomS	465±109/137±70	4.79±1.23/1.81±0.56	3.33±0.29/0.62±0.24	4.1±0.3/2.3±0.1	30±3/52±15
rRom/CanNP	518±188/164±74	4.53±0.79/1.87±1.0	3.15±0.29/0.62±0.07	4.1±0.3/2.3±0.4	28±1/46±9
rCandid #1	447±110/464±190	5.60±1.5/6.14±1.64	3.73±1.22/4.48±1.07	3.8±0.0/4.0±0.3	27±6/33±10
rRomL/CanS	493±165/484±124	5.29±0.88/7.44±1.61	3.38±0.47/5.34±1.89	4.2±0.5/3.8±0.4	30±7/29±8
rRom/CanGPC	447±53/590±103	5.01±0.67/9.22±4.17	3.22±0.72/4.01±1.14	4.6±0.6/3.9±0.2	30±4/34±6
rRom/G2/F427I	544±107/528±101	3.96±0.6/6.41±2.3	2.75±0.64/4.81±1.68	4.1±0.2/3.8±0.3	29±5/32±2

Table 4.1. Hematology and blood chemistry parameters in guinea pigs infected with virulent and attenuated chimeric JUNV variants.
(a) Blood was collected preinfection (day −7) and postinfection (day +12), and hematology and blood chemistry parameters were analyzed.
(b) Hartley guinea pigs were inoculated i.p. with 10^3 PFU of rJUNVs.

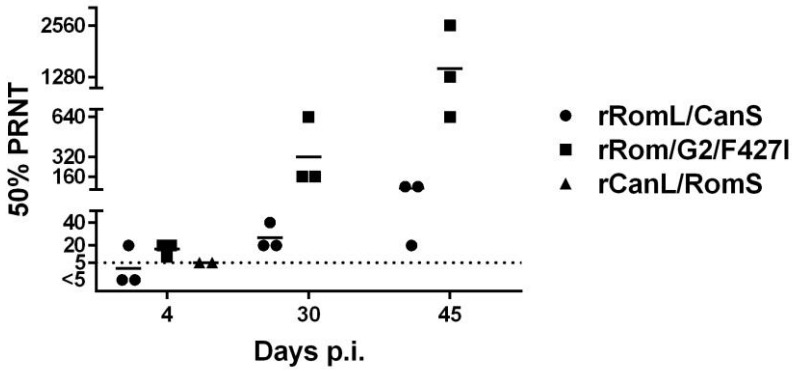

Figure 4.4. Imunogenicity comparison between intersegment chimeric viruses and rRomero expressing the F427I mutation in G2. Serum samples were collected from guinea pigs at the indicated time points and the titers of Candid #1-specific neutralizing antibodies were determined by 50% plaque reduction neutralization test (PRNT). Horizontal dashes indicate average titer values.

immunized guinea pigs (Fig. 3.3D), suggesting that rRomL/CanS exhibits similar *in vivo* biological properties to rCandid #1. Interestingly, rRom/G2/F427I infection induced much higher neutralizing antibody titers at 30 and 45 days p.i. than rRomL/CanS infection (Fig. 4.4), which, together with the ability of rRom/G2/F427I to induce a mild disease in infected guinea pigs, may suggest that replication of rRom/G2/F427I is less restricted in infected animals than replication of rRomL/CanS. Therefore, it can be concluded that, the genetic factors encoded by the S segment of viral genome are the major determinants of JUNV virulence in guinea pigs. In line with previously published results from a study with a murine model of JUNV neurovirulence (Albariño et al., 2011b), the F427I mutation in the transmembrane domain of GP2 significantly attenuated the Romero strain of JUNV; however, other mutations present in the S segment of Candid #1 are required for complete attenuation of the virus.

To further investigate the compatibility of JUNV proteins between the pathogenic Romero and the attenuated Candid #1 strains of the virus and evaluate the role of each protein in its virulence, pathogenesis, and attenuation, Hartley guinea pigs were infected with either the intra-S segment chimeric viruses rRom/CanNP and rRom/CanGPC, or the intra-L segment chimeric viruses rRom/CanZ and rRom/CanLP (Fig. 4.5). Surprisingly,

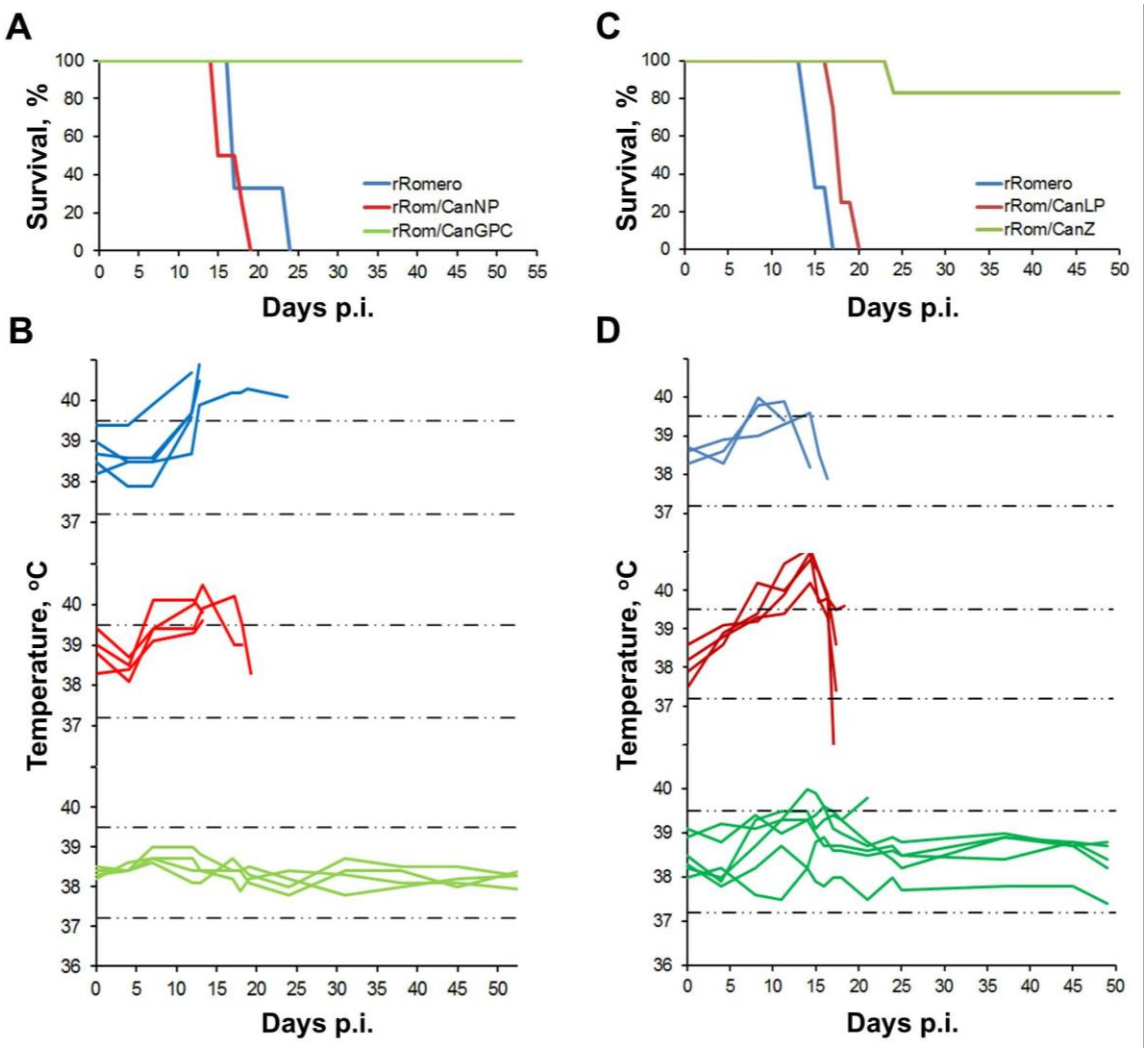

Figure 4.5. Survival and disease characteristics of guinea pigs infected with intra-S and –L segment chimeric viruses between Romero and Candid #1 strains of JUNV. (A and C) Hartley guinea pigs were inoculated i.p. with 10^3 PFU of rJUNVs and monitored for 50 days for survival. **(B and D)** Body temperatures were recorded throughout the course of the study. The range of normal guinea pig body temperature (37.2 -39.5 C^o) is flanked by dashed lines on temperature graphs.

substitution for the NP of Candid #1 origin in the genome of Romero did not cause attenuation of rRom/CanNP virus. All infected animals developed a disease characteristic of Romero infection, accompanied with weight loss (data not shown) and fever (Fig. 4.5B), and died by 20 days p.i. (Fig. 4.5A). On the other hand, inoculation of guinea pigs with rRom/CanGPC that expresses the GPC of Candid #1 and all the other viral proteins of Romero, did not result in a detectable disease (Fig. 4.5B) and all the animals survived

the infection (Fig. 4.5A). Although all guinea pigs inoculated with rRom/CanLP (rRomero expressing the LP of Candid #1) succumbed to infection (Fig. 4.5C), these animals exhibited delayed disease development with peak fever recorded at 13-14 days p.i., which was approximately 2-3 days later than that for rRomero-infected animals (Fig. 4.5D). Interestingly, 3 out of 6 guinea pigs inoculated with rRom/CanZ (rRomero that encodes only the Z of Candid #1), that exhibited delayed growth in cultured cells, developed a transient fever between 8 and 17 days p.i. that lasted on average for 3-4 days (Fig. 4.5D). However, only one out 3 animals that developed disease symptoms ultimately succumbed to infection on day 24 p.i. (Fig. 4.5C). All survived animals developed high titers of neutralizing antibodies (PRNT50 titers of >>160) by 38 days p.i. Collectively, the obtained data demonstrated that the amino acid changes accumulated in the GPC during *in vivo* and *in vitro* passaging are the main determinants of the attenuated phenotype of Candid #1. On the other hand, mutations in the NP of Candid #1 did not attenuate the virulence of the pathogenic strain of JUNV, suggesting that these mutations occurred as a result of adaptation to amino acid changes in other viral proteins. Intriguingly, the chimeric virus (rRom/CanLP) that expresses the LP of Candid #1 and Z, NP, and GPC of Romero exhibited a lower level of virulence than rRomero, which may have indicated suboptimal expression of viral genes by the chimeric polymerase complex that resulted in partial virus attenuation. Importantly, rRom/CanZ chimeric JUNV that exhibited highly attenuated growth in tissue culture was able to induce disease and caused partial mortality in inoculated guinea pigs, suggesting that the attenuated phenotype of this virus was most likely solely associated with impaired virion production by infected cells.

To confirm that the complete attenuation of JUNV was only achieved when the full-length GPC of Candid #1 origin was expressed, histopathological manifestations in the spleen and liver were compared between guinea pigs infected with either intersegment chimeric viruses (rRomL/CanS and rCanL/RomS), intra-S segment

Viruses[a]	Virulence for guinea pigs	Histological changes[b]	
		Spleen	Liver
rRomero rCanL/RomS rRom/CanNP	Yes	• congested and depleted red pulp • depleted, non-reactive white pulp • scattered macrophages and polymorphonuclear cells	• microvesicular and macrovesicular steatosis • periportal and lobular inflammation
rCandid #1 rRomL/CanS rRom/CanGPC rRom/G2/F427I	No	unremarkable	• rare foci of periportal and lobular inflammation

Table 4.2. Histophatological findings in tissues of guinea pigs infected with chimeric JUNV variants.
(a) Guinea pigs were inoculated i.p. with 10^3 PFU of rJUNVs and euthanized at 12 dpi.
(b) Histopathologic analysis was performed on H&E-stained tissue sections.

chimeric viruses (rRom/CanNP and rRom/CanGPC), rRomero expressing the F427I mutation in G2 (rRom/G2/F427I), or parental viruses rRomero and rCandid #1. These organs were selected based on the results from animal experiments with rRomero, where the most pronounced pathological changes were observed in the spleen and liver. Thus, histological sections from three animals randomly selected in each group that were euthanized at 11 days p.i. were subjected to standard hematoxylin and eosin staining and evaluated by a pathologist blinded to the conditions of the experiment. A summary of histopathological findings is presented in Table 4.2. All animals that were inoculated with virulent variants of JUNV (rCanL/RomS and rRom/CanNP) and succumbed to infection exhibited histopathological changes highly similar to those found in the organs of rRomero-infected animals (Fig. 3.4). The changes in the spleen were characterized by congestion and decreased cellularity of the red pulp, presence of macrophages and scattered polymorphonuclear cells, and depletion of the white pulp without overt necrosis. The manifestations in the liver were characterized by diffuse microvesicular and, sometimes, macrovesicular steatosis, periportal and lobular inflammation, and the presence of nuclear debris in portal triads. In general, the spleen and liver of guinea pigs that were inoculated with avirulent variants of JUNV (rRomL/CanL, rRom/CanGPC, and rRom/G2/F427I) did not show any significant pathological changes; however,

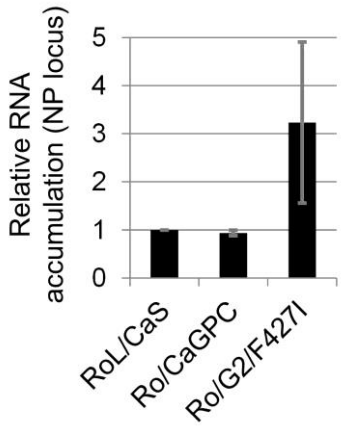

Figure 4.6. Relative levels of viral RNA in the brains of infected guinea pigs. Total RNA was extracted from brain tissues of rJUNV-infected guinea pigs euthanized at 12 dpi. Quantitative RT-PCR using SYBR Green dye was performed in triplicates. Levels of RNA derived from NP locus normalized to GAPDH mRNA are expressed as the ratio relative to the NP RNA level in rRomL/CanS brain tissue sample. Average values and standard deviations are shown. RoL/CaS, rRomL/CanS. Ro/CaGPC, rRom/CanGPC. Ro/G2/F427I, rRom/G2/F427I.

occasionally, rare foci of periportal and lobular inflammation were observed in the liver and the presence of scattered macrophages was detected in the white pulp of the spleen. Intriguingly, the histopathological manifestations in the organs of rRom/G2/F427I-infected guinea pigs were more pronounced than the changes observed in the organs rRomL/CanS- or rRom/CanGPC-infected animals. Specifically, the livers of guinea pigs infected with rRom/G2/F427I showed more foci of mononuclear cell inflammation with the presence of hepatocyte apoptosis. These results supported the hypothesis that rRom/G2/F427I replicates more efficiently in the organs of infected guinea pigs than rRomL/CanS and rRom/CanGPC. To further confirm greater organ distribution of rRom/G2/F427I, compared to rRomL/CanS and rRom/CanGPC, the levels of viral RNA in the brain, spleen and liver at 11 days p.i. were evaluated. Although virus presence could not be detected in the spleen and liver of infected animals in any of the experimental groups, the rRom/G2/F427I-infected animals contained greater amounts of viral RNA in the brain than rRomL/CanS- and rRom/CanGPC-infected animals (Fig. 4.6). Therefore, the F427I amino acid change in the transmembrane region of G2 was

identified as a major attenuating mutation of JUNV in guinea pigs; however, other mutations in the GPC of Candid #1 were required to restrict viral replication in the organs of infected animals below pathogenic levels.

DISCUSSION

Here, I have described the rescue of inter- and intrasegment recombinant chimeric JUNVs between the pathogenic Romero and the attenuated Candid #1 strains. For this, a pol-I/pol-II reverse genetics system, described in the previous chapter, was utilized to either exchange the genome RNA segments, L and S, between Romero and Candid #1 (rRomL/CanS and rCanL/RomS (Fig. 4.1A)) or genetically engineer variants of Romero virus where individual viral genes were substituted with the corresponding counterparts of Candid #1 origin (rRom/CanGPC, rRom/CanNP, rRom/CanZ, and rRom/CanLP (Figs. 4.1A and 4.2A)). Analysis of the *in vitro* growth properties of the intersegment chimeric viruses containing one RNA segment derived from the genome of Romero and the other from the genome of Candid #1 showed that the GPC/NP and Z/LP combinations encoded by the S and L segments, respectively, were fully exchangeable between the two strains as both chimeric viruses exhibited similar cell culture replication kinetics to each other and both parental viruses, rRomero and rCandid #1. The plaque phenotypes of both intersegment chimeric viruses were determined by the origin of the S segment in the genome; the virus containing the S segment of Romero produced large plaques similar to those produced by rRomero and the virus containing the S segment of Candid #1 produced small plaques similar to those produced by rCandid #1 (Fig. 4.1B). Further analysis of intra-S and –L segment chimeric viruses revealed that GPC, NP, and LP of Candid #1 were fully compatible with the proteins and genetic material of Romero, since all three combinations of the viral proteins between Candid #1 and Romero were able to efficiently support the growth of chimeric viruses rRom/CanGPC, rRom/CanNP, and

rRom/CanLP, respectively, in IFN-deficient Vero and IFN-competent A549 cells (Figs. 4.1D and 4.2D & E). Interestingly, both inter-S segment chimeric viruses rRom/CanNP and rRom/CanGPC produced plaques of intermediate size between plaques produced by rRomero and rCandid #1, indicating that both viral proteins are involved in the process of plaque formation. One possible explanation for the small plaque phenotype of rCandid #1 and chimeric JUNVs containing genes encoded by the S segment of Candid #1 could be that these viruses are more potent apoptosis inducers in the infected cells than rRomero and rRomero-like viruses, which, on the other hand, could lead to early cell death and limited cell-to-cell viral spread under agarose overlay (see Materials and Methods). However, the exact mechanism of this process requires further investigation. Surprisingly, the intra-L segment chimeric virus encoding the Z of Candid #1 in the background of Romero, rRom/CanZ, produced very small plaques and exhibited delayed *in vitro* growth in Vero cells (Fig. 4.2). In contrast, the chimeric virus that encodes the LP of Candid #1 and all the other viral proteins, including Z, of Romero, rRom/CanLP, did not display attenuated growth in cell culture. These results strongly suggest specific incompatibility between the LP of Romero and Z of Candid #1 that has likely resulted from the coevolution of Z with LP during generation of Candid #1 (Ambrosio et al., 2011) to accommodate amino acid changes in the viral polymerase. Of note, the single amino acid change F427I in the G2 that has been demonstrated to attenuate JUNV neurovirulence in mice (Albariño et al., 2011b) neither affected the growth kinetics nor changed the plaque phenotype of rRomero (Fig. 4.1). Nevertheless, the obtained results clearly indicated that the plaque phenotype of the chimeric viruses did not correlate with their ability replicate and produce infectious progeny in cultured cells.

The next step was to investigate the *in vivo* pathogenicity and virulence of the chimeric viruses in a guinea pig model of lethal JUNV infection that closely reproduces the features of human AHF (Yun et al., 2008). In general, all generated recombinant viruses could be divided into two groups based on virulence, pathogenicity, and clinical

disease parameters observed in infected guinea pigs: the Romero-like viruses and the Candid #1-like viruses. Interestingly, all viruses that encoded the GPC derived from the genome of Romero (rCanL/RomS, rRom/CanNP, rRom/CanLP, and rRom/CanZ) exhibited a virulent phenotype in infected guinea pigs. Although, the rRomero virus expressing the Z of Candid #1, rRom/CanZ, induced an AHF-like disease in 50% of inoculated guinea pigs (3 out of 6) (Fig. 4.5D) that resulted in the death of only one animal (Fig. 4.5C), the observed partial attenuation of this virus was most likely caused by impaired growth in infected cells due to functional incompatibility between Romero LP and Candid #1 Z (Fig. 4.2E). In line with these data, the guinea pigs inoculated with rRom/CanLP, expressing the LP of Candid #1 and the Z of Romero, developed disease and died approximately 2-3 days later than rRomero-infected animals (Fig. 4.5C & D), which may have indicated impaired ability of the Candid #1 Z to control the activity of the Romero LP (Kranzusch and Whelan, 2011) leading to more efficient recognition of viral replication by the RIG-I-mediated mechanisms (Huang et al., 2012). Overall, these results demonstrated that the glycoproteins of JUNV were the major virulence determinant in a representative animal model of AHF; however, the optimal interaction between the viral polymerase and the matrix protein Z was also important for *in vivo* virulence of the virus.

On the other hand, the recombinant viruses that encoded either the full-length GPC of Candid #1 (rRomL/CanS and rRom/CanGPC) or the GPC of Romero containing the F427I mutation in G2 (rRom/G2/F427I) were highly attenuated and did not cause any mortality in inoculated guinea pigs (Figs. 4.3A and 4.5A). However, the animals that were inoculated with rRom/G2/F427I contracted a mild non-lethal disease that fully resolved by the end of observation period (Fig. 4.3). These animals developed much higher neutralizing antibody levels than rRomL/CanS-inoculated guinea pigs (Fig. 4.4) and had greater amounts of viral RNA in the brain than the animals inoculated either with the intersegment chimeric JUNV containing the entire S segment of Candid #1

(rRomL/CanS) or the variant of rRomero expressing only the GPC of the attenuated parental strain (rRom/CanGPC) (Fig. 4.6) most likely due to a better ability of rRom/G2/F427I to replicate and disseminate in the tissues of infected guinea pigs. This hypothesis was further supported by histological analysis of tissue sections from infected guinea pigs that revealed higher levels of immune cell infiltration in the organs of the rRom/G2/F427I-infected animals compared to the rRomL/CanS- and rRom/CanGPC-infected animals (Table 4.2). Therefore, an overall conclusion can be drown that although the single amino acid change F427I in the transmembrane region of G2 that likely impacts the ability of the glycoprotein complex to mediate cell entry (Droniou-Bonzom et al., 2011) is indeed a major determinant of JUNV attenuation, other amino acid changes that occurred in the GPC of Candid #1 during *in vivo* and *in vitro* passaging are (Ambrosio et al., 2011) required for complete *in vivo* attenuation of the virus.

CHAPTER 5: THE ROLE THE ENVELOPE GLYCOPROTEINS IN THE REPLICATION CYCLE OF JUNIN VIRUS

INTRODUCTION

Replication and expression of arenavirus genome is strictly regulated during infection. After the genetic material is delivered into the cytoplasm, the viral polymerase initiates synthesis of genomic and anti-genomic segment RNA species, as well as mRNA of viral genes. Studies of the prototypic arenavirus LCMV-infected cells demonstrated that the maximal level of viral RNA synthesis that preceded peak virus titers was followed by a marked decrease in the rate of RNA production (Cornu and de la Torre, 2001). Therefore two phases of arenavirus replication cycle have been proposed: the active genome replication and expression phase and the virion assembly and budding phase. In the same study, a MG system was utilized to demonstrate that the small arenavirus RING finger protein Z inhibited *in vitro* transcription and replication of an S segment-based construct (Cornu and de la Torre, 2001). Later, Z of MACV was demonstrated to form a direct heterodimeric complex with the homologous LP and lock it in a promoter-bound form, thus preventing from processing the template genome RNA. Interestingly, the ability of Z to inhibit LP activity was found to be conserved between closely related arenavirus species, as the Z of the New World arenavirus JUNV exhibited similar ability to block RNA synthesis by the MACV replication complex. In contrast, the Z of a distantly related Old World arenavirus LCMV neither interacted nor inhibited the functional activity of MACV LP (Kranzusch and Whelan, 2011). The mechanism of interaction between LP and Z has been proposed to be involved in the regulation of the arenavirus life cycle. Thus, in the early phase of infection, low concentration of Z allows for active viral RNA synthesis; however, accumulation of high levels of Z in infected

cells over time leads to the blockade of the Z-LP complex bound the viral promoter, which may also be important to ensure inclusion of the viral polymerase into arenavirus virions (Kranzusch et al., 2010; Kranzusch and Whelan, 2011).

A single amino acid change in the transmembrane region of the envelope glycoprotein G2 of Candid #1 strain of JUNV has been demonstrated to significantly attenuate the virus neurovirulence in mice (Albariño et al., 2011b) and virulence in a guinea pig model closely reproducing the features of human AHF (this dissertation, Chapter 4). This mutation, F427I, has been shown to destabilize the metastable conformation of the glycoprotein complex triggering transition to a fusogenic conformation at neutral pH. This could possibly limit tissue dissemination of Candid #1 (Droniou-Bonzom et al., 2011). However, the F427I mutation occurred during final passaging of Candid #1 in fetal rhesus monkey lung FRhL-2 cells (Ambrosio et al., 2011) and does not explain the attenuated phenotype of the predecessor to Candid #1 strains XJ37 and XJ44 (Yun et al., 2008).

Previously, the GPC of LCMV have been demonstrated to induce ER stress and trigger UPR (Pasqual et al., 2011). Thus, acute infection with LCMV induced production of BiP, an ER-resident protein that provides initial folding assistance to completely unfolded or unstructured nascent polypeptide chains (Schröder, 2008), and selectively activated the ATF6-controlled branch of UPR while the PERK- and IRE1-regulated pathways were neither activated nor blocked. Expression of the individual LCMV proteins demonstrated that only production of the GPC triggered ATF6-mediated UPR, observed during LCMV-infection. Importantly, rapid down regulation of GPC expression during transition from acute to persistent LCMV infection resolved ER stress conditions and returned UPR signaling to basal levels (Pasqual et al., 2011).

In this chapter, I present a detailed comparison of the transcriptional and protein expression profiles between the inter- and intrasegment chimeric JUNV variants described in the previous chapter. The recombinant viruses expressing the GPC of

Candid #1 that exhibited an attenuated phenotype in guinea pigs demonstrated markedly higher levels of RNA synthesis and protein production in infected cells than the virulent viruses expressing the GPC of Romero. The GPs of Candid #1 were demonstrated to undergo abnormal post-translational processing resulting in the induction of ER stress response and may have a diminished ability to interact with the RING finger protein Z that may lead to dysregulated replication and expression of the viral genome, which could potentially facilitate immune recognition of JUNV infection.

RESULTS

Virulent and attenuated variants of JUNV exhibit different patterns and kinetics of protein expression in infected cells

To further investigate molecular mechanisms that could lead to attenuation of JUNV, the expression patterns and kinetics of viral protein production was compared between the rescued inter- and intrasegment chimeric viruses (Figs. 4.1A and 4.2A) and parental rRomero and rCandid #1. The anti-G2, anti-NP, and anti-Z antibodies used in the Western blot experiments were raised against conserved regions of the viral proteins between Romero and Candid #1. Analysis of GP expression in Vero cells revealed two distinct Western blot patterns for the viruses that exhibited a virulent phenotype in guinea pigs and expressed the GPC of Romero (rRomero, rCanL/RomS, rRom/CanNP, rRom/CanLP, and rRom/CanZ) and the viruses that were attenuated in guinea pigs and expressed the GPC of Candid #1 (rCandid #1, rRomL/CanS, and rRom/CanGPC) (Fig. 5.1A). Thus, the lysates of cells infected with the attenuated viruses contained additional bands between the G2 and the uncleaved G1G2 precursor and the proportion between the amounts of G2 and G1G2 was shifted towards the unprocessed precursor (Fig. 5.1A). The total amounts G2 and G1G2 and the amounts of NP accumulated in cells 44 hours after

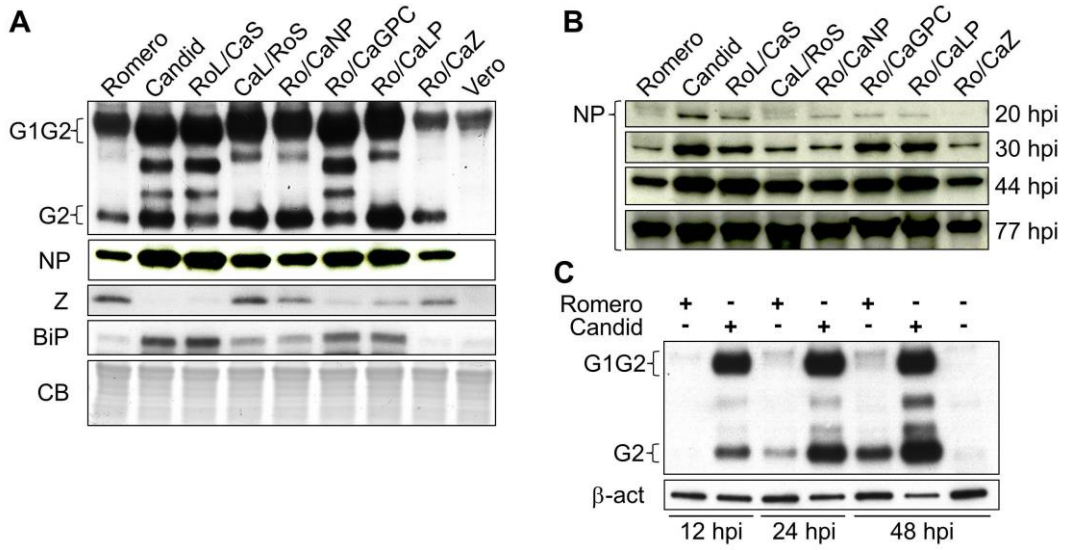

Figure 5.1. Protein expression profiles and kinetics of chimeric JUNV variants. (A) Differential expression of proteins by Vero cells infected at an MOI of 0.1. Cells were lysed in Laemmli's SDS sample buffer at 44 hours post-infection (hpi). Viral proteins were detected by Western blotting using antibodies raised against conserved regions of G2, NP, and Z between Romero and Candid #1. The gel was pre-stained with Coomassie blue (CB) to ensure equal sample loading. **(B)** Kinetics of NP expression. Vero cells infected in the same conditions as in (A) (MOI 0.1) were collected at the indicated time points and the levels of NP expression were determined by Western blotting. Equal sample loading was monitored by CB staining (not shown). **(C)** GP banding pattern and kinetics of expression between rRomero (Romero) and rCandid #1 (Candid). Vero cells were infected at an MOI of 5 and cell lysate samples were collected at the indicated time points. Western blot was probed with anti-G2 antibody. β-actin was used to control for equal sample loading.

infection were higher for the JUNV variants that were attenuated in guinea pigs and rRom/CanLP, infection of guinea pigs with which resulted in delayed disease development and mortality, compared to the viruses that were virulent for guinea pigs (Fig. 5.1A). The differences between the NP levels appeared early after infection and persisted until late stages of viral growth (Fig. 5.1B). Intriguingly, the differences in the GP banding patterns and the total amounts of produced G1 and G1G2 observed between the virulent and attenuated variants of JUNV at 44 hours p.i. (Fig. 5.1A), also occurred early and persisted throughout the course of infection in cells infected with virulent rRomero and attenuated rCandid #1 (Fig. 5.1C). Interestingly, all samples that showed additional bands between the fully processed G2 and the uncleaved G1G2 precursor also

had lower amounts of Z than the samples that predominantly showed the G2 and G1G2 bands (Fig. 5.1A). These results clearly demonstrated that the attenuated and virulent variants of JUNV exhibited different protein expression profiles in infected cells.

Attenuated variants of JUNV exhibit higher levels of RNA synthesis than virulent variants

The next step was to investigate whether the observed differences in protein expression between the virulent and attenuated variants of JUNV were due to higher levels of functional activity of the polymerase complexes of attenuated viruses resulting in the synthesis of greater amounts of viral mRNA. To this end, Vero cells were infected with the inter- and intrasegment chimeric JUNVs and intracellular levels of viral RNA at early (24 hours p.i.) and late (48 hours p.i.) phases of viral growth were determined by Northern blot analysis (Fig. 5.2A). The accumulated amounts of antigenomic S segment RNA and NP mRNA precisely correlated with the amounts of NP produced in the infected cells between virulent and attenuated virus variants (compare Figs. 5.1B and 5.2A). Interestingly, the high level of NP mRNA synthesis detected early in infection (24 hours p.i.) markedly decreased in the late phase of viral growth (48 hours p.i.) (Fig. 5.2A) when the rate of infectious particle production had already plateaued (Fig. 4.1D). Similar results were obtained for the levels of genomic S RNA and GPC mRNA (Fig. 5.2B). To investigate the nature of observed discrepancies in the levels viral RNA production, the activity levels of Romero and Candid #1 LPs were tested using MG constructs expressing the firefly luciferase marker in lieu of viral genes that were generated based on the S segments of Romero and Candid # genomes. Surprisingly, similar levels of activity were achieved when homologous LP/NP combinations of Romero and Candid #1 were used to express luciferase from both viral gene loci, GPC and NP, of homologous MG templates (Fig. 5.2C). This finding indicated that in JUNV-infected cells the level of viral RNA

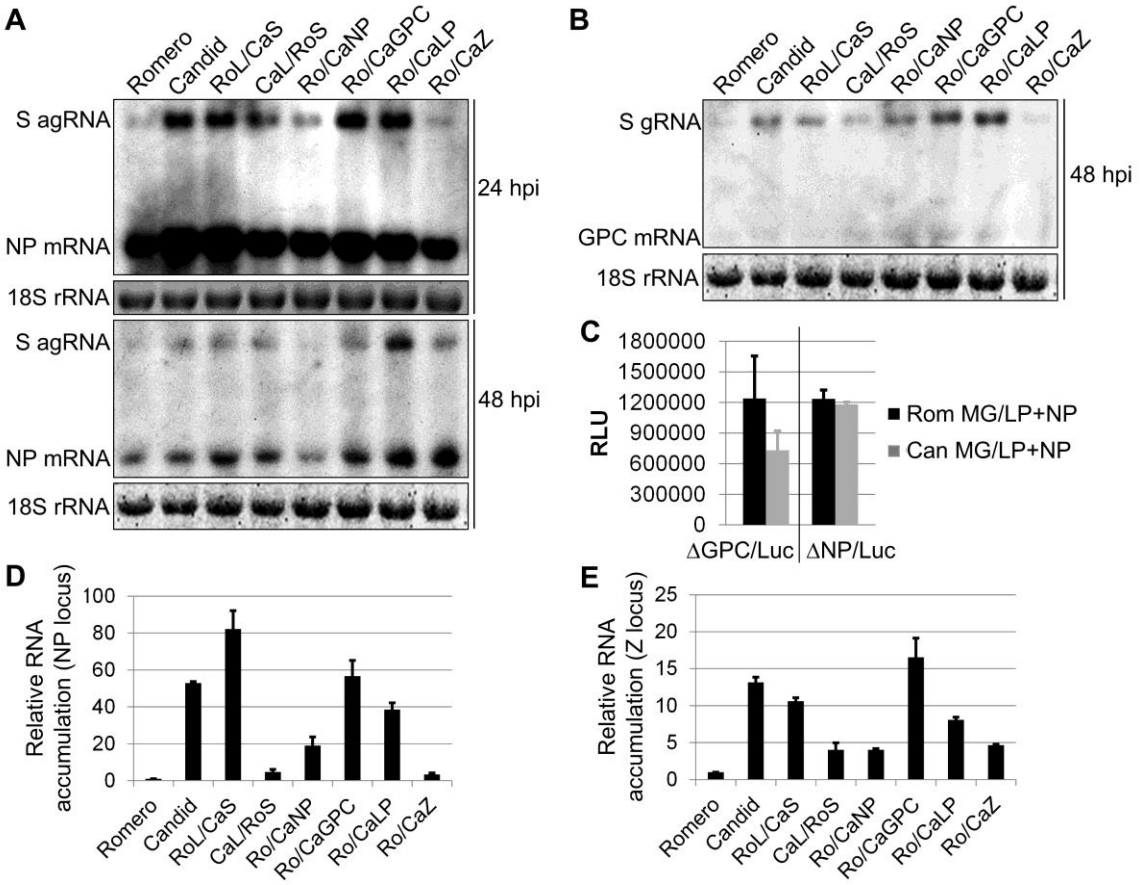

Figure 5.2. Comparison of transcriptional activity between the polymerase complexes of chimeric JUNV variants. (A and B) Levels of genomic (gRNA) and anti-genomic (agRNA) S serment RNA species, and mRNA of the GPC and NP genes in Vero cells infected with rJUNVs. Cells were infected at an MOI of 5 and harvested at the indicated time points. Total RNA was isolated and analyzed by Northern blot for viral RNA species. Equal sample loading and RNA integrity was controlled by EtBr staining of 18S rRNA. **(C)** Comparison between the activities of Romero LP and Candid #1 LP in minigenome (MG) assays. BHK-21S cells were transfected with murine pol-I promoter-driven S segment-based minigenome (MG) constructs expressing firefly luciferase in lieu of either GPC (ΔGPC/Luc) or NP (ΔNP/Luc) gene together with pol-II expression constructs for LP and NP. The levels of luciferase expression were determined at 48 hours after transfection with Romero (Rom MG/LP+NP) or Candid #1 (Can MG/LP+NP) constructs. RLU, relative light units. **(D and E)** Relative viral RNA accumulation transcribed from either NP **(D)** or Z **(E)** gene locus. Vero cells were infected in the same conditions as in (A) and (B) (MOI 5) and harvested at 24 hours p.i. Quantitative RT-PCR using SYBR Green dye was performed in triplicates. Levels of viral RNA normalized to GAPDH mRNA are expressed as the ratio relative to the level of viral RNA in cells infected with rRomero. Average values and standard deviations are shown. Romero, rRomero. Candid, rCandid #1. RoL/CaS, rRomL/CanS. CaL/RoS, rCanL/RomS. Ro/CaNP, rRom/CanNP. Ro/CaGPC, rRom/CanGPC. Ro/CaLP, rRom/CanLP. Ro/CaZ, rRom/CanZ.

synthesis is determined rather by the viral regulatory mechanisms controlling the polymerase complex mediated by LP/Z interaction than the functional activity of LP.

Next, the total levels of L segment RNA and Z mRNA synthesis were evaluated by quantitative PCR (qPCR). This method of viral RNA detection was chosen because of the small size of the Z protein gene, which greatly limited the sensitivity of Northern blot analysis (data not shown). In line with the results from Northern blot experiments, the total levels of S segment RNA and NP mRNA were higher at 24 hours p.i. in Vero cells infected with the attenuated variants of JUNV (Fig. 5.2A & D). This indicated that the experimental data obtained by qPCR was in good correlation with the data obtained in Northern blot experiments. Intriguingly, the intracellular levels of L segment RNA and Z mRNA detected by qPCR were proportional to the levels of S segment RNA and NP mRNA detected by Northern blot and qPCR assays between the attenuated and virulent viruses (Fig. 5.2, compare panel E to panels A & D). However, in the Western blot experiments, the amounts of Z accumulated in infected cells were lower for the attenuated variants of JUNV compared to the virulent variants (Fig. 5.1A). These data strongly suggested that the low levels of Z in Vero cells infected with the attenuated JUNV variants were not caused by impaired transcription of the genes encoded by the L segment, but were rather due to excretion of Z from the cells by an unknown mechanism.

Abnormal post-translational processing of the envelope glycoproteins of attenuated Candid #1 strain of Junin virus induces endoplasmic reticulum stress response

The inter- and intrasegment chimeric JUNVs expressing the GPC of *in vivo* attenuated Candid #1 strain of JUNV exhibited a distinct viral protein expression profile in Vero cells that markedly differed from that of the viruses expressing the GPC of the virulent Romero strain (Fig. 5.3). Comparison of the protein expression profiles in

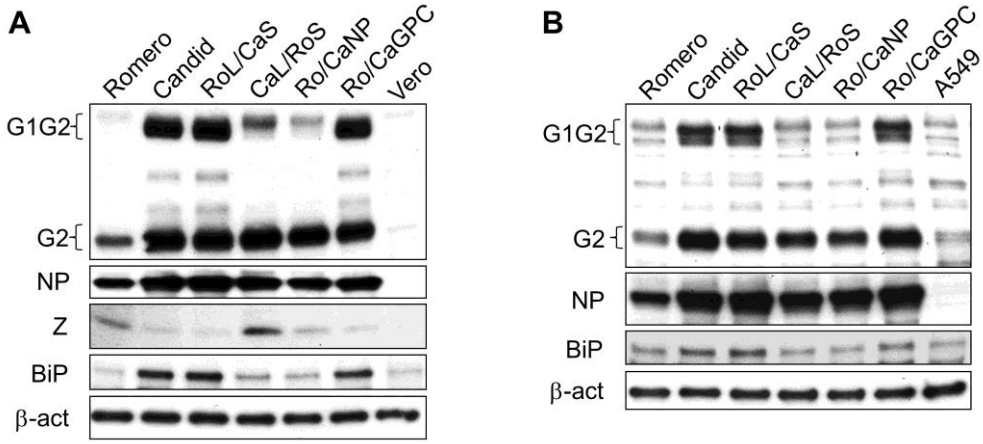

Figure 5.3. Protein expression profiles of chimeric JUNV variants in Vero and A549 cells. Differential expression of viral proteins and the UPR marker BiP in Vero **(A)** and A549 **(B)** cells infected with chimeric JUNV variants. Cells were infected at an MOI of 5 and harvested at 48 hours p.i. The levels of viral and cellular proteins were determined by Western blotting. Romero, rRomero. Candid, rCandid #1. RoL/CaS, rRomL/CanS. CaL/RoS, rCanL/RomS. Ro/CaNP, rRom/CanNP. Ro/CaGPC, rRom/CanGPC. Ro/CaLP, Vero, lysate of mock-infected Vero cells. A549, lysate of mock-infected A549 cells.

infected IFN-deficient primate Vero (Fig. 5.3A) and IFN-competent human A549 (Fig. 5.3B) cells clearly demonstrated that the expression patterns of the viral proteins and specifically the presence of additional GP bands of intermediate sizes between G2 and G1G2 for the chimeric viruses expressing the GPC of Candid #1 was highly similar in both nonhuman primate and human cells, the species for which Candid #1 is highly attenuated (McKee et al., 1992; McKee et al., 1993), and was independent of the functional state of IFN signaling. These results allowed to hypothesize that the nascent GPC of Candid #1 undergoes abnormal post-translational processing that leads to decreased production of fully processed G2 and induction of ER stress. To test this hypothesis the lysates of Vero and A549 cells infected with the recombinant viruses expressing the GPC of either Candid #1 or Romero were analyzed for intracellular accumulation of the ER chaperon protein BiP that senses unfolded proteins in ER lumen and activates the UPR under stress conditions (Liu et al., 2003). Activation of BiP expression has previously been utilized to demonstrate UPR induction in LCMV-infected cells (Pasqual et al., 2011). Remarkably, both Vero (Fig. 5.3A) and A549 (Fig. 5.3B)

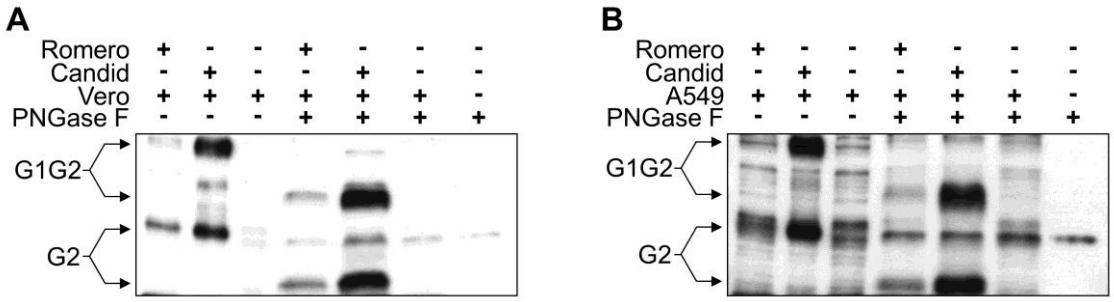

Figure 5.4. N-linked glycosylation status of the GPs of Romero and Candid #1 in Vero and A549 cells. Lysates of Vero **(A)** or A549 **(B)** cells infected at an MOI of 5 with either rRomero (Romero) or rCandid #1 (Candid) were treated with PNGase F to remove N-linked oligosaccharides from protein backbone. The GP banding patterns were analyzed by Western blotting using an anti-G2 antibody.

cells exhibited marked upregulation of BiP expression upon infection with JUNV variants expressing the GPC of Candid #1. In contrast, the levels of BiP expression were only slightly elevated in cells infected with viruses expressing the GPC of Romero (Fig. 5.3). Therefore, the obtained results suggested that expression of Candid #1 GPC, but not Romero GPC, in infected cells results in ER stress and induction of UPR.

To further investigate whether the appearance of additional GP bands was due to abnormal posttranslational modification of Candid #1 GPs, the lysates of infected Vero (Fig. 5.4A) and A549 (Fig. 5.4B) cells were treated with the peptide -N-glycosidase F (PNGase F) (New England Biolabs) to remove N-linked glycanes from the protein backbone. As expected, the treatment almost completely eliminated the protein bands of intermediated size observed in untreated samples containing Candid #1 GPC and the Western blot samples predominantly showed two protein bands corresponding to unglycosylated G2 and G1G2 (Fig. 5.4). Of note, the anti-G2 antibody used in Western blot experiments exhibited a high degree of nonspecific binding to PNGase F; however, this band had a higher mobility than the GP bands in untreated samples and could not mask any of the bands between untreated G2 and G1G2 (Fig. 5.4). Thus, the observed difference in the GP banding patterns between Romero and Candid #1 was caused by abnormal post-translational glycosylation of Candid #1 GPs.

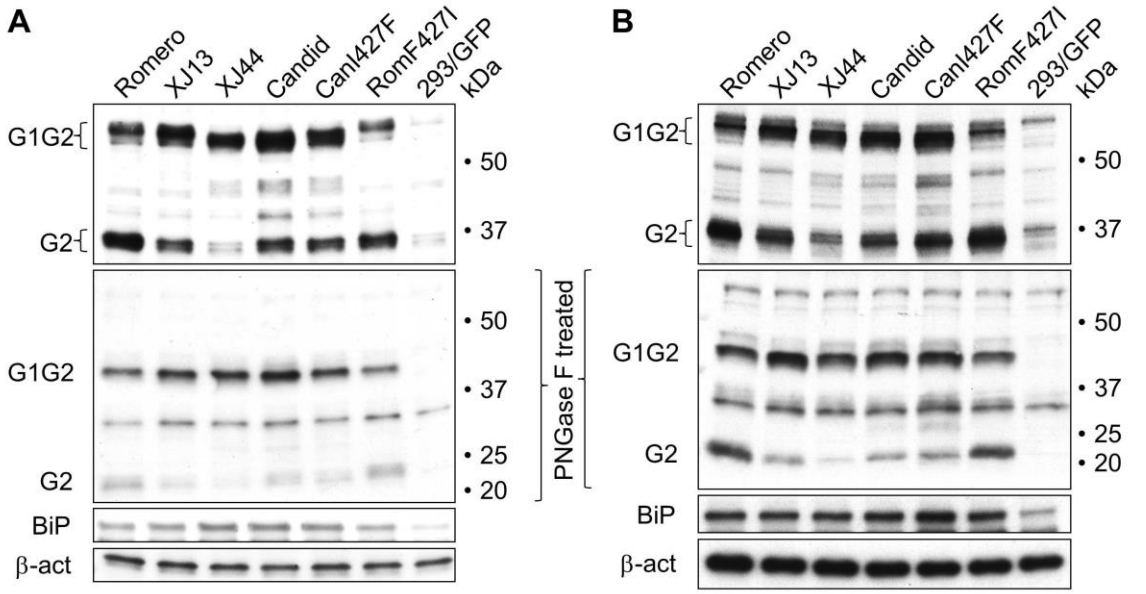

Figure 5.5. Activation of the UPR in HEK 293 cells transfected with the GPCs of JUNV strains differing in *in vivo* attenuation status. HEK 293 cells were transfected with equal amounts of expression plasmids for the GPCs of Romero (Romero), Candid #1 (Candid), Candid #1 predecessor strains XJ13 and XJ44, and the GPCs of Candid #1 and Romero bearing I427F (CandidI427F) and F427I (RomeroF427I) amino acid changes in the G2 subunit, respectively. Cell lysates were harvested at 24 (A) and 48 (B) hours post-transfection and divided into two equal aliquots that were either mock-treated (top panels) or treated with PNGase F (PNGase F treated). Expression of viral GPs and UPR marker BiP was analyzed by Western blotting. An anti-G2 antibody was used to detect viral GPs. β-actin was used as a sample loading control. 293/GFP, HEK 293 cells transfected with a GFP expressing construct that shares the same plasmid backbone with the expression constructs for JUNV GPCs.

Attenuated Candid #1 strain of JUNV was generated by serial *in vivo* and *in vitro* passaging of a virus that was isolated from a clinical human case of AHF (Parodi et al., 1958). During this process the virus had gradually lost its virulence for guinea pigs, non-human primates, mice, and humans (Fig. 1.3). To investigate whether the attenuation of Candid #1 correlates with the effectiveness of post-translational GP modification and processing, expression constructs were generated for the GPCs of Romero, Candid #1, and two predecessor to Candid #1 strains, XJ13 and XJ44 (Fig. 1.3). Two additional constructs encoding the GPC of Romero containing the F427I mutation and the GPC of Candid #1 containing the reverse I427F mutation were also generated to test whether this amino acid position that was critical for JUNV neurovirulence in mice (Albariño et al.,

2011b) and virulence in guinea pigs (Fig. 4.3) would also play a role in post-translational glycosylation of GPs. To this end, human embryonic kidney (HEK) 293 cells were transfected with the generated constructs and the GP banding patterns, as well as the levels of BiP were analyzed in cell lysates by Western blot at 24 (Fig. 5.5A) and 48 (Fig. 5.5B) hours post-transfection (p.t.). Remarkably, the processing efficiency and glycosylation pattern of GPs gradually changed for the expressed GPCs form Romero-like to Candid #1-like (Fig. 5.5). In addition, the level of intracellular BiP also gradually increased in accordance with the state of post-translational modification of JUNV GPs (Fig. 5.5A). Interestingly, mutation of the amino acid at position 427 in both Romero and Candid #1 GPCs neither affected post-translational processing or glycosylation of either of the GPCs nor changed the level of BiP expression (Fig. 5.5). Notably, at 48 hours p.t. high levels of BiP were detected in all samples indicating that prolonged overexpression of JUNV GPC triggers UPR regardless the efficiency of post-translational processing and the glycosylation state of the GPs (Fig. 5.5B). Collectively, these results demonstrated correlation between the ability of ER to correctly process nascent GPC and the state of JUNV *in vivo* attenuation.

Overexpression of the glycoprotein precursor of virulent Romero strain of Junin virus induces the unfolded protein response, but to a lesser extent than the overexpression of the glycoprotein precursor of attenuated Candid #1 strain

Inoculation of guinea pigs with the chimeric JUNV virus encoding the LP of Candid #1 in the background of Romero genome, rRom/CanLP (Fig. 4.2A) resulted in a delayed disease onset and prolonged survival of infected animals (Fig. 4.5C & D). Although, this virus exhibited a Romero-like GP banding pattern in Western blot, the overall levels of viral RNA synthesis (Fig. 5.2) and protein production were elevated

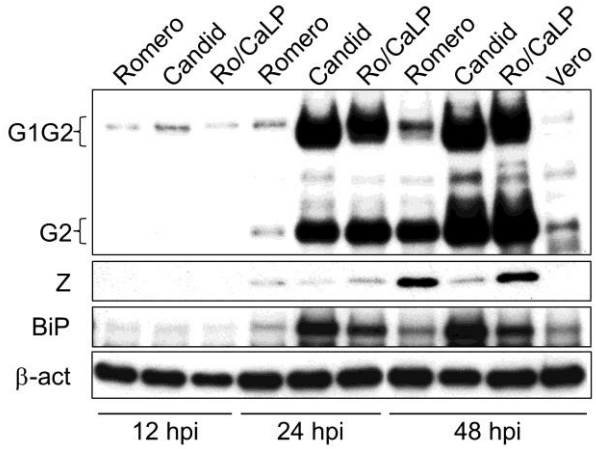

Figure 5.6. Activation of the UPR in response to overexpression of the GPC of Romero and Candid #1. Vero cells infected at an MOI of 5 with either rRomero (Romero), rCandid #1 (Candid), or rRom/CanLP (Ro/CaLP) were harvested at the indicated time points. Protein expression was analyzed by Western blotting using appropriate antibodies. An anti-G2 antibody was used to detect viral GPs. β-actin was used as a sample loading control. Vero, lysate of mock-infected Vero cells.

(Fig. 5.1A). Interestingly, the intersegment chimeric virus rCanL/RomS (Fig. 4.1A) that contains the entire L segment of Candid #1, exhibited a fully virulent phenotype in guinea pigs and the levels of viral gene expression similar to that of rRomero (Figs. 5.1A and 5.2). These findings suggested that the Z of Candid #1 has a better ability to control the functional activity of the LP of Candid #1 (Kranzusch and Whelan, 2011) that the Z of Romero. Given that prolonged plasmid-driven overexpression of the GPC of Romero triggered UPR induction (Fig. 5.5B), it could be possible that the slight attenuation of rRom/CanLP virulence in guinea pigs was associated with higher levels of Romero GPC expression by Candid #1 LP complexed with the Z of Romero that could lead to UPR-triggered induction of an inflammatory response (Zhang and Kaufman, 2008). Comparison of GPC expression between rRomero, rCandid #1, and rRom/CanLP in an independent experiment confirmed that Vero cells infected with rRom/CanLP produce much larger total amounts of GPs than those produced by rRomero-infected cells and similar to those produced by rCandid #1-infected cells (Fig. 5.6). The GP banding pattern for rRom/CanLP remained Romero-like and was different from the rCandid #1 GP banding pattern. Intriguingly, rRom/CanLP infection of Vero cells, similarly to prolonged

plasmid-driven overexpression of Romero GPC in HEK 293 cells, also induced production of BiP but to a lesser extent than rCandid #1 infection (Fig. 5.6). Thus, the obtained results demonstrated that overexpression of the GPC of Romero during viral infection results in the induction of UPR; however, the similar level of expression of the GPC of Candid #1 led to a markedly higher production of the ER stress response marker BiP.

Small RING finger protein Z is retained in infected cells if coexpressed with the glycoproteins of Romero strain of Junin virus, but not the glycoproteins of Candid #1 strain

In contrast with the elevated production of GPC and NP in cells infected with JUNV variants expressing the GPC of Candid #1 that were attenuated in guinea pigs compared to the virulent virus variants expressing the GPC of Romero (Figs. 4.3 and 4.5), the levels of intracellular Z, regardless of the JUNV strain of origin, were lower for the attenuated viruses than for the virulent viruses (Fig. 5.1A). However, the total intracellular amounts of the S (Fig. 5.2D) and L (Fig. 5.2E) segment RNA and the mRNA from genes encoded by both segments were higher for the attenuated viruses than for the virulent viruses. It has previously been demonstrated that the Z of arenaviruses exhibits a self-budding activity that does not require the presence of other viral proteins (Perez et al., 2003). Interestingly, the release of JUNV Z from transfected cells was impaired by co-expression of JUNV GPs (Groseth et al., 2010). Therefore, to test if the GPs of Candid #1 could not efficiently interact with Z and sequester it in the cytosol, viral particles were purified from aliquots of rRomero and rCandid #1 stocks containing equal amounts of PFUs and the total amounts of the G2 and Z were determined by Western blot. Remarkably, the virions of rRomero contained 60% more of G2 and 62% less of Z than

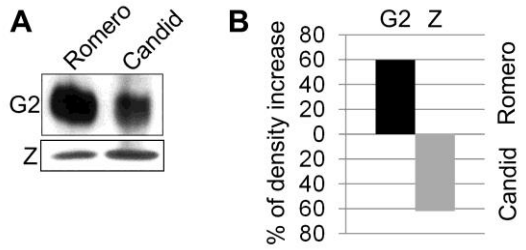

Figure 5.7. G2 and Z composition of Romero and Candid #1 virions. (A) Aliquots of rRomero (Romero) and rCandid #1 (Candid) containing equal amounts of PFUs were lysed in Laemmli's SDS loading buffer and virion protein composition was analyzed by Western blotting. **(B)** Comparison of G2 and Z band densities between rRomero and rCandid #1 virion samples shown in (A). Band densities were measured using the AlphaEaseFC software (Alpha Innotech).

the virions of rCandid #1 (Fig. 5.7). Given that rCandid #1 exhibited markedly higher levels of viral RNA synthesis (Fig. 5.2), the obtained results allowed to propose a mechanism for the observed difference in the LP activity between Romero and Candid #1 (Fig. 5.2): the GPs of Romero interact with the Z protein retaining it in the cytosol and allowing for efficient control of the LP functional activity; however, the interaction between the GPs of Candid #1 and Z (of Romero or Candid #1) is diminished leading to the release of Z from the cytosol and uncontrolled viral RNA synthesis (Fig. 5.8).

Notably, rRom/CanLP virus expressing the LP of Candid #1 and the Z and GPC of Romero also exhibited high levels of viral RNA synthesis; however, the Z protein was efficiently retained in the cytosol (Fig. 5.6). This suggested that the Z of Romero was unable to control the functional activity of the LP of Candid #1, again putting an emphasis on the importance of the functional compatibility between the viral LP and Z for JUNV *in vitro* and *in vivo* replication.

DISCUSSION

The mechanism of attenuation of the Candid #1 strain of JUNV that is currently used as a live-attenuated vaccine in AHF-endemic regions of Argentina (Ambrosio et al., 2011) is still largely elusive. Recently, the single F427I amino acid change in the

transmembrane region of the G2 subunit of the envelope glycoprotein complex was demonstrated to significantly attenuate neurovirulence of JUNV in mice (Albariño et al., 2011b). Although the rRomero virus containing this single amino acid sustitution did not cause any mortality in a guinea pig model of lethal JUNV infection (Fig. 4.3A) that adequately reproduces the features of human AHF (Emonet et al., 2010; Yun et al., 2008), the inoculated animals developed an acute self-limiting illness (Fig. 4.3B) indicating that the occurrence of this mutation in the G2 can only partially account for the highly attenuated phenotype of Candid #1 in all tested animal models and unprecedented safety in human patients (Ambrosio et al., 2011). Further studies revealed that the occurrence of the F427I mutation resulted in destabilization of the metastable conformation of the glycoprotein complex promoting its transition to a fusogenic conformation at neutral pH, and thus possibly impacting the ability of the virus to disseminate in infected tissues (Droniou-Bonzom et al., 2011). In addition, the same study identified an increased dependence of the glycoprotein complex of Candid #1 on the human TfR-1 receptor for the entry into target cells, which may affect the *in vivo* tissue tropism of Candid #1 (Droniou-Bonzom et al., 2011). However, the receptor recognition activity has been mapped to the G1 subunit of the glycoprotein complex (Buchmeier, 2013; Nunberg and York, 2012), further indicating that other mutations in the GPC of Candid #1 are also important for JUNV attenuation. In line with the results of these studies, only JUNV variants expressing the full-length GPC of Candid #1, rCandid #1, rRomL/CanS and rRom/CanGPC (Fig. 4.1A), were completely attenuated and did not induce any detectable disease in inoculated guinea pigs (Figs. 4.3 and 4.5). Most importantly, the F427I mutation occurred in the GPC of Candid #1 during the final passaging of the parental XJ44 strain of JUNV in the fetal rhesus monkey lung FRhL-2 cells (Albariño et al., 2011b; Albarino et al., 1997). However, this virus already exhibited an attenuated phenotype in NHPs and guinea pigs, the two animal models most closely reproducing human AHF (Ambrosio et al., 2011). Therefore, the role of other molecular

mechanisms than those associated with the F427I amino acid change in G2 in attenuation of JUNV would have to be investigated.

A recent study demonstrated the involvement of the cellular pattern recognition receptor RIG-I in immune recognition of JUNV replication (Huang et al., 2012). This cytoplasmic receptor senses double-stranded (ds) RNA intermediates produced during replication of RNA viruses, which triggers activation of type I IFN signaling (Kato et al., 2006). Intriguingly, the variants of JUNV expressing the GPC of Candid #1 (rCandid #1, rRomL/CanS, and rRom/CanGPC) that were completely attenuated in guinea pigs (Figs. 4.3 and 4.5), exhibited markedly higher levels of RNA synthesis (Fig. 5.2) and viral protein production (Fig. 5.1) than the variants of JUNV expressing the GPC of Romero (rRomero, rCanL/RomS, rRom/CanNP) that induced a uniformly lethal AHF-like disease in inoculated guinea pigs. Therefore, increased production of type I IFN in infected animals caused by RIG-I-mediated recognition of the high levels of viral RNA synthesis may have contributed to the attenuated phenotype of these viruses.

Interestingly, the chimeric virus expressing the LP of Romero and the Z of Candid #1, rRom/CanZ, that exhibited a highly impaired growth in tissue culture (Fig. 4.2D) and a partially attenuated phenotype in guinea pigs (Fig. 4.5C), expressed RNA synthesis and protein production levels similar to those of rRomero (Figs. 5.2 and 5.1A, respectively), indicating the ability of Candid #1 Z to support the functional activity of Romero LP. These results suggested that the delayed *in vitro* growth of this virus and, most likely, *in vivo* attenuation was associated with other functions of Z than regulation of viral RNA synthesis, such as formation and budding of nascent viral particles. In contrast, the JUNV variant expressing the LP of Candid #1 and the Z of Romero, rRom/CanLP, demonstrated the levels of viral RNA synthesis and protein production comparable to those of rCandid #1 (Figs. 5.2 and 5.1A, respectively) and guinea pigs inoculated with this virus exhibited a delayed, although uniformly lethal, disease (Fig. 4.5C). Thus, the obtained experimental

data demonstrated that the Z of Romero could not efficiently control the activity of Candid #1 LP and the overproduction of viral RNA possibly leading to increased expression of type I IFN may have resulted in diminished virulence of this virus in infected animals.

Notably, complete attenuation of JUNV chimeric variants was invariably associated with expression of the full-length GPC of Candid #1. Interestingly, the banding pattern of Candid #1 GPs in Western blot was markedly different from that of Romero GPs and showed additional bands between the G2 and uncleaved G1G2 precursor (Fig. 5.1C). N-linked glycosylation of nascent polypeptide chains is an essential process for correct post-translational protein folding (Schröder, 2008). Therefore, to investigate whether the additional bands in samples containing the GPs of Candid #1 resulted from altered GP glycosylation, the N-linked oligosaccharide groups were removed from the protein backbone by PNGase F treatment (Mijnes et al., 1998). As expected, the treatment resolved the additional bands in Candid #1 GP samples (Fig. 5.4), indicating that the GP of Candid #1 undergo abnormal post-translational modification in the ER. Of note, the observed banding pattern for Candid #1 GPs could not result from the differences in the level of GP expression, since elevated production of Romero GPs in cells infected with rRom/CanLP did not change the Romero GP banding pattern (Fig. 5.1A). Improper post-translational modification of nascent proteins can result in accumulation of unfolded proteins in ER lumen, which can causes ER stress. The ER chaperon protein BiP is the primary sensor of ER stress and controls the activation of three main branches of the UPR mediated by the three signal transducers IRE1, PERK, and ATF6 (Schröder, 2008). Upregulation of BiP expression constitutes a robust marker of ER stress and UPR activation (Bertolotti et al., 2000; Schröder, 2008; Schroder and Kaufman, 2005), and has previously been used to demonstrate the activation of ER stress response in LCMV infected cells (Pasqual et al., 2011). Therefore, the lysates of cells infected with the JUNV variants expressing the GPC of Candid #1

were analyzed for the levels of BiP expression. As expected, all samples containing the GPs of Candid #1 also showed high amounts of BiP indicative of the induction of cellular UPR (Fig. 5.3). Importantly, the GP banding pattern and the level of BiP production in cells expressing the GPs of two parental to Candid #1 strains XJ13 and XJ44 correlated with their *in vivo* attenuation status with XJ13 (less attenuated) being closer related to virulent Romero and XJ44 (more attenuated) being closer related to attenuated Candid #1 (Fig. 5.5). Of note, the observed Western blot GP banding patters and BiP expression levels appeared not to be cell line or species specific, since similar results were obtained in African green monkey kidney epithelial Vero cells (Fig. 5.3A), human alveolar basal epithelial A549 cells (Fig. 5.3B), and human embryonic kidney 293 cells (Fig. 5.5). The goal of the UPR is to restore the folding capacity of ER; however, prolonged unresolved ER stress can result in the induction of apoptosis and inflammatory signaling (Schröder, 2008). UPR induced by a number of viruses have been reported to involve proapoptotic signaling (Barry et al., 2010; Dimcheff et al., 2004; Medigeshi et al., 2007). Thus, a clear correlation was demonstrated between the state of JUNV attenuation and GP-triggered induction of the UPR, which may contribute to protective immune response development in patients and laboratory animals by activating proapoptotic and proinflammatory signaling in infected cells (Schröder, 2008; Zhang and Kaufman, 2008).

The obtained experimental data indicated that all cell lysate samples containing the GPs of Candid #1 also contained much lower amounts of Z than the samples containing the GPs of Romero, regardless the strain of Z origin (Fig. 5.1A) and despite the high levels of viral RNA synthesis detected in these samples (Fig. 5.2). Interestingly, the analysis of rCandid #1 and rRomero stocks revealed that virions of rRomero contained 60% more GPC and 62% less of Z, suggesting that the GPs of Candid #1 cannot efficiently interact with Z (Groseth et al., 2010) leading to its release from cytoplasm likely in a form of GP-free viral particles (Perez et al., 2003). The results also

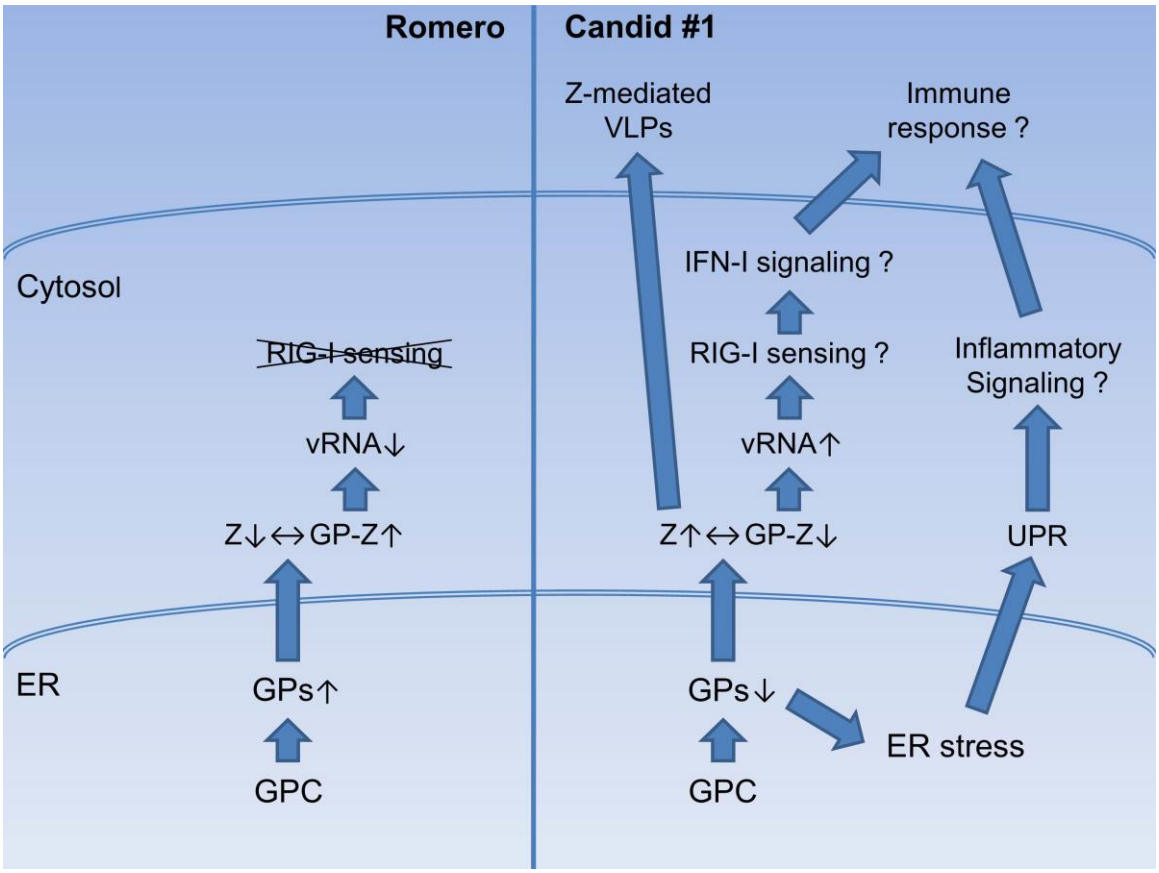

Figure 5.8. Role of envelope glycoproteins in attenuation of JUNV. A detailed description is provided in the text.

suggested that the GP interaction site is conserved between the Z proteins of Romero and Candid #1, since the origin of GPs but not Z determined the observed results.

Analysis of the results obtained in *in vivo* and *in vitro* experiments with inter- and intrasegment chimeric JUNV variants allowed to propose a model describing a sequence of events that may contribute to the virulent phenotype of Romero and attenuated phenotype of Candid #1 strain of JUNV. Therefore, upon expression, the GPC of Romero undergoes efficient processing in the ER and Golgi (Nunberg and York, 2012) producing the individual GP subunits: G1, G2, and SSP. The fully processed GPs can efficiently interact with the RING finger protein Z, facilitating its sequestration in the cytosol that leads to efficient control of the viral polymerase complex activity (Fig. 5.8, left). However, in cells infected with the Candid #1 strain of JUNV, the GPC undergoes an

abnormal post-translational modification that leads to accumulation of unprocessed/unfolded GP precursors and strong induction of the UPR. The prolonged ER stress may trigger proapoptotic and proinflammatory signaling (Schröder, 2008). Notably, mouse macrophages have previously been demonstrated to secrete inflammatory cytokines in response to Candid #1 infection (Cuevas et al., 2011). In addition, the accumulated mutations (other than the F427I mutation) prevent the GPs of Candid #1 from efficient interaction with the Z protein leading to its release from the cell. Resulting low concentration of Z leads to uncontrolled viral RNA synthesis, which may further boost innate immune signaling via RIG-I-mediated recognition of viral replication (Huang et al., 2012) (Fig. 5.8, right).

The model described above is supported by the result from several studies conducted by different research groups. The GPCs of arenaviruses undergo co- and post-translational glycosylation and proteolytic processing in order for the envelope GPs to acquire functional conformation (Beyer et al., 2003; Eichler et al., 2006; Lenz et al., 2001a; Rojek et al., 2008). Thus, eleven potential N-glycosylation sites have been identified in the amino acid sequence of the LASV GPC. Disruption of six sites blocked proteolytic processing of the GPC; however, did not prevent transportation to the cleavage-defective mutants to the cell surface (Eichler et al., 2006). Expression of the GPC of LCMV has been demonstrated to induce ER stress and trigger transient UPR in transfected and infected cells, that was monitored by the level of BiP expression (Pasqual et al., 2011). On the other hand, Z protein of arenaviruses interacts with the GPs in order to mediate their requirement in nascent viral particles (Capul, 2007; Schlie et al., 2010). Interestingly, plasmid-driven overexpression of GPC results in a diminished ability of the Z protein to inhibit the activity of the viral L polymerase in a MG assay, suggesting that the GP-Z interaction may play a role in the regulation of RNA replication/translation (Capul, 2007). This hypothesis is further supported by the notions that the Z protein of arenaviruses exhibits a self-budding activity (Perez et al., 2003) and the release of Z is

inhibited by co-expression of GPC (Groseth et al., 2010),which may determine the amount of Z available for the interaction with the viral L polymerase.

The obtained experimental results provided valuable insights into the mechanisms that underlie the attenuation of the Candid #1 vaccine strain of JUNV. There are three main directions that can be proposed for further continuation of this project: investigation of the functional interactions of Z with GPs and LP, elucidation of the UPR signaling pathways that are activated in response to Candid #1 GPC expression, and characterization of the role of individual amino acid changes in the GPC between virulent Romero and attenuated Candid #1 strains of JUNV. This knowledge would allow for complete description of the molecular mechanisms determining JUNV attenuation and, most importantly, would permit the development of novel safe and highly efficient vaccine candidates against JUNV and other members of *Arenaveridae* virus family.

BIBLIOGRAPHY

1. Abraham, J., Corbett, K.D., Farzan, M., Choe, H., Harrison, S.C., 2010. Structural basis for receptor recognition by New World hemorrhagic fever arenaviruses. Nat Struct Mol Biol 17.

2. Abraham, J., Kwong, J.A., Albariño, C.G., Lu, J.G., Radoshitzky, S.R., Salazar-Bravo, J., Farzan, M., Spiropoulou, C.F., Choe, H., 2009. Host-Species Transferrin Receptor 1 Orthologs Are Cellular Receptors for Nonpathogenic New World Clade B Arenaviruses. PLoS Pathog 5, e1000358.

3. Agnihothram, S.S., York, J., Nunberg, J.H., 2006. Role of the stable signal peptide and cytoplasmic domain of G2 in regulating intracellular transport of the Junin virus envelope glycoprotein complex. J Virol 80, 5189-5198.

4. Agnihothram, S.S., York, J., Trahey, M., Nunberg, J.H., 2007. Bitopic membrane topology of the stable signal peptide in the tripartite Junin virus GP-C envelope glycoprotein complex. J Virol 81, 4331-4337.

5. Aisen, P., Listowsky, I., 1980. Iron Transport and Storage Proteins. Annual Review of Biochemistry 49, 357-393.

6. Albariño, C.G., Bergeron, É., Erickson, B.R., Khristova, M.L., Rollin, P.E., Nichol, S.T., 2009. Efficient Reverse Genetics Generation of Infectious Junin Viruses Differing in Glycoprotein Processing. Journal of Virology 83, 5606-5614.

7. Albariño, C.G., Bird, B.H., Chakrabarti, A.K., Dodd, K.A., Erickson, B.R., Nichol, S.T., 2011a. Efficient Rescue of Recombinant Lassa Virus Reveals the Influence of S Segment Noncoding Regions on Virus Replication and Virulence. Journal of Virology 85, 4020-4024.

8. Albariño, C.G., Bird, B.H., Chakrabarti, A.K., Dodd, K.A., Flint, M., Bergeron, É., White, D.M., Nichol, S.T., 2011b. The Major Determinant of Attenuation in Mice of the Candid1 Vaccine for Argentine Hemorrhagic Fever Is Located in the G2 Glycoprotein Transmembrane Domain. Journal of Virology 85, 10404-10408.

9. Albarino, C.G., Ghiringhelli, P.D., Posik, D.M., Lozano, M.E., Ambrosio, A.M., Sanchez, A., Romanowski, V., 1997. Molecular characterization of attenuated Junin virus strains. J Gen Virol 78 (Pt 7), 1605-1610.

10. Ambrosio, A., Saavedra, M., Mariani, M., Gamboa, G., Maiza, A., 2011. Argentine hemorrhagic fever vaccines. Human Vaccines 7, 694-700.

11. Ambrosio, A.M., Gamboa, G.S., Feuillade, M.R., Briggiler, A.M., Rimoldi, M.T., 1992. Peripheral blood leukocytes of patients with Argentine hemorrhagic fever as effectors of antibody-dependent cell-cytotoxicity. J Med Virol 37, 232-236.

12. Andrei, G., De Clercq, E., 1993. Molecular approaches for the treatment of hemorrhagic fever virus infections. Antiviral Res 22, 45-75.

13. Archer, A.M., Rico-Hesse, R., 2002. High Genetic Divergence and Recombination in Arenaviruses from the Americas. Virology 304, 274-281.

14. Avila, M.M., Samoilovich, S.R., Laguens, R.P., Merani, M.S., Weissenbacher, M.C., 1987. Protection of Junin virus-infected marmosets by passive administration of immune serum: association with late neurologic signs. J Med Virol 21, 67-74.

15. Avila, M.M., Samoilovich, S.R., Weissenbacher, M.C., 1979. Infection of guinea pigs with an attenuated strain of Junin virus XJCL3. Medicina (B Aires) 39, 597-603.

16. Baird, N.L., York, J., Nunberg, J.H., 2012. Arenavirus Infection Induces Discrete Cytosolic Structures for RNA Replication. Journal of Virology 86, 11301-11310.

17. Baize, S., Kaplon, J., Faure, C., Pannetier, D., Georges-Courbot, M.C., Deubel, V., 2004. Lassa virus infection of human dendritic cells and macrophages is productive but fails to activate cells. J Immunol 172, 2861-2869.

18. Barry, G., Fragkoudis, R., Ferguson, M.C., Lulla, A., Merits, A., Kohl, A., Fazakerley, J.K., 2010. Semliki Forest Virus-Induced Endoplasmic Reticulum Stress Accelerates Apoptotic Death of Mammalian Cells. Journal of Virology 84, 7369-7377.

19. Bertolotti, A., Zhang, Y., Hendershot, L.M., Harding, H.P., Ron, D., 2000. Dynamic interaction of BiP and ER stress transducers in the unfolded-protein response. Nat Cell Biol 2, 326-332.

20. Beyer, W.R., Popplau, D., Garten, W., von Laer, D., Lenz, O., 2003. Endoproteolytic processing of the lymphocytic choriomeningitis virus glycoprotein by the subtilase SKI-1/S1P. J Virol 77, 2866-2872.

21. Bonhomme, C.J., Capul, A.A., Lauron, E.J., Bederka, L.H., Knopp, K.A., Buchmeier, M.J., 2011. Glycosylation modulates arenavirus glycoprotein expression and function. Virology 409, 223-233.

22. Borden, K.L., Campbell Dwyer, E.J., Salvato, M.S., 1998. An arenavirus RING (zinc-binding) protein binds the oncoprotein promyelocyte leukemia protein (PML) and relocates PML nuclear bodies to the cytoplasm. J Virol 72, 758-766.

23. Borrow, P., Oldstone, M.B., 1994. Mechanism of lymphocytic choriomeningitis virus entry into cells. Virology 198, 1-9.

24. Bowen, M.D., Peters, C.J., Nichol, S.T., 1997. Phylogenetic analysis of the Arenaviridae: patterns of virus evolution and evidence for cospeciation between arenaviruses and their rodent hosts. Mol Phylogenet Evol 8, 301-316.

25. Braakman, I., Van Anken, E., 2000. Folding of Viral Envelope Glycoproteins in the Endoplasmic Reticulum. Traffic 1, 533-539.

26. Buchmeier, M.J., de la Torre, J.C., and Peters, C.J., 2013. Arenaviridae, in: Knipe, D.M., Holey, P.M. (Ed.), Fields Virology, Sixth Edition, pp. 1283-1303.

27. Burri, D.J., Palma, J.R., Kunz, S., Pasquato, A., 2012. Envelope Glycoprotein of Arenaviruses. Viruses 4, 2162-2181.

28. Cajimat, M.N.B., Milazzo, M.L., Borchert, J.N., Abbott, K.D., Bradley, R.D., Fulhorst, C.F., 2008. Diversity among Tacaribe serocomplex viruses (family Arenaviridae) naturally associated with the Mexican woodrat (Neotoma mexicana). Virus Research 133, 211-217.

29. Cajimat, M.N.B., Milazzo, M.L., Bradley, R.D., Fulhorst, C.F., 2007. Catarina Virus, an Arenaviral Species Principally Associated with Neotoma micropus (Southern Plains Woodrat) in Texas. The American Journal of Tropical Medicine and Hygiene 77, 732-736.

30. Cajimat, M.N.B., Milazzo, M.L., Haynie, M.L., Hanson, J.D., Bradley, R.D., Fulhorst, C.F., 2011. Diversity and phylogenetic relationships among the North American Tacaribe serocomplex viruses (Family Arenaviridae). Virology 421, 87-95.

31. Campbell Dwyer, E.J., Lai, H., MacDonald, R.C., Salvato, M.S., Borden, K.L., 2000. The lymphocytic choriomeningitis virus RING protein Z associates with eukaryotic initiation factor 4E and selectively represses translation in a RING-dependent manner. J Virol 74, 3293-3300.

32. Campetella, O.E., Galassi, N.V., Barrios, H.A., 1990. Contrasuppressor cells induced by Junin virus. Immunology 69, 629-631.

33. Campetella, O.E., Galassi, N.V., Sanjuan, N., Barrios, H.A., 1988. Susceptible adult murine model for Junin virus. J Med Virol 26, 443-451.

34. Candurra, N.A., Damonte, E.B., Coto, C.E., 1989. Antigenic relationships between attenuated and pathogenic strains of Junin virus. J Med Virol 27, 145-150.

35. Cao, W., Henry, M.D., Borrow, P., Yamada, H., Elder, J.H., Ravkov, E.V., Nichol, S.T., Compans, R.W., Campbell, K.P., Oldstone, M.B., 1998.

Identification of alpha-dystroglycan as a receptor for lymphocytic choriomeningitis virus and Lassa fever virus [see comments]. Science 282, 2079-2081.

36. Capul, A.A., Perez, M., Burke, E., Kunz, S., Buchmeier, M.J., de la Torre, J.C, 2007. Arenavirus Z-GP association requires Z myristoylation but not functional RING or L domains. J.Virology 81.

37. Charrel, R.N., Coutard, B., Baronti, C., Canard, B., Nougairede, A., Frangeul, A., Morin, B., Jamal, S., Schmidt, C.L., Hilgenfeld, R., Klempa, B., de Lamballerie, X., 2011. Arenaviruses and hantaviruses: From epidemiology and genomics to antivirals. Antiviral Research 90, 102-114.

38. Charrel, R.N., Feldmann, H., Fulhorst, C.F., Khelifa, R., Chesse, R.d., Lamballerie, X.d., 2002. Phylogeny of New World arenaviruses based on the complete coding sequences of the small genomic segment identified an evolutionary lineage produced by intrasegmental recombination. Biochemical and Biophysical Research Communications 296, 1118-1124.

39. Chen, M., Lan, S., Ou, R., Price, G.E., Jiang, H., de la Torre, J.C., Moskophidis, D., 2008. Genomic and biological characterization of aggressive and docile strains of lymphocytic choriomeningitis virus rescued from a plasmid-based reverse-genetics system. Journal of General Virology 89, 1421-1433.

40. Chiappero, M.B., Gardenal, C.N., 2003. Restricted gene flow in Calomys musculinus (Rodentia, Muridae), the natural reservoir of Junin virus. J Hered 94, 490-495.

41. Comai, L., 2004. Mechanism of RNA Polymerase I Transcription, in: Ronald, C.C., Joan Weliky, C. (Eds.), Advances in Protein Chemistry. Academic Press, pp. 123-155.

42. Condit, R.C., 2013. Principles of Virology, in: Knipe, D.M., Holey, P.M. (Ed.), Fields Virology, Sixth Edition, pp. 21-51.

43. Cornu, T.I., de la Torre, J.C., 2001. RING finger Z protein of lymphocytic choriomeningitis virus (LCMV) inhibits transcription and RNA replication of an LCMV S-segment minigenome. J Virol 75, 9415-9426.

44. Cornu, T.I., de la Torre, J.C., 2002. Characterization of the arenavirus RING finger Z protein regions required for Z-mediated inhibition of viral RNA synthesis. J Virol 76, 6678-6688.

45. Cornu, T.I., Feldmann, H., de la Torre, J.C., 2004. Cells expressing the RING finger Z protein are resistant to arenavirus infection. J Virol 78, 2979-2983.

46. Cresta, B., Padula, P., de Martinez Segovia, M., 1980. Biological properties of Junin virus proteins. I. Identification of the immunogenic glycoprotein. Intervirology 13, 284-288.

47. Cuevas, C.D., Lavanya, M., Wang, E., Ross, S.R., 2011. Junín Virus Infects Mouse Cells and Induces Innate Immune Responses. Journal of Virology 85, 11058-11068.

48. Damonte, E.B., Coto, C.E., 2002. Treatment of arenavirus infections: from basic studies to the challenge of antiviral therapy. Adv Virus Res 58, 125-155.

49. Damonte, E.B., Mersich, S.E., Candurra, N.A., 1994. Intracellular processing and transport of Junin virus glycoproteins influences virion infectivity. Virus Res 34, 317-326.

50. de Guerrero, L.B., Boxaca, M.C., Malumbres, E., Dejean, C., Caruso, E., 1985. Early protection to Junín virus of guinea pig with an attenuated Junín virus strain. Acta Virol 29, 334-337.

51. Dejean, C.B., Ayerra, B.L., Teyssié, A.R., 198. Interferon response in the guinea pig infected with Junín virus. J Med Virol 23, 83-91.

52. Dimcheff, D.E., Faasse, M.A., McAtee, F.J., Portis, J.L., 2004. Endoplasmic reticulum (ER) stress induced by a neurovirulent mouse retrovirus is associated with prolonged BiP binding and retention of a viral protein in the ER. J Biol Chem. 279, 33782-33790. Epub 32004 Jun 33783.

53. Djavani, M., Rodas, J., Lukashevich, I.S., Horejsh, D., Pandolfi, P.P., Borden, K.L., Salvato, M.S., 2001. Role of the promyelocytic leukemia protein PML in the interferon sensitivity of lymphocytic choriomeningitis virus. J Virol 75, 6204-6208.

54. Downs, W.G., Anderson, C.R., Spence, L., Aitken, T.H.G., Greenhall, A.H., 1963. Tacaribe Virus, a New Agent Isolated from Artibeus Bats and Mosquitoes in Trinidad, West Indies. The American Journal of Tropical Medicine and Hygiene 12, 640-646.

55. Droniou-Bonzom, M.E., Reignier, T., Oldenburg, J.E., Cox, A.U., Exline, C.M., Rathbun, J.Y., Cannon, P.M., 2011. Substitutions in the Glycoprotein (GP) of the Candid#1 Vaccine Strain of Junin Virus Increase Dependence on Human Transferrin Receptor 1 for Entry and Destabilize the Metastable Conformation of GP. Journal of Virology 85, 13457-13462.

56. Eckerle, L.D., Becker, M.M., Halpin, R.A., Li, K., Venter, E., Lu, X., Scherbakova, S., Graham, R.L., Baric, R.S., Stockwell, T.B., Spiro, D.J., Denison, M.R., 2010. Infidelity of SARS-CoV Nsp14-Exonuclease Mutant Virus Replication Is Revealed by Complete Genome Sequencing. PLoS Pathog 6, e1000896.

57. Eichler, R., Lenz, O., Garten, W., Strecker, T., 2006. The role of single N-glycans in proteolytic processing and cell surface transport of the Lassa virus glycoprotein GP-C, p. 41.

58. Eichler, R., Lenz, O., Strecker, T., Garten, W., 2003. Signal peptide of Lassa virus glycoprotein GP-C exhibits an unusual length. FEBS Lett 538, 203-206.

59. Elagoz, A., Benjannet, S., Mammarbassi, A., Wickham, L., Seidah, N.G., 2002. Biosynthesis and cellular trafficking of the convertase SKI-1/S1P: ectodomain shedding requires SKI-1 activity. J Biol Chem. 277, 11265-11275. Epub 12001 Dec 11226.

60. Elsner, B., Schwarz, E., Mando, O.G., Maiztegui, J., Vilches, A., 1973. Pathology of 12 fatal cases of Argentine hemorrhagic fever. The American Journal of Tropical Medicine and Hygiene 22, 229-236.

61. Emonet, S.E., Urata, S., de la Torre, J.C., 2011a. Arenavirus reverse genetics: New approaches for the investigation of arenavirus biology and development of antiviral strategies. Virology 411, 416-425.

62. Emonet, S.F., Garidou, L., McGavern, D.B., de la Torre, J.C., 2009. Generation of recombinant lymphocytic choriomeningitis viruses with trisegmented genomes stably expressing two additional genes of interest, pp. 3473-3478.

63. Emonet, S.F., Seregin, A.V., Yun, N.E., Poussard, A.L., Walker, A.G., de la Torre, J.C., Paessler, S., 2010. Rescue From Cloned cDNAs And In Vivo Characterization of Recombinant Pathogenic Romero And Life-Attenuated Candid #1 Strains Of Junin Virus, The Causative Agent Of Argentine Hemorrhagic Fever Disease. J Virol 85, 1473-1483.

64. Emonet, S.F., Seregin, A.V., Yun, N.E., Poussard, A.L., Walker, A.G., de la Torre, J.C., Paessler, S., 2011b. Rescue from Cloned cDNAs and In Vivo Characterization of Recombinant Pathogenic Romero and Live-Attenuated Candid #1 Strains of Junin Virus, the Causative Agent of Argentine Hemorrhagic Fever Disease. Journal of Virology 85, 1473-1483.

65. Enria, D., Bowen, M.D., Mills, J.N., Shieh, W.J., Bausch, D., Peters, C.J., 2004. Arenavirus infections, in: Guerrant, R.L., Walker, D.H., Weller, P.F., Saunders, W.B. (Eds.), Tropical Infectious Diseases: Principles, Pathogens, and Practice. Saunders, pp. 1191–1212.

66. Enria, D., Feuillade, M.R., 1998. Argentine Haemorrhagic Fever (Junin virus - Arenaviridae): a review on clinical, epidemiological, ecological, treatment, and preventive aspects of the disease, in: Travassos de Rosa, A.P.A., Vasconcelos, P.F.C., Travasos da Rosa, J.F.S. (Ed.), An overview of arbovirology in Brazil and neighboring countries. Chaggas Belem Brasil, pp. 219-232.

67. Enria, D.A., Barrera Oro, J.G., 2002. Junin virus vaccines. Curr Top Microbiol Immunol 263, 239-261.

68. Enria, D.A., Briggiler, A.M., Sánchez, Z., 2008. Treatment of Argentine hemorrhagic fever. Antiviral Research 78, 132-139.

69. Enria, D.A., de Damilano, A.J., Briggiler, A.M., Ambrosio, A.M., Fernandez, N.J., Feuillade, M.R., Maiztegui, J.I., 1985. [Late neurologic syndrome in patients with Argentinian hemorrhagic fever treated with immune plasma]. Medicina (B Aires) 45, 615-620.

70. Enria, D.A., Mills, J.N., Bausch, D.G., Shieh, W., Peters, C.J., 2011. Arenavirus Infections, in: Guerrant, R.L., Walker, D.H., Weller, P.F. (Eds.), Tropical Infectious Diseases: Principles, Pathogenesis, & Practice, 3rd ed. Elsevier Saunders, Edinburg, London, New York, Oxford, Philadelphia, St. Louis, Sydney, Toronto, pp. 449-461.

71. Espenshade, P.J., Cheng, D., Goldstein, J.L., Brown, M.S., 1999. Autocatalytic Processing of Site-1 Protease Removes Propeptide and Permits Cleavage of Sterol Regulatory Element-binding Proteins. Journal of Biological Chemistry 274, 22795-22804.

72. Fan, L., Briese, T., Lipkin, W.I., 2010. Z Proteins of New World Arenaviruses Bind RIG-I and Interfere with Type I Interferon Induction. J Virol 84, 1785-1791.

73. Fennewald, S.M., Aronson, J.F., Zhang, L., Herzog, N.K., 2002. Alterations in NF-kappaB and RBP-Jkappa by arenavirus infection of macrophages in vitro and in vivo. J Virol 76, 1154-1162.

74. Flanagan, M.L., Oldenburg, J., Reignier, T., Holt, N., Hamilton, G.A., Martin, V.K., Cannon, P.M., 2008. New World Clade B Arenaviruses Can Use Transferrin Receptor 1 (TfR1)-Dependent and -Independent Entry Pathways, and Glycoproteins from Human Pathogenic Strains Are Associated with the Use of TfR1. Journal of Virology 82, 938-948.

75. Flatz, L., Bergthaler, A., de la Torre, J.C., Pinschewer, D.D., 2006. Recovery of an arenavirus entirely from RNA polymerase I/II-driven cDNA. Proc Natl Acad Sci U S A 103, 4663-4668.

76. Franze-Fernandez, M.-T., Zetina, C., Iapalucci, S., Lucero, M.A., Bouissou, C., Lopez, R., Rey, O., Daheli, M., Cohen, G.N., Zakin, M.M., 1987. Molecular structure and early events in the replication of Tacaribe arenavirus S RNA. Virus Research 7, 309-324.

77. Freiden, P.J., Gaut, J.R., Hendershot, L.M., 1992. Interconversion of three differentially modified and assembled forms of BiP. Embo J 11, 63-70.

78. Froeschke, M., Basler, M., Groettrup, M., Dobberstein, B., 2003. Long-lived signal peptide of lymphocytic choriomeningitis virus glycoprotein pGP-C. J Biol Chem 278, 41914-41920.

79. Fulhorst, C.F., Charrel, R.N., Weaver, S.C., Ksiazek, T.G., Bradley, R.D., Milazzo, M.L., Tesh, R.B., Bowen, M.D., 2001. Geographic distribution and genetic diversity of Whitewater Arroyo virus in the southwestern United States. Emerg Infect Dis 7, 403-407.

80. Garcin, D., Kolakofsky, D., 1990. A novel mechanism for the initiation of Tacaribe arenavirus genome replication. J Virol 64, 6196-6203.

81. Garcin, D., Kolakofsky, D., 1992. Tacaribe arenavirus RNA synthesis in vitro is primer dependent and suggests an unusual model for the initiation of genome replication. J Virol 66, 1370-1376.

82. Giovanniello, O.A., Nejamkis, M.R., Galassi, N.V., Nota, N.R., 1980. Immunosuppression in experimental Junin virus infection of mice. Intervirology 13, 122-125.

83. Gómez, R.M., Jaquenod de Giusti, C., Sanchez Vallduvi, M.M., Frik, J., Ferrer, M.F., Schattner, M., 2011. Junín virus. A XXI century update. Microbes and Infection 13, 303-311.

84. Goñi, S., Iserte, J., Stephan, B., Borio, C., Ghiringhelli, P., Lozano, M., 2010. Molecular analysis of the virulence attenuation process in Junín virus vaccine genealogy. Virus Genes 40, 320-328.

85. Goni, S.E., Iserte, J.A., Ambrosio, A.M., Romanowski, V., Ghiringhelli, P.D., Lozano, M.E., 2006. Genomic features of attenuated Junin virus vaccine strain candidate. Virus Genes 32, 37-41.

86. Gonzalez, J.P., Emonet, S., Lamballerie, X.d., Charrel, R., 2007. Arenaviruses, in: Childs, J.E., Mackenzie, J.S., Richt, J.A. (Eds.), Wildlife and Emerging Zoonotic Diseases: The Biology, Circumstances and Consequences of Cross-Species Transmission. Springer Berlin Heidelberg, pp. 253-288.

87. González, P.H., Cossio, P.M., Arana, R.M., J.I., Laguens, R.P., 1980. Lymphatic tissue in Argentine hemorrhagic fever. Pathologic features. Arch Pathol Lab Med 104, 250-254.

88. Grant, A., Seregin, A., Huang, C., Kolokoltsova, O., Brasier, A., Peters, C., Paessler, S., 2012. Junín virus pathogenesis and virus replication. Viruses 4, 2317-2339.

89. Groseth, A., Hoenen, T., Weber, M., Wolff, S., Herwig, A., Kaufmann, A., Becker, S., 2011. Tacaribe Virus but Not Junin Virus Infection Induces

Cytokine Release from Primary Human Monocytes and Macrophages. PLoS Negl Trop Dis 5, e1137.

90. Groseth, A., Wolff, S., Strecker, T., Hoenen, T., Becker, S., 2010. Efficient Budding of the Tacaribe Virus Matrix Protein Z Requires the Nucleoprotein. Journal of Virology 84, 3603-3611.

91. Habjan, M., Penski, N., Spiegel, M., Weber, F., 2008. T7 RNA polymerase-dependent and -independent systems for cDNA-based rescue of Rift Valley fever virus. Journal of General Virology 89, 2157-2166.

92. Harrison, L.H., Halsey, N.A., McKee, K.T., Jr., Peters, C.J., Barrera Oro, J.G., Briggiler, A.M., Feuillade, M.R., Maiztegui, J.I., 1999. Clinical case definitions for Argentine hemorrhagic fever. Clin Infect Dis 28, 1091-1094.

93. Hass, M., Golnitz, U., Muller, S., Becker-Ziaja, B., Gunther, S., 2004. Replicon system for Lassa virus. J Virol 78, 13793-13803.

94. Hass, M., Lelke, M., Busch, C., Becker-Ziaja, B., Günther, S., 2008. Mutational Evidence for a Structural Model of the Lassa Virus RNA Polymerase Domain and Identification of Two Residues, Gly1394 and Asp1395, That Are Critical for Transcription but Not Replication of the Genome. Journal of Virology 82, 10207-10217.

95. Hass, M., Westerkofsky, M., Müller, S., Becker-Ziaja, B., Busch, C., Günther, S., 2006. Mutational Analysis of the Lassa Virus Promoter. Journal of Virology 80, 12414-12419.

96. Heller, M.V., Marta, R.F., Sturk, A., Maiztegui, J.I., Hack, C.E., Cate, J.W., Molinas, F.C., 1995. Early markers of blood coagulation and fibrinolysis activation in Argentine hemorrhagic fever. Thromb Haemost 73, 368-373.

97. Huang, C., Kolokoltsova, O.A., Yun, N.E., Seregin, A.V., Poussard, A.L., Walker, A.G., Brasier, A.R., Zhao, Y., Tian, B., de la Torre, J.C., Paessler, S., 2012. Junín Virus Infection Activates the Type I Interferon Pathway in a RIG-I-Dependent Manner. PLoS Negl Trop Dis 6, e1659.

98. Kato, H., Takeuchi, O., Sato, S., Yoneyama, M., Yamamoto, M., Matsui, K., Uematsu, S., Jung, A., Kawai, T., Ishii, K.J., Yamaguchi, O., Otsu, K., Tsujimura, T., Koh, C.-S., Reis e Sousa, C., Matsuura, Y., Fujita, T., Akira, S., 2006. Differential roles of MDA5 and RIG-I helicases in the recognition of RNA viruses. Nature 441, 101-105.

99. Kenyon, R.H., Canonico, P.G., Green, D.E., Peters, C.J., 1986a. Effect of ribavirin and tributylribavirin on argentine hemorrhagic fever (Junin virus) in guinea pigs. Antimicrobial Agents and Chemotherapy 29, 521-523.

100. Kenyon, R.H., Condie, R.M., Jahrling, P.B., Peters, C.J., 1990. Protection of guinea pigs against experimental Argentine hemorrhagic fever by purified human IgG: importance of elimination of infected cells. Microbial Pathogenesis 9, 219-226.

101. Kenyon, R.H., Green, D.E., Eddy, G.A., Peters, C.J., 1986b. Treatment of Junin virus-infected guinea pigs with immune serum: development of late neurological disease. J Med Virol 20, 207-218.

102. Kenyon, R.H., Green, D.E., Maiztegui, J.I., Peters, C.J., 1988. Viral strain dependent differences in experimental Argentine hemorrhagic fever. Intervirology 29, 133-143.

103. Kenyon, R.H., Green, D.E., Peters, C.J., 1985. Effect of immunosuppression on experimental Argentine hemorrhagic fever in guinea pigs. J Virol 53, 75-80.

104. Kenyon, R.H., McKee, K.T., Jr., Zack, P.M., Rippy, M.K., Vogel, A.P., York, C., Meegan, J., Crabbs, C., Peters, C.J., 1992. Aerosol infection of rhesus macaques with Junin virus. Intervirology 33, 23-31.

105. Kirk, W.E., Cash, P., Peters, C.J., Bishop, D.H.L., 1980. Formation and Characterization of an Intertypic Lymphocytic Choriomeningitis Recombinant Virus. Journal of General Virology 51, 213-218.

106. Kolokoltsova, O.A., Yun, N.E., Poussard, A.L., Smith, J.K., Smith, J.N., Salazar, M., Walker, A., Tseng, C.-T.K., Aronson, J.F., Paessler, S., 2010. Mice Lacking Alpha/Beta and Gamma Interferon Receptors Are Susceptible to Junin Virus Infection. J Virol 84, 13063-13067.

107. Kranzusch, P.J., Schenk, A.D., Rahmeh, A.A., Radoshitzky, S.R., Bavari, S., Walz, T., Whelan, S.P.J., 2010. Assembly of a functional Machupo virus polymerase complex. Proceedings of the National Academy of Sciences 107, 20069-20074.

108. Kranzusch, P.J., Whelan, S.P.J., 2011. Arenavirus Z protein controls viral RNA synthesis by locking a polymerase–promoter complex. Proceedings of the National Academy of Sciences 108, 19743-19748.

109. Kunz, S., 2009. Receptor binding and cell entry of Old World arenaviruses reveal novel aspects of virus–host interaction. Virology 387, 245-249.

110. Laguens, R.M., Avila, M.M., Samoilovich, S.R., Weissenbacher, M.C., Laguens, R.P., 1983. Pathogenicity of an Attenuated Strain (XJCl₃) of Junin Virus. Intervirology 20, 195-201.

111. Lampuri, J.S., Vidal, M.D., Coto, C.E., 1982. [Response of calomys musculinus to experimental infection with Junin virus] [Article in Spanish]. Medicina (B Aires) 42, 61-66.

112. Lan, S., McLay Schelde, L., Wang, J., Kumar, N., Ly, H., Liang, Y., 2009. Development of Infectious Clones for Virulent and Avirulent Pichinde Viruses: a Model Virus To Study Arenavirus-Induced Hemorrhagic Fevers. Journal of Virology 83, 6357-6362.

113. Lee, K.J., Novella, I.S., Teng, M.N., Oldstone, M.B., de La Torre, J.C., 2000. NP and L proteins of lymphocytic choriomeningitis virus (LCMV) are sufficient for efficient transcription and replication of LCMV genomic RNA analogs. J Virol 74, 3470-3477.

114. Lelke, M., Brunotte, L., Busch, C., Günther, S., 2010. An N-Terminal Region of Lassa Virus L Protein Plays a Critical Role in Transcription but Not Replication of the Virus Genome. Journal of Virology 84, 1934-1944.

115. Lenz, O., ter Meulen, J., Klenk, H.-D., Seidah, N.G., Garten, W., 2001a. The Lassa virus glycoprotein precursor GP-C is proteolytically processed by subtilase SKI-1/S1P, pp. 12701-12705.

116. Lenz, O., ter Meulen, J., Klenk, H.D., Seidah, N.G., Garten, W., 2001b. The Lassa virus glycoprotein precursor GP-C is proteolytically processed by subtilase SKI-1/S1P. Proc Natl Acad Sci U S A 98, 12701-12705.

117. Lerer, G.D., Saavedra, M.C., Falcoff, R., Maiztegui, J.I., Molinas, F.C., 1991. Activity of a platelet protein kinase that phosphorylates fibrinogen and histone in Argentine hemorrhagic fever. Acta Physiol Pharmacol Ther Latinoam 41, 377-386.

118. Levis, S.C., Saavedra, M.C., Ceccoli, C., Falcoff, E., Feuillade, M.R., Enria, D.A.M., Maiztegui, J.I., Falcoff, R., 1984. Endogenous Interferon in Argentine Hemorrhagic Fever. Journal of Infectious Diseases 149, 428-433.

119. Levis, S.C., Saavedra, M.C., Ceccoli, C., Feuillade, M.R., Enria, D.A., Maiztegui, J.I., Falcoff, R., 1985. Correlation between endogenous interferon and the clinical evolution of patients with Argentine hemorrhagic fever. J Interferon Res 5, 383-389.

120. Liu, C.Y., Xu, Z., Kaufman, R.J., 2003. Structure and Intermolecular Interactions of the Luminal Dimerization Domain of Human IRE1α. Journal of Biological Chemistry 278, 17680-17687.

121. Lopez, N., Jacamo, R., Franze-Fernandez, M.T., 2001. Transcription and RNA replication of tacaribe virus genome and antigenome analogs require N and L proteins: z protein is an inhibitor of these processes. J Virol 75, 12241-12251.

122. Lukashevich, I.S., 1992. Generation of reassortants between African arenaviruses. Virology 188, 600-605.

123. Lukashevich, I.S., Carrion Jr, R., Salvato, M.S., Mansfield, K., Brasky, K., Zapata, J., Cairo, C., Goicochea, M., Hoosien, G.E., Ticer, A., Bryant, J., Davis, H., Hammamieh, R., Mayda, M., Jett, M., Patterson, J., 2008. Safety, immunogenicity, and efficacy of the ML29 reassortant vaccine for Lassa fever in small non-human primates. Vaccine 26, 5246-5254.

124. Lukashevich, I.S., Maryankova, R., Vladyko, A.S., Nashkevich, N., Koleda, S., Djavani, M., Horejsh, D., Voitenok, N.N., Salvato, M.S., 1999. Lassa and Mopeia virus replication in human monocytes/macrophages and in endothelial cells: different effects on IL-8 and TNF-alpha gene expression. J Med Virol 59, 552-560.

125. Lukashevich, I.S., Patterson, J., Carrion, R., Moshkoff, D., Ticer, A., Zapata, J., Brasky, K., Geiger, R., Hubbard, G.B., Bryant, J., Salvato, M.S., 2005. A live attenuated vaccine for Lassa fever made by reassortment of Lassa and Mopeia viruses. J Virol 79, 13934-13942.

126. Mahanty, S., Bausch, D.G., Thomas, R.L., Goba, A., Bah, A., Peters, C.J., Rollin, P.E., 2001. Low Levels of Interleukin-8 and Interferon-Inducible Protein–10 in Serum Are Associated with Fatal Infections in Acute Lassa Fever. Journal of Infectious Diseases 183, 1713-1721.

127. Maiztegui, J.I., 1975. Clinical and epidemiological patterns of Argentine haemorrhagic fever. Bull World Health Organ 52, 567–575.

128. Maiztegui, J.I., Fernandez, N.J., de Damilano, A.J., 1979. Efficacy of immune plasma in treatment of Argentine haemorrhagic fever and association between treatment and a late neurological syndrome. Lancet 2, 1216-1217.

129. Maiztegui, J.I., McKee, K.T., Jr., Barrera Oro, J.G., Harrison, L.H., Gibbs, P.H., Feuillade, M.R., Enria, D.A., Briggiler, A.M., Levis, S.C., Ambrosio, A.M., Halsey, N.A., Peters, C.J., 1998. Protective efficacy of a live attenuated vaccine against Argentine hemorrhagic fever. AHF Study Group. J Infect Dis 177, 277-283.

130. Marq, J.-B., Kolakofsky, D., Garcin, D., 2010. Unpaired 5′ ppp-Nucleotides, as Found in Arenavirus Double-stranded RNA Panhandles, Are Not Recognized by RIG-I. Journal of Biological Chemistry 285, 18208-18216.

131. Marta, R.F., Enria, D., Molinas, F.C., 2000. Relationship between hematopoietic growth factors levels and hematological parameters in Argentine hemorrhagic fever. Am J Hematol 64, 1-6.

132. Marta, R.F., Montero, V.S., Hack, C.E., Sturk, A., Maiztegui, J.I., Molinas, F.C., 1999. Proinflammatory cytokines and elastase-alpha-1-antitrypsin in Argentine hemorrhagic fever. Am J Trop Med Hyg 60, 85-89.

133. Marta, R.F., Montero, V.S., Molinas, F.C., 1998. Systemic disorders in Argentine haemorrhagic fever. Bulletin de l'Institut Pasteur 96, 115-124.

134. Martínez-Sobrido , L., Emonet, S., Giannakas, P., Cubitt, B., García-Sastre, A., de la Torre, J.C., 2009. Identification of Amino Acid Residues Critical for the Anti-Interferon Activity of the Nucleoprotein of the Prototypic Arenavirus Lymphocytic Choriomeningitis Virus. Journal of Virology 83, 11330-11340.

135. Martinez-Sobrido, L., Giannakas, P., Cubitt, B., Garcia-Sastre, A., de la Torre, J.C., 2007. Differential Inhibition of Type I Interferon Induction by Arenavirus Nucleoproteins. J Virol 81, 12696-12703.

136. Martinez-Sobrido, L., Zuniga, E.I., Rosario, D., Garcia-Sastre, A., de la Torre, J.C., 2006. Inhibition of the type I interferon response by the nucleoprotein of the prototypic arenavirus lymphocytic choriomeningitis virus. J Virol 80, 9192-9199.

137. Martinez, M.G., Cordo, S.M., Candurra, N.A., 2007. Characterization of Junin arenavirus cell entry. J Gen Virol. 88, 1776-1784.

138. Matloubian, M., Kolhekar, S.R., Somasundaram, T., Ahmed, R., 1993. Molecular determinants of macrophage tropism and viral persistence: importance of single amino acid changes in the polymerase and glycoprotein of lymphocytic choriomeningitis virus. Journal of Virology 67, 7340-7349.

139. Matloubian, M., Somasundaram, T., Kolhekar, S.R., Selvakumar, R., Ahmed, R., 1990. Genetic basis of viral persistence: single amino acid change in the viral glycoprotein affects ability of lymphocytic choriomeningitis virus to persist in adult mice. The Journal of Experimental Medicine 172, 1043-1048.

140. McCormick, J.B., Fisher-Hoch, S.P., 2002. Lassa Fever, in: Oldstone, M.B. (Ed.), Arenaviruses I. Springer-Verlag, Berlin, Heidelberg, New York, pp. 75-110.

141. McKee, K.T., Oro, J.G., Kuehne, A.I., Spisso, J.A., Mahlandt, B.G., 1992. Candid No. 1 Argentine hemorrhagic fever vaccine protects against lethal Junin virus challenge in rhesus macaques. Intervirology 34, 154-163.

142. McKee, K.T., Oro, J.G.B., Kuehne, A.I., Spisso, J.A., Mahlandt, B.G., 1993. Safety and Immunogenicity of a Live-Attenuated Junin (Argentine Hemorrhagic Fever) Vaccine in Rhesus Macaques. The American Journal of Tropical Medicine and Hygiene 48, 403-411.

143. Medeot, S.I., Contigiani, M.S., Brandan, E.R., Sabattini, M.S., 1990. Neurovirulence of wild and laboratory Junin virus strains in animal hosts. J Med Virol 32, 171-182.

144. Medigeshi, G.R., Lancaster, A.M., Hirsch, A.J., Briese, T., Lipkin, W.I., Defilippis, V., Fruh, K., Mason, P.W., Nikolich-Zugich, J., Nelson, J.A., 2007. West Nile virus infection activates the unfolded protein response leading to CHOP induction and apoptosis. J Virol 8, 8.

145. Meyer, B.J., Southern, P.J., 1993. Concurrent sequence analysis of 5' and 3' RNA termini by intramolecular circularization reveals 5' nontemplated bases and 3' terminal heterogeneity for lymphocytic choriomeningitis virus mRNAs. J Virol 67, 2621-2627.

146. Meyer, B.J., Southern, P.J., 1994. Sequence heterogeneity in the termini of lymphocytic choriomeningitis virus genomic and antigenomic RNAs. J Virol 68, 7659-7664.

147. Mijnes, J.D.F., Lutters, B.C.H., Vlot, A.C., Horzinek, M.C., Rottier, P.J.M., de Groot, R.J., 1998. The Disulfide-Bonded Structure of Feline Herpesvirus Glycoprotein I. Journal of Virology 72, 7245-7254.

148. Milazzo M.L., C.M.N., Haynie M.L., Abbott K.D., Bradley R.D., and Fulhorst C.F., 2008. Diversity Among Tacaribe Serocomplex Viruses (Family Arenaviridae) Naturally Associated with the White-Throated Woodrat (Neotoma albigula) in the Southwestern United States. Vector Borne Zoonotic Dis 8, 523-540.

149. Molinas, F.C., de Bracco, M.M.E., Maiztegui, J.I., 1981. Coagulation Studies in Argentine Hemorrhagic Fever. Journal of Infectious Diseases 143, 1-6.

150. Molinas, F.C., Kordich, L., Porterie, P., Lerer, G., Maiztegui, J.I., 1987. Plasminogen abnormalities in patients with argentine hemorrhagic fever. Thrombosis Research 48, 713-720.

151. Morin, B., Coutard, B., Lelke, M., Ferron, F., Kerber, R., Jamal, S., Frangeul, A., Baronti, C., Charrel, R., de Lamballerie, X., Vonrhein, C., Lescar, J., Bricogne, G., Günther, S., Canard, B., 2010. The N-Terminal Domain of the Arenavirus L Protein Is an RNA Endonuclease Essential in mRNA Transcription. PLoS Pathog 6, e1001038.

152. Murphy, F.A., Whitfield, S.G., 1975. Morphology and morphogenesis of arenaviruses. Bull World Health Organ 52, 409–419.

153. Nota, N.R., Nejamkis, M.R., Giovanniello, O.A., 1976. Further experiments on the action of antithymocyte serum in experimental Junín virus infection. Acta Virol 20, 61-65.

154. Nunberg, J.H., York, J., 2012. The curious case of arenavirus entry, and its inhibition. Viruses 4, 83-101.

155. Ohoka, N., Yoshii, S., Hattori, T., Onozaki, K., Hayashi, H., 2005. TRB3, a novel ER stress-inducible gene, is induced via ATF4–CHOP pathway and is involved in cell death. The EMBO Journal 24, 1243-1255.

156. Parker, W.B., 2005. Metabolism and antiviral activity of ribavirin. Virus Res 107, 165-171.

157. Parodi, A.S., Greenway, D.J., Rugiero, H.R., Frigerio, M., de la Barrera, J.M., Mettler, N., Garzon, F., Boxaca, M., Guerrero, L., Nota, N., 1958. Concerning the epidemic outbreak in Junin. Dia Med. 30, 2300-2301.

158. Pasqual, G., Burri, D.J., Pasquato, A., de la Torre, J.C., Kunz, S., 2011. Role of the Host Cell's Unfolded Protein Response in Arenavirus Infection. Journal of Virology 85, 1662-1670.

159. Pasquato, A., Burri, D.J., Traba, E.G.-I., Hanna-El-Daher, L., Seidah, N.G., Kunz, S., 2011. Arenavirus envelope glycoproteins mimic autoprocessing sites of the cellular proprotein convertase subtilisin kexin isozyme-1/site-1 protease. Virology 417, 18-26.

160. Patterson, M., Seregin, A., Huang, C., Kolokoltsova, O., Smith, J., Miller, M., Smith, J., Yun, N., Poussard, A., Grant, A., Tigabu, B., Walker, A., Paessler, S., 2014. Rescue of a Recombinant Machupo Virus from Cloned cDNAs and In Vivo Characterization in Interferon (αβ/γ) Receptor Double Knockout Mice. Journal of Virology 88, 1914-1923.

161. Perez, M., Craven, R.C., de la Torre, J.C., 2003. The small RING finger protein Z drives arenavirus budding: implications for antiviral strategies. Proc Natl Acad Sci U S A 100, 12978-12983.

162. Perez, M., de la Torre, J.C., 2003. Characterization of the Genomic Promoter of the Prototypic Arenavirus Lymphocytic Choriomeningitis Virus. J Virol 77, 1184-1194.

163. Peters, C.J., 2002. Human Infection with Arenaviruses in the Americas, in: Oldstone, M.B. (Ed.), Arenaviruses I. Springer-Verlag, Berlin Heidelberg, pp. 65-74.

164. Peters, C.J., 2006. Emerging infections: lessons from the viral hemorrhagic fevers. Trans Am Clin Climatol Assoc 117, 189-197.

165. Peters, C.J., Jahrling, P.B., Liu, C.T., Kenyon, R.H., McKee, K.T., Jr., Barrera Oro, J.G., 1987. Experimental studies of arenaviral hemorrhagic fevers. Curr Top Microbiol Immunol 134, 5-68.

166. Pinschewer, D.D., Perez, M., de la Torre, J.C., 2003. Role of the virus nucleoprotein in the regulation of lymphocytic choriomeningitis virus transcription and RNA replication. J Virol 77, 3882-3887.

167. Pinschewer, D.D., Perez, M., de la Torre, J.C., 2005. Dual role of the lymphocytic choriomeningitis virus intergenic region in transcription termination and virus propagation. J Virol 79, 4519-4526.

168. Pozner, R.G., Ure, A.E., Jaquenod de Giusti, C., D'Atri, L.P., Italiano, J.E., Torres, O., Romanowski, V., Schattner, M., Gómez, R.M., 2010. Junín Virus Infection of Human Hematopoietic Progenitors Impairs In Vitro Proplatelet Formation and Platelet Release via a Bystander Effect Involving Type I IFN Signaling. PLoS Pathog 6, e1000847.

169. Pythoud, C., Rodrigo, W.W.S.I., Pasqual, G., Rothenberger, S., Martínez-Sobrido, L., de la Torre, J.C., Kunz, S., 2012. Arenavirus Nucleoprotein Targets Interferon Regulatory Factor-Activating Kinase IKKε. Journal of Virology 86, 7728-7738.

170. Qi, X., Lan, S., Wang, W., Schelde, L.M., Dong, H., Wallat, G.D., Ly, H., Liang, Y., Dong, C., 2010. Cap binding and immune evasion revealed by Lassa nucleoprotein structure. Nature 468, 779-783.

171. Quirin, K., Eschli, B., Scheu, I., Poort, L., Kartenbeck, J., Helenius, A., 2008. Lymphocytic choriomeningitis virus uses a novel endocytic pathway for infectious entry via late endosomes. Virology 378, 21-33.

172. Radoshitzky, S.R., Abraham, J., Spiropoulou, C.F., Kuhn, J.H., Nguyen, D., Li, W., Nagel, J., Schmidt, P.J., Nunberg, J.H., Andrews, N.C., Farzan, M., Choe, H., 2007. Transferrin receptor 1 is a cellular receptor for New World haemorrhagic fever arenaviruses. Nature. 446, 92-96. Epub 2007 Feb 2007.

173. Radoshitzky, S.R., Kuhn, J.H., Spiropoulou, C.F., Albariño, C.G., Nguyen, D.P., Salazar-Bravo, J., Dorfman, T., Lee, A.S., Wang, E., Ross, S.R., Choe, H., Farzan, M., 2008. Receptor determinants of zoonotic transmission of New World hemorrhagic fever arenaviruses. Proceedings of the National Academy of Sciences 105, 2664-2669.

174. Riviere, Y., Ahmed, R., Oldstone, M., 1986. The use of lymphocytic choriomeningitis virus reassortants to map viral genes causing virulence. Medical Microbiology and Immunology 175, 191-192.

175. Riviere, Y., Ahmed, R., Southern, P.J., Buchmeier, M.J., Oldstone, M.B., 1985. Genetic mapping of lymphocytic choriomeningitis virus pathogenicity: virulence in guinea pigs is associated with the L RNA segment. Journal of Virology 55, 704-709.

176. Rodrigo, W.W.S.I., Ortiz-Riaño, E., Pythoud, C., Kunz, S., de la Torre, J.C., Martínez-Sobrido, L., 2012. Arenavirus Nucleoproteins Prevent Activation of Nuclear Factor Kappa B. Journal of Virology 86, 8185-8197.

177. Rojek, J.M., Lee, A.M., Nguyen, N., Spiropoulou, C.F., Kunz, S., 2008. Site 1 protease is required for proteolytic processing of the glycoproteins of the South American hemorrhagic fever viruses Junin, Machupo, and Guanarito. J Virol 82, 6045-6051.

178. Ruggiero, H.A., Magnoni, C., De Guerrero, L.B., Milani, H.A., Izquierdo, F.P., Milani, H.L., Weber, E.L., 1981. Persistence of antibodies and clinical evaluation in volunteers 7 to 9 years following the vaccination against Argentine hemorrhagic fever. Journal of Medical Virology 7, 227-232.

179. Sabattini, M.S., Gonzalez, L.E., de Rios Diaz, G., Vega, V.R., 1977. Infeccion natural y experimental de roedores con virus junin. Medicina (B Aires) 37, 149-161.

180. Sabattini, M.S., Maiztegui, J.I., 1970. Fiebre Hemorragica Argentina. Medicina (B Aires) 30, 111-128.

181. Salazar, M., Yun, N.E., Poussard, A.L., Smith, J.N., Smith, J.K., Kolokoltsova, O.A., Patterson, M.J., Linde, J., Paessler, S., 2012. Effect of Ribavirin on Junin Virus Infection in Guinea Pigs. Zoonoses and Public Health 59, 278-285.

182. Salvato, M.S., Clegg, J.C.S., Buchmeier, M.J., Charrel, R.N., Gonzales, J.P., Lukashevich, I.S., Peters, C.J., Rico-Hesse, R., Romanowski, V., 2012. Family Arenaviridae, in: King, A.M.Q., Adams, M.J., Carstens, E.B., Lefkowitz, E.F. (Eds.), Virus Taxonomy: Ninth Report of the International Committee on Taxonomy of Viruses. Academic Press, pp. 714-723.

183. Salvato, M.S., Shimomaye, E.M., 1989. The completed sequence of lymphocytic choriomeningitis virus reveals a unique RNA structure and a gene for a zinc finger protein. Virology 173, 1-10.

184. Samoilovich, S.R., Calello, M.A., Laguens, R.P., Weissenbacher, M.C., 1988. Long-term protection against Argentine hemorrhagic fever in Tacaribe virus infected marmosets: virologic and histopathologic findings. J Med Virol 24, 229-236.

185. Samoilovich, S.R., Pecci Saavedra, J., Frigerio, M.J., Weissenbacher, M.C., 1984. Nasal and intrathalamic inoculations of primates with Tacaribe virus: protection against Argentine hemorrhagic fever and absence of neurovirulence. Acta Virol 28, 277-281.

186. Sánchez, A.B., de la Torre, J.C., 2006. Rescue of the prototypic Arenavirus LCMV entirely from plasmid. Virology 350, 370-380.

187. Schlie, K., Maisa, A., Freiberg, F., Groseth, A., Strecker, T., Garten, W., 2010. Viral Protein Determinants of Lassa Virus Entry and Release from Polarized Epithelial Cells. Journal of Virology 84, 3178-3188.

188. Schröder, M., 2008. Endoplasmic reticulum stress responses. Cell. Mol. Life Sci. 65, 862-894.

189. Schroder, M., Kaufman, R.J., 2005. The mammalian unfolded protein response. Annu Rev Biochem. 74, 739-789.

190. Seregin, A.V., Yun, N.E., Poussard, A.L., Peng, B.-H., Smith, J.K., Smith, J.N., Salazar, M., Paessler, S., 2010. TC83 replicon vectored vaccine provides protection against Junin virus in guinea pigs. Vaccine 28, 4713-4718.

191. Shimojima, M., Kawaoka, Y., 2012. Cell Surface Molecules Involved in Infection Mediated by Lymphocytic Choriomeningitis Virus Glycoprotein. Journal of Veterinary Medical Science 74, 1363-1366.

192. Shimojima, M., Ströher, U., Ebihara, H., Feldmann, H., Kawaoka, Y., 2012. Identification of Cell Surface Molecules Involved in Dystroglycan-Independent Lassa Virus Cell Entry. Journal of Virology 86, 2067-2078.

193. Spiropoulou, C.F., Kunz, S., Rollin, P.E., Campbell, K.P., Oldstone, M.B., 2002. New World arenavirus clade C, but not clade A and B viruses, utilizes alpha-dystroglycan as its major receptor. J Virol 76, 5140-5146.

194. Stephen, E.L., Jones, D.E., Peters, C.J., Eddy, G.A., Loizeaux, P.S., Jahrling, P.B., 1980. Ribavirin treatment of toga-, arena-, and bunyavirus infections in subhuman primates and other laboratory animal species, in: Smith, R.A., Kirkpatrick, W. (Eds.), Ribavirin: a broad spectrum antiviral agent. Academic Press, Inc., New York, N.Y., pp. 169-183.

195. Strecker, T., Eichler, R., Meulen, J., Weissenhorn, W., Dieter Klenk, H., Garten, W., Lenz, O., 2003. Lassa virus Z protein is a matrix protein and sufficient for the release of virus-like particles [corrected]. J Virol 77, 10700-10705.

196. Tortorici, M.A., Albarino, C.G., Posik, D.M., Ghiringhelli, P.D., Lozano, M.E., Rivera Pomar, R., Romanowski, V., 2001. Arenavirus nucleocapsid protein displays a transcriptional antitermination activity in vivo. Virus Res 73, 41-55.

197. Urata, S., Noda, T., Kawaoka, Y., Yokosawa, H., Yasuda, J., 2006. Cellular factors required for Lassa virus budding. J Virol 80, 4191-4195.

198. Vallejos, D.A., Ambrosio, A.M., Feuillade, M.R., Maiztegui, J.I., 1989. Lymphocyte subsets alteration in patients with argentine hemorrhagic fever. J Med Virol 27, 160-163.

199. Videla, C., Carballal, G., Remorini, P., la Torre, J., 1989. Formalin inactivated Junin virus: immunogenicity and protection assays. J Med Virol 29, 215-220.

200. Vitullo, A.D., Hodara, V.L., Merani, M.S., 1987. Effect of persistent infection with Junin virus on growth and reproduction of its natural reservoir, Calomys musculinus. Am J Trop Med Hyg 37, 663-669.

201. Volpon, L., Osborne, M.J., Capul, A.A., de la Torre, J.C., Borden, K.L.B., 2010. Structural characterization of the Z RING-eIF4E complex reveals a distinct mode of control for eIF4E. Proceedings of the National Academy of Sciences 107, 5441-5446.

202. Weissenbacher, M.C., Avila, M.M., Calello, M.A., Merani, M.S., McCormick, J.B., Rodriguez, M., 1986. Effect of ribavirin and immune serum on Junin virus-infected primates. Med Microbiol Immunol 175, 183-186.

203. Weissenbacher, M.C., Calello, M.A., Colillas, O.J., Rondinone, S.N., Frigerio, M.J., 1979. Argentine hemorrhagic fever: a primate model. Intervirology 11, 363-365.

204. Weissenbacher, M.C., Coto, C.E., Calello, M.A., 1975-1976. Cross-protection between Tacaribe complex viruses. Presence of neutralizing antibodies against Junin virus (Argentine hemorrhagic fever) in guinea pigs infected with Tacaribe virus. Intervirology 6, 42-49.

205. Weissenbacher, M.C., Coto, C.E., Calello, M.A., Rondinone, S.N., Damonte, E.B., Frigerio, M.J., 1982. Cross-protection in nonhuman primates against Argentine hemorrhagic fever. Infection and Immunity 35, 425-430.

206. Weissenbacher, M.C., de Guerrero, L.B., Boxaca, M.C., 1975. Experimental biology and pathogenesis of Junin virus infection in animals and man. Bull World Health Organ 52, 507-515.

207. Weissenbacher, M.C., Laguens, R.P., Coto, C.E., 1987. Argentine hemorrhagic fever. Curr Top Microbiol Immunol 134, 79-116.

208. Wulff, H., Lange, J.V., Webb, P.A., 1978. Interrelationships Among Arenaviruses Measured by Indirect Immunofluorescence. Intervirology 9, 344-350.

209. Yamaguchi, H., Wang, H.-G., 2004. CHOP Is Involved in Endoplasmic Reticulum Stress-induced Apoptosis by Enhancing DR5 Expression in Human Carcinoma Cells. Journal of Biological Chemistry 279, 45495-45502.

210. Ye, J., Rawson, R.B., Komuro, R., Chen, X., Davé, U.P., Prywes, R., Brown, M.S., Goldstein, J.L., 2000. ER Stress Induces Cleavage of Membrane-Bound ATF6 by the Same Proteases that Process SREBPs. Molecular Cell 6, 1355-1364.

211. York, J., Nunberg, J.H., 2006. Role of the stable signal peptide of Junin arenavirus envelope glycoprotein in pH-dependent membrane fusion. J Virol 80, 7775-7780.

212. York, J., Nunberg, J.H., 2007. A Novel Zinc-Binding Domain Is Essential for Formation of the Functional Junín Virus Envelope Glycoprotein Complex. Journal of Virology 81, 13385-13391.

213. York, J., Nunberg, J.H., 2009. Intersubunit Interactions Modulate pH-Induced Activation of Membrane Fusion by the Junín Virus Envelope Glycoprotein GPC. Journal of Virology 83, 4121-4126.

214. York, J., Romanowski, V., Lu, M., Nunberg, J.H., 2004. The signal peptide of the Junin arenavirus envelope glycoprotein is myristoylated and forms an essential subunit of the mature G1-G2 complex. J Virol 78, 10783-10792.

215. Yun, N.E., Linde, N.S., Dziuba, N., Zacks, M.A., Smith, J.N., Smith, J.K., Aronson, J.F., Chumakova, O.V., Lander, H.M., Peters, C.J., Paessler, S., 2008. Pathogenesis of XJ and Romero Strains of Junin Virus in Two Strains of Guinea Pigs. Am J Trop Med Hyg 79, 275-282.

216. Zhang, K., Kaufman, R.J., 2006. The unfolded protein response: a stress signaling pathway critical for health and disease. Neurology. 66, S102-109.

217. Zhang, K., Kaufman, R.J., 2008. From endoplasmic-reticulum stress to the inflammatory response. Nature 454, 455-462.

218. Zhang, L., Marriott, K.A., Harnish, D.G., Aronson, J.F., 2001. Reassortant Analysis of Guinea Pig Virulence of Pichinde Virus Variants. Virology 290, 30-38.

VITA

Alexey V. Seregin was born in Omsk, Russia, on May 10th, 1980. He obtained a B.S. and M.S. degree in Cytology and Genetics from the Novosibirsk State University, Novosibirsk, Russia. In 2002, he joined a newly established research group at the University of Kansas, Lawrence, KS, as a research assistant. His projects were primarily focused on the molecular mechanisms of virulence and pathogenicity of West Nile virus. In 2010, he entered the Experimental Pathology graduate program at the University of Texas Medical Branch (UTMB), Galveston, TX, and began working with the hemorrhagic fever arenaviruses Junin and Lassa under the mentorship of Dr. Slobodan Paessler. His dissertation project was focused on the molecular mechanisms of arenavirus pathogenesis and attenuation. During his graduate career at UTMB, Alexey received 10 highly prestigious scholarships and travel awards and was the recipient of a T32 Biodefense fellowship from the National Institutes of Health. His work was presented at several major national and international conferences and contributed to 15 publications in peer-reviewed scientific journals including 3 first-author articles.

Education

B.S. and M.S., June 2002, Novosibirsk State University, Novosibirsk, Russia

Publications

1. Patterson M, Seregin A, Huang C, Kolokoltsova O, Smith J, Miller M, Smith J, Yun N, Poussard A, Grant A, Tigabu B, Walker A, Paessler S. Rescue of a Recombinant Machupo Virus from Cloned cDNAs and In Vivo Characterization in Interferon (αβ/γ) Receptor Double Knockout Mice. J Virol. 2013 Nov 27. [Epub ahead of print]

2. Yun NE, Seregin AV, Walker DH, Popov VL, Walker AG, Smith JN, Miller M, de la Torre JC, Smith JK, Borisevich V, Fair JN, Wauquier N, Grant DS, Bockarie B, Bente D, Paessler S. Mice lacking functional STAT1 are highly susceptible to lethal infection with Lassa virus. J Virol. 2013 Oct;87(19):10908-11. doi: 10.1128/JVI.01433-13. Epub 2013 Jul 31.

3. Poussard A, Patterson M, Taylor K, Seregin A, Smith J, Smith J, Salazar M, Paessler S. In vivo imaging systems (IVIS) detection of a neuro-invasive encephalitic virus. J Vis Exp. 2012 Dec 2;(70):e4429. doi: 10.3791/4429.

4. Grant A, Seregin A, Huang C, Kolokoltsova O, Brasier A, Peters C, Paessler S. Junín Virus Pathogenesis and Virus Replication. Review. Viruses 2012, 4, 2317-2339; doi:10.3390/v4102317

5. Huang C, Kolokoltsova OA, Yun NE, Seregin AV, Poussard AL, Walker AG, Brasier AR, Zhao Y, Tian B, de la Torre JC, Paessler S. Junín virus infection activates the type I interferon pathway in a RIG-I-dependent manner. PLoS Negl Trop Dis. 2012; 6(5):e1659. Epub 2012 May 22.

6. Yun NE, Poussard AL, Seregin AV, Walker AG, Smith JK, Aronson JF, Smith JN, Soong L, Paessler S. Functional interferon system is required for clearance of lassa virus. J Virol. 2012 Mar; 86(6):3389-92. Epub 2012 Jan 11.

7. Patterson M, Poussard A, Taylor K, Seregin A, Smith J, Peng BH, Walker A, Linde J, Smith J, Salazar M, Paessler S. Rapid, non-invasive imaging of alphaviral brain infection: reducing animal numbers and morbidity to identify efficacy of potential vaccines and antivirals. Vaccine. 2011 Nov 21;29(50):9345-51. Epub 2011 Oct 12.

8. Emonet SF*, Seregin AV*, Yun NE, Poussard AL, Walker AG, de la Torre JC, Paessler S. Rescue from cloned cDNAs and in vivo characterization of recombinant pathogenic Romero and live-attenuated Candid #1 strains of Junin virus, the causative agent of Argentine hemorrhagic fever disease. J Virol. 2011 Feb;85(4):1473-83. Epub 2010 Dec 1. (*-equal contribution)

9. Seregin AV, Yun NE, Poussard AL, Peng BH, Smith JK, Smith JN, Salazar M, Paessler S. TC83 replicon vectored vaccine provides protection against Junin virus in guinea pigs. Vaccine. 2010 Jul 5;28(30):4713-8. Epub 2010 May 7.

10. Paessler S, Rijnbrand R, Stein DA, Ni H, Yun NE, Dziuba N, Borisevich V, Seregin A, Ma Y, Blouch R, Iversen PL, Zacks MA. Inhibition of alphavirus infection in cell culture and in mice with antisense morpholino oligomers. Virology. 2008 Jul 5;376(2):357-70. Epub 2008 May 12.

11. Borisevich V, Nistler R, Hudman D, Yamshchikov G, Seregin A, Yamshchikov VF. 2008. A highly sensitive and versatile virus titration assay in the 96-well microplate format. J Virol Methods 147(2), 197-205.

12. Seregin AV, Nistler R, Borisevich V, Yamshchikov G, Chaporgina E, Kwok CW, Yamshchikov, VF. Immunogenicity of West Nile virus infectious DNA and its noninfectious derivatives. 2006. Virology 356(1-2), 115-25.

13. Borisevich V, Seregin A, Nistler R, Mutabazi D, Yamshchikov VF. Biological properties of chimeric West Nile viruses. 2006. Virology 349(2), 371-81.

14. Yamshchikov G, Borisevich V, Kwok CW, Nistler R, Kohlmeier J, Seregin A, Chaporgina E, Benedict S, Yamshchikov VF. The suitability of yellow fever and Japanese encephalitis vaccines for immunization against West Nile virus. 2005. Vaccine 23(39), 4785-92.

15. Yamshchikov G, Borisevich V, Seregin A, Chaporgina E, Mishina M, Mishin V, Kwok CW, Yamshchikov VF. An attenuated West Nile prototype virus is highly immunogenic and protects against the deadly NY99 strain: a candidate for live WN vaccine development. 2004. Virology 330(1), 304-12.

Selected Abstracts

1. Seregin AV, Yun NE, Poussard AL, Paessler S. Genetic determinants of Junin virus attenuation (oral presentation). The American Society for Virology, 32th Annual Meeting, State College, PA, 2013.

2. Seregin AV, Yun NE, Paessler S. Genetic determinants of Junin virus attenuation (poster). 15th International Negative Strand Virus Meeting, Granada, Spain, 2013.

3. Seregin AV, Emonet S, Yun NE, Poussard AL, Walker AG, de la Torre JC, Paessler S. Recombinant genetics for Junin virus (oral presentation). The American Society for Virology, 30th Annual Meeting, Minneapolis, MN, 2011.

4. Seregin AV, Yun NE, Poussard AL, Paessler S. Rescue of the arenavirus Junin from a polymerase I/II-driven plasmid system (poster). The American Society for Virology, 29th Annual Meeting, Bozeman, MT, 2010.

5. Seregin AV, Yun NE, Salazar M, Poussard AL, Smith JK, Smith JN, Zacks MA, Paessler S. Immunogenicity and efficacy of a novel recombinant vaccine against argentine hemorrhagic fever (poster). 58th Annual Meeting of the American Society of Tropical Medicine and Hygiene, Washington, DC, USA, 2009.

6. Seregin AV, Yun NE, Paessler S. Alphavirus vector-based vaccine development against Argentine hemorrhagic fever (poster). 2nd Vaccine Congress Boston, MA, USA, 2008.

7. Seregin AV, Borisevich V, Hudman D and Yamshchikov V. Infectious DNA is more immunogenic than attenuated virus carrying mutations affecting its infectivity (poster). The changing Landscape of Vaccine Development - Vaccines for Global Health, Galveston, TX, 2006.

8. Seregin AV, VG Borisevich, RJ Nistler, VF Yamshchikov. Infectious DNA methodology as a valuable tool in development of live vaccines (poster). Poster. KCALSI Research Day. Kansas City, KS, 2005.

9. Seregin AV, Puzakov MV, Menzorov AG. Chromosome segregation in intra- and interspecific cell hybrids obtained by fusion of murine embryonic stem cells with somatic cells and analysis of their pluripotency (oral presentation). XL International Scientific Student Conference "Student and Progress in Science and Technology". Novosibirsk, Russian Federation, 2002.

Summary of Dissertation

The New World arenavirus Junin (JUNV) is the causative agent of the Argentine hemorrhagic fever (AHF), a deadly disease endemic to central regions of Argentina. The live-attenuated Candid #1 strain of JUNV is currently used to vaccinate human population at risk. However, the mechanism of attenuation of this strain is still largely unknown. Therefore, the identification and functional characterization of viral genetic factors implicated in JUNV pathogenesis or attenuation would significantly improve the understanding of the molecular mechanisms underlying AHF and facilitate the development of novel, effective and safe vaccines. To this end, an RNA polymerase I/II-based reverse genetics system was utilized to rescue the wild type pathogenic Romero and attenuated Candid #1 strains of JUNV. Both recombinant viruses exhibited similar in vitro growth kinetics and in vivo biological properties to their parental counterparts. This system was further used to generate chimeric JUNV variants encoding different gene combinations of Romero and Candid #1. Analysis of virulence of the chimeric viruses in a guinea pigs model of lethal infection that closely reproduces the features of AHF, identified the envelope glycoproteins (GPs) as the major determinants of pathogenesis and attenuation of JUNV. Therefore, the chimeric viruses expressing the GPs of Romero

and Candid #1 exhibited virulent and attenuated phenotypes in guinea pigs, respectively. Comparison of the transcriptional and protein expression profiles of the chimeric JUNV variants demonstrated marked differences in the levels of viral RNA synthesis and protein expression between the attenuated and virulent JUNV variants. Further analysis showed that the GPC of Candid #1 undergoes abnormal post-translational modification and induces endoplasmic reticulum (ER) stress, which may facilitate immune recognition of JUNV infection. In addition, the small RING finger protein Z that is a negative regulator of the viral polymerase complex was retained in infected cells when it was coexpressed with the GPs of Romero, but not the GPs of Candid #1, therefore suggesting a molecular mechanism for the higher levels of viral RNA synthesis in cells infected with attenuated JUNV variants expressing the GPC of Candid #1. Thus, these findings provided further insights into the mechanism of JUNV attenuation.